Local insight into hydrological interactions from water quantity and vegetation monitoring

A study based on the sensor station network implemented in the drainage catchment of the Grote Masloot

Waterschap Noorderzijlvest – University of Twente

Bachelor thesis Civil Engineering

1st of July 2022

Preface

A research opportunity from the regional water authority Waterschap Noorderzijlvest related to their program "Voldoende en Gezond Water" on sufficient and healthy water frames this bachelor thesis for the Civil Engineering program at the University of Twente. The execution of the assignment has been supervised by M. Hooghiem from Waterschap Noorderzijlvest and J.F. Schyns of the University of Twente during the period of April 25th to July 1st.

Through the project "Duurzaam Agrarisch Waterbeheer", DAW, Waterschap Noorderzijlvest cooperates with an organization of local agricultural exploiters, named Boermarke Zeijen, looking for solutions to deal with contemporary water issues (Boermarke Zeijen, 2021). Following the introduction of the sustainable agricultural water management project DAW in 2018, Waterschap Noorderzijlvest has access to time series data on surface and groundwater with supplementing soil moisture and drain flow measurement alongside meteorological records. This data has been collected on local private properties occurring at defined measuring points within the catchment of the Grote Masloot. Waterschap Noorderzijlvest is interested in an empirical analysis of the relations between the water quantity data variables to uncover potential strain inducing components on prevailing local activities under pressures of meteorological conditions. On the side of Boermarke Zeijen, the members of this organization want to develop their businesses to the economic and ecological benefit (Glansbeek, 2021). The current interest in the data gathered is further explained by how, according to the planning of Waterschap Noorderzijlvest (2021), the current DAW project phase is to be concluded in 2022. An understanding of what insights the currently collected data offers about the area for water management would be beneficial to make arrangements for after 2022.

Summary

Following the introduction of the sustainable agricultural water management project in 2018, for the catchment of the Grote Masloot, Waterschap Noorderzijlvest has access to monitoring data. The sensor network collects time series of surface and groundwater level alongside soil moisture content, drain flow volume and precipitation records. The objective of this research project is to obtain insight in the relations amongst those variables of water quantity, supplemented with data on vegetation. This to identify if drainage management is adapted accordingly under wet and dry conditions. A temporal empirical analysis of the onsite collected records and remote sensing data is therefore used. Vegetation vigor is characterized by the normalized difference vegetation index, NDVI, using satellite data of the Copernicus Land Monitoring Service from the open access database of the European Space Agency.

The objective dictates two sequential levels that the methodology needs to address, processing the study objects up to the set target. The first part seeks for a directed relational analysis of the onsite collected water quantity time series alongside processed remote sensing imagery for the locations of the sensing stations. More specifically, focus is on the response of surface and groundwater levels alongside drain flow volumes to precipitation. While this response is also of interest for soil moisture content, the relation to groundwater level needs to be simultaneously considered. Further, the extent to which the derived vegetation vigor relates to the recorded soil moisture content is also incorporated. The second part subsequently uses gained insights to identify to what extent the drainage management supports land use based on the observed hydrological relations under wet and dry conditions.

For the first part, studying the relation between groundwater level and precipitation allows to state that the median lag time of peaks following a precipitation event ranges from 5 hours 45 minutes to 10 hours depending on the location. The rate of change during precipitation absence does follow a linear decrease that is variable per station and ranges from 1.45 to 2.92 cm per day. The groundwater table annual cycle amplitude is lower for the less elevated, more surface water occupied, locations. Further, the distance between monitoring stations alone is insufficient to account for the full variance between time series.

In the analysis of the response of surface water to precipitation, it should be noted that surface water level is maintained within close bounds with deviations principally being short term. This is further highlighted by how the surface water response lag time to precipitation tends to be concentrated in the range of 6 hours 30 minutes to 7 hours. Nevertheless, surface water is very variably affected by dry periods. Drain flow volume records on the other hand are prone to short term fluctuation, with for all but one station no perceivable yearly cyclicity. Because drain flow lag time to precipitation ranges from 6 to 9 hours, it should further be noted how these values exceed those for surface water for the comparable stations along the Grote Masloot. While drains do continue to flow during dry conditions there is no perceivable pattern. This is likely the result of the unreliability of the drain flow data set that contains entries of unrealistic magnitude following from the immersion or clogging of the equipment.

In the investigation of the dual relation between soil moisture to both groundwater and precipitation, it is found how soil moisture content features yearly cyclicity that is most prominent for the shallowest soil layers. Only the non grassland parcels, covered with deciduous trees or used for crops, experience less of a decay in the yearly amplitude as the measuring depth is increased. Following the better corresponding yearly cyclicity, soil moisture is most strongly correlated with groundwater for the shallowest soil layers. However according to the stable nature of the time series from 50 cm below the ground surface downwards, the moisture content is well upheld while uninfluenced by prevailing meteorological conditions. Indeed groundwater tables do annually rise to saturate the soil layers monitored, with superficiality and duration being most prominent for the low elevated grasslands. Further, predominantly the upper soil layers respond to precipitation occurrence and absence. While the dry conditions do tend to affect solely the first 20 cm, rainfall still usually shows effects until the 40 cm depth.

Considering the relation between soil moisture content and vegetation vigor, NDVI values do not feature cyclicity for grassland but do so for areas covered with deciduous trees or used for growing crops. While NDVI is not correlated to soil moisture content directly, for all non grassland parcels the soil moisture and NDVI series are out of phase with the deciduous trees parcel being perfect opposites. Consequently for land on which crops are grown, the lowest soil moisture content coincides with the part of the NDVI series that shows vegetation developing in its growth phase.

For the second part, using the relational insights in a discussion of the implications of drainage systems and the influences on the latter, allows to interpret how drain flow volume appears unaffected by groundwater fluctuations in terms of that it does not rise sufficiently to trigger extra drain flow in winter. However, because it was found that groundwater does tend to rise to the lower layers in which soil moisture content is measured for the less elevated parts of the catchment, it is more likely that the already mentioned errors in the collected drain flow data hide patterns. Hence drainage seems effective following from how, for the lower elevated grassland, the soil moisture states are more stable at increasing depths. This, because drainage targets to control groundwater level by limiting recharge through inducing the discharge of excess soil moisture content. Nevertheless it may be an option to reconsider the targets for utilizing the grasslands along the Grote Masloot, thereby revising perceptions on drainage.

Based on the findings of the executed data oriented analysis, in the context of the broader sustainable agricultural management project Waterschap Noorderzijlvest is involved with, it can be recommended to improve drainage monitoring. This in terms of record reliability and in combination with advancements of combined measuring in fields where groundwater level and soil moisture content are also monitored. Further, from a more environmental perspective, it can be interesting to reinforce monitoring of nonagricultural parcels for awareness of local agricultural influences.

Table of Contents

1. Introduction

The high dependability of agricultural practices on the local environment and weather conditions makes them in turn influencing and affecting the water quantity and quality characteristics of a region. The interest in informed management choices from the Dutch regional water authority Waterschap Noorderzijlvest and organization of local agricultural exploiters, named Boermark Zeijen, led to initiate a data collection initiative. The study area is restricted to the catchment of the Grote Masloot located in the southern district of Waterschap Noorderzijlvest where a sensor network has been implemented for monitoring from a water and agricultural management perspective. To understand the set research objective, the broader context is clarified and complemented with an overview of the interests involved.

1.1. Problem definition

Across the Grote Masloot catchment, the different land use functions of agriculture, nature, residential and work are accommodated (Glansbeek, 2021). For each, the water availability requirements differ per period and location. In specific, the soil moisture conditions agriculture requires do not correspond with natural seasonal conditions (Glansbeek, 2021). Hence, Waterschap Noorderzijlvest considers the water requirements from the various land use functions to direct management strategies (Glansbeek, 2021).

Rozemeijer et al. (2020) concluded that the local landscape of the study area dictates hydrologic behavior since the water quality and quantity in the stream valley is dependent upon the activities taking place on higher grounds. This suggests that there is potential to retain water and nutrients more effectively on a local scale. Indeed, due to its placement, the land around the stream is quickly too wet while the more elevated areas rapidly become too dry (Vinkenvleugel, 2019). Consequently, Rozemeijer et al. (2020), have identified the need to establish a better balanced relation between water management practices and land use functions. More specifically, they mention issues related to unnecessary water discharge, drought damage, soil compaction, nutrient outwash, fallow land and crop selection.

Based upon these observations, there is the need for a location tailored approach to manage water. The problem is formulated in terms of the insufficient resilience to fluctuating weather patterns and specifically extreme events. Waterschap Noorderzijlvest is interested in balancing water inflow and outflow to not shift pressures of water extraction and discharge to surrounding areas. Adjointly the agricultural exploiters have the desire to make their businesses more sustainable (Vinkenvleugel, 2019) while being financially directly impacted by drought damage and nutrients leaching away from the land.

1.2 Local interests and previously conducted research

To address the deficiency of knowledge on the response of the catchment to meteorological conditions and how this is location dependent, the local stakeholders have undertaken action. In 2018, the project "Duurzaam Agrarisch Waterbeheer", DAW, about sustainable agricultural water management within the Grote Masloot catchment was initiated. Waterschap Noorderzijlvest and Boermarke Zeijen jointly implemented a system to monitor water levels and quality (Vinkenvleugel, 2019).

Deltares and Nutriënten Management Instituut, NMI, have been involved to develop tools and formulate advice around the data collected. In the first phase, interest has been on exploring the potential of onsite sensor data collection and understanding its benefit for regional management of water resources, soil quality and agricultural exploitation (Rozemeijer et al., 2020). As such the reports of Rozemeijer et al. (2020) and van Rotterdam & van Doorn (2021) provide insight on the specific study area and expectations from data collection. Specifically, Rozemeijer et al. (2020) demonstrate the usefulness for developing models that can make predictions based on weather forecasts on a per parcel basis. That information would help Waterschap Noorderzijlvest to tune management strategies more effectively to the different local functions. They want to use such a model to investigate management for improved water storage, seeking to retain more water naturally, limiting drought and pollution damage (Rozemeijer et al. 2020).

Already, Boermarke Zeijen has focused attention on what they can do related to water management to optimize their production processes (Glansbeek, 2021). For this they have used the advice formulated by van Rotterdam & van Doorn (2021) following the detailed study of the six parcels in the area by NMI (Glansbeek, 2021). The Boermarke Zeijen organization hopes that based on the collected records the suboptimal locations, where it is too wet or dry can be identified, and possibly addressed with a tailored water inflow and outflow strategy (Vinkenvleugel, 2019). Overall, they benefit from reducing unnecessary nutrient losses, improving soil composition and texture alongside making the most of the local water resources while keeping their land accessible. Nevertheless, Waterschap Noorderzijlvest needs to consider the wider context in delineating their management strategies. Their target is set at using local interventions to improve water quality while considering the necessity to have increased water storage capacity to prepare for weather extremes.

1.3. Research objective and questions

Rozemeijer et al. (2020) offer their perspective on the continuation of the project to benefit the objectives of Waterschap Noorderzijlvest and Boermarke Zeijen. This set up enables to deduce a target contribution from the existing research gap running parallel to the potential second phase of the Deltares/NMI project. Figure 1 offers an overview of how the research framework partially contributes to the research gap formulated within the larger project context envisioned.

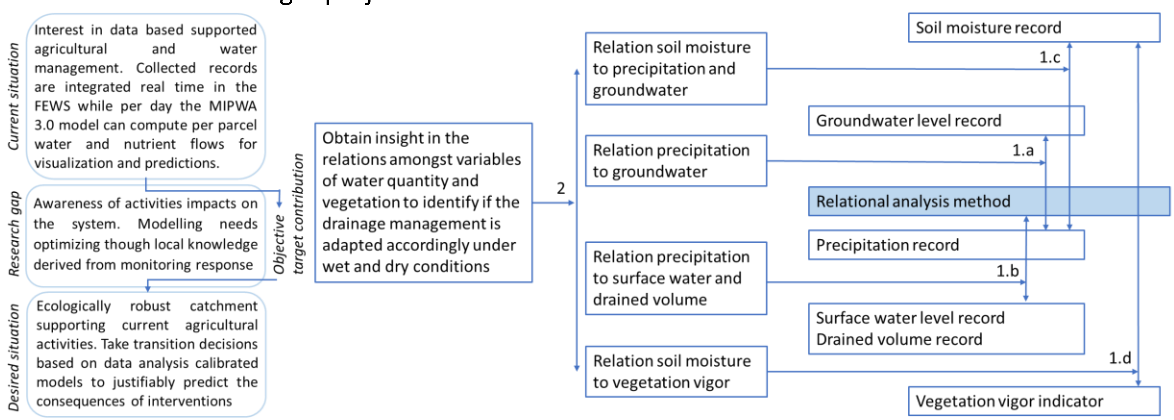

Figure 1: First establishing a research objective by identifying the research gap for the project sustainable agricultural water management Boermarke Zeijen based on the reporting of Rozemijer et al. (2020) and van Rotterdam & van Doorn (2021), allows to in the subsequent deconstruction of this aim recognize the components to be researched.

From Figure 1 the interconnectivity of water resource storage as groundwater and the discharge of water at the land surface, both contributing to the soil moisture available for vegetation, is uncovered. Accordingly, this leads to the formulation of following research objective:

The objective of this research project is to obtain insight in the relations amongst variables of water quantity and vegetation to identify if the drainage management is adapted accordingly under wet and dry conditions for the Grote Masloot catchment by a temporal empirical analysis of the onsite collected records and remote sensing data.

The variables of the water quantity component this formulation refers to include precipitation, surface water, soil moisture, groundwater and drainflow. In turn, the vegetation element alludes to the health and biomass of the ground cover. Eamus et al. (2015), who use the normalized difference vegetation index, NDVI, in their investigation to relate vegetation to groundwater in arid to semi-arid regions, reveal the potential of remote sensing data for this purpose. An empirical data analysis into the relation between the different water quantity related fluxes of the hydrological cycle and the connection to processed remote sensing data to understand vegetation ground cover thereby follows.

Overall, the twofold nature of the research objective is uncovered through Figure 1. Deconstructing the objective deduces two sequential levels that the methodology needs to address to process the study objects up to the set target. Indeed, Figure 1 shows the record components of interest and depicts the relational analysis amongst these by the vertical arrows that confront those elements. The confrontations thus mark the levels of the executed research. The numbering of the mentioned confrontations is the basis for the research questions. Acknowledging how the first part seeks for directed relational analysis with associated interpretation, while the second part is predominantly dedicated to the reflection on those, this leads to the research questions being formulated as follows:

1) Which insights are revealed by empirically analyzing the collected onsite water quantity time series alongside processed remote sensing imagery for the locations of the sensing stations within the Grote Masloot catchment?
   - 1.a) To what extent do the recorded groundwater levels respond to precipitation?
   - 1.b) To what extent do the recorded surface water levels and drainage volumes respond to precipitation?
   - 1.c) To what extent do the recorded soil moisture contents relate to groundwater levels and precipitation?
   - 1.d) To what extent does the derived vegetation vigor relate to recorded soil moisture contents?
2) To what extent does the drainage management, characterized by the drain flows, support land use based on the observed hydrological relations under wet and dry conditions?

1.4. Report outline

First elaborating on the data collection for the study area gives the overview required to secondly present the method executed for each research question, acknowledging the overlap in strategies applied. Thirdly discussing the required processing of the stored data allows to present the properties of the record sets available to work with. The results are then fourthly reported using the sequential format dictated by the research questions. Fifthly, a discussion to put in perspective the performed analysis allows to finally transparently conclude and present recommendations.

2. Data available from the study area

The time series of interest all have a spatial component adjoint to their temporal and thematic characteristics. Therefore prior to presenting the properties of both the onsite and remotely sensed data available, an overview is given of the integration of data collection within the study area.

2.1. The catchment sensor station network

The stream valley is enclosed between two, drought sensitive, sand ridges where excess precipitation can infiltrate (Rozemeijer et al., 2020). Part of this further contributes to the availability of soil moisture in the peat layer of the valley itself (Rozemeijer et al., 2020). Figure 2 presents the characteristics of the catchment showing where data collection, useful for the set research questions, takes place. The sensor locations provide point data to monitor the soil moisture, groundwater levels, surface water levels, and local drain flows. Furthermore, a weather station is in place to collect meteorological data. Precipitation records are not only taken at this station but also four of the combined soil moisture and groundwater measuring locations are equipped with rain meters. For surface water measurements, the sensing equipment is positioned on the upstream side of the associated weir. Drain flow data is however collected downstream if discharging in the Grote Masloot. Finally soil moisture sensors are calibrated to the local soil type. They provide records as a scaled frequency unit, SFU, from 10 to 60 cm in depth every 10 cm.

From the perspective of Waterschap Noorderzijlvest, the sensors allow to get insight into the conditions in the field at real time (Rozemeijer et al. 2020). The latter gives Waterschap Noorderzijlvest the ability to quickly respond to changes in the water system. If the relations between the stakeholders and the influence of their activities on the environment is transparent, the management practices can be tailored to the local situation (Vinkenvleugel, 2019).

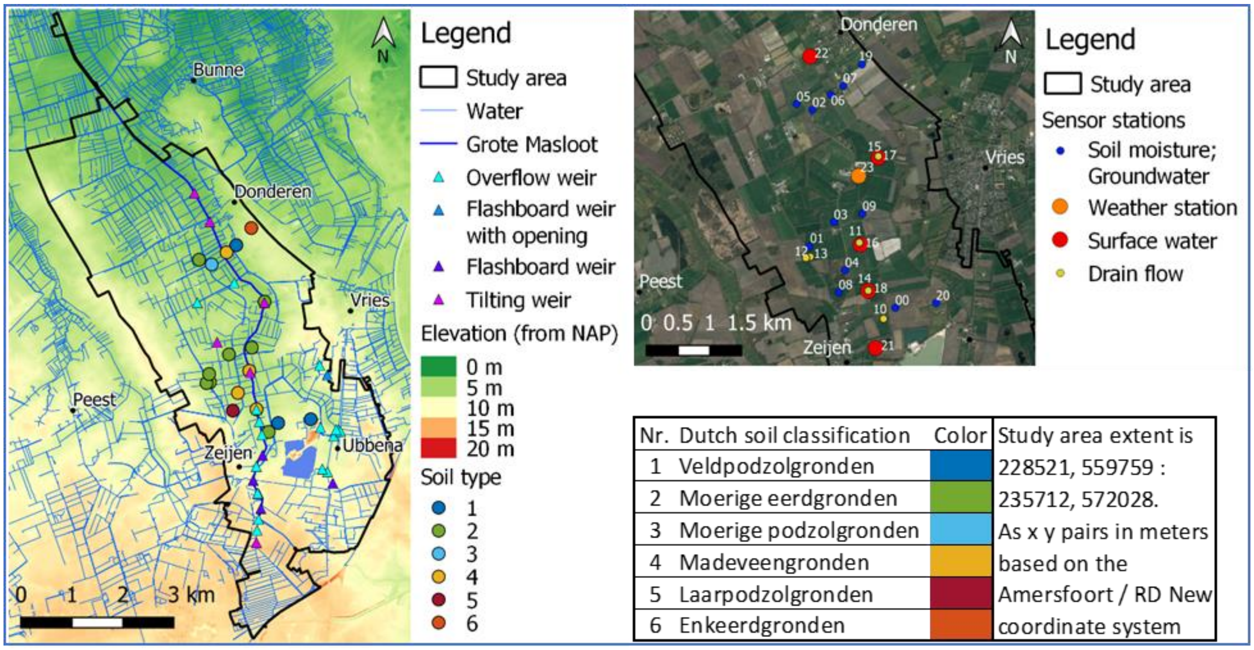

Figure 2: Overview of the study area characteristics and the sensor station network. Elevation data from Actueel Hoogtebestand Nederland (2014-2019), aerial imagery from Bing (2021). Other layers and information are adapted from Waterschap Noorderzijlvest.

2.3. Available records

A distinction can be made between system state and system input record sets. The latter focuses on precipitation, dictating if it is dry or wet, with the former referring to the components of the catchment system in terms of surface and groundwater level alongside soil moisture, drain flow and vegetation vigor. The data is however presented according to its origin due to the influence of the latter for processing.

2.3.1. Onsite collected data

The data from Waterschap Noorderzijlvest is made available in addVANTAGE Pro 6.8 from ADCON. The data can be downloaded as spreadsheets, containing a date time value per record entry, to facilitate analysis based on dedicated data handling tools such as MATLAB. While data collection is ongoing, the files have been retrieved on the 12th of April 2022. The exact monitoring start day in 2018 does vary per sensing location. Table 1 gives an overview of the material available in line with the established research questions, while a detailed per sensor overview of the data collection properties is provided in Appendix 1. Records are intended to be stored in the data base at each 15 minute instance.

Table 1: Onsite collected time series data available.

Sensor type	Nr. of stations	Data of interest collected	Units	Smallest unit	Data collection start period in 2018
Drain flow	6	Volume drained	l	0.1	28 May - 9 July
Weather station	1	Precipitation	mm	0.2	8 February
Surface water	5	Surface water level	m*	0.01	4 July - 9 July
Soil moisture; Groundwater	12	Soil moisture content	SFU**	0.01	6 March - 5 June
		Groundwater level	m***	0.01	6 March - 5 June
		Precipitation****	mm	0.2	6 March - 15 March

* to Amsterdam ordnance datum (NAP) *** with refference to NAP
** Scaled Frequency Unit **** at four locations

2.3.2. Remote sensing data

Vegetation state can be assessed through satellite data provided by the Copernicus Land Monitoring Service, CLMS. The Copernicus open access database from the European Space Agency, ESA, retrievable from (European Space Agency, n.d.-a), allows to browse high resolution satellite images by location, sensing period and mission. The Sentinel-2 mission is most applicable to dispose of optical imagery for monitoring vegetation (Copernicus, n.d.). This mission is composed of two satellite platforms that are in a polar sun synchronous orbit phased 180 degrees from each other (European Space Agency, n.d.-d). Equatorial revisit time is five days (European Space Agency, n.d.-d) and consequently will be slightly shorter for the interest site. However, cloud coverage may increase the interval between usable images.

Both Sentinel-2A and Sentinel-2B platforms are equipped with a MultiSpectral Instrument that passively collects reflected radiation (European Space Agency, n.d.-c). Thirteen spectral bands are available. The pixel resolution differs per band but is 10 meters for band number 4, red, and 8, near infrared, used for NDVI. The data availability period range exceeds the onsite records. Accordingly, the files can be downloaded from the start of April 2018 to the end of March 2022. It is useful that ESA facilitates the download of level-2A imagery directly that has been georeferenced in the WSG 84 geographic coordinate system and geocoded. Level 2 data refers to ground surface reflectance and has undergone radiometric calibration to transform raw digital numbers, level 0, to top of the atmosphere radiances, level 1, followed by atmospheric correction to obtain the level 2 data (European Space Agency, n.d.-b). The third level of data processing into the application product is to be performed using the vegetation index.

3. Method

The used methods are described below for each of the two central research questions defined.

3.1. Investigating hydrological relations

The analysis for the first research question is focused on interpreting time series from individual stations of a single nature and combining those metrics in a dual comparison. In this, it is justifiable to consider local terrain and subsoil characteristics as background conditions. Investigating the hydrological relations requires four analysis strategies based upon what data set types are manipulated as presented in Figure 3. Since each sub-question uses a subset of these methods. They are first defined in terms of applicability to a general metric of interest to then be contextualized for the application to each sub research question.

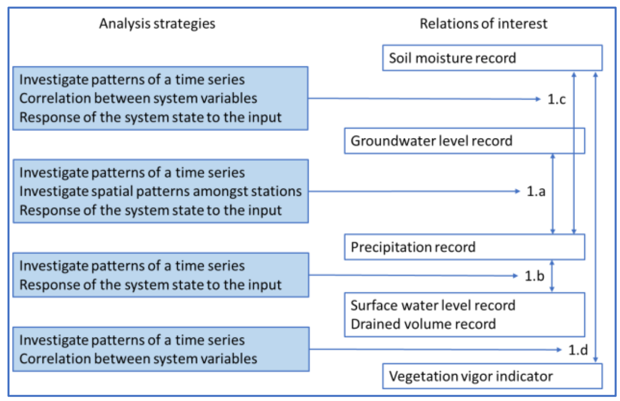

Figure 3: Deducing what data analysis strategies are required for each sub research question

Investigate patterns of a time series

The fundamental input to each sub-question is time series data. Understanding how each single metric changes across time per sensor station offers the basis to place in perspective subsequent relational insights. Accordingly, Pal & Prakash (2017, p.16) prescribe to first investigate series in the context of their internal structure. The target is to sequentially delink the chain portrayed in Figure 4 to separate random and nonrandom components. The nonrandom component, arising from a combination of a general trend alongside seasonality and cyclic movements, allows to understand the patterns in the phenomenon. For cases where the nonrandom element is present, successive entries are not independent (Matalas, 1963).

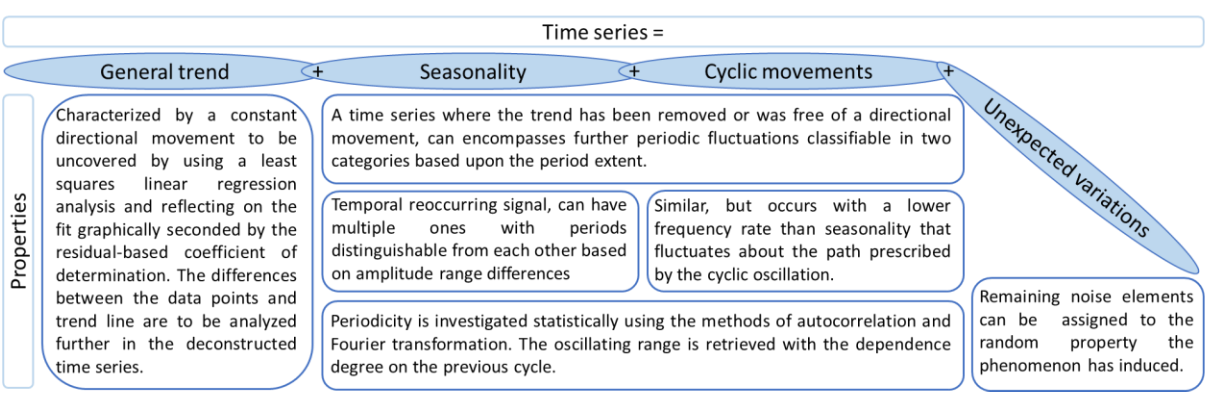

Figure 4: Time series structure, integrating concepts from (Pal & Prakash p. 21-32)

Figure 4 prescribes the initiation of the analysis through extracting the general trend if present. The importance of visual inspection is highlighted due to how the coefficient of determination, to portray the fit of the data points to the generated linear regression, may return a low value while there is directional change. The coefficient of determination as the square of the correlation coefficient between the recorded observations and the linear fit is decremented by seasonality and cyclic movement fluctuation.

To obtain the period of seasonal and cyclic oscillation, in combination with the amplitude and supplemented with the general degree of similarity to the previous cycle, the application of an autocorrelation analysis is complemented by the use of a Fourier transform. To locate the frequency of periodicity, the Fourier transform has first been applied. This mathematical formulation relates a time series to the frequency sampled version of itself (MathWorks, n.d.). The fast Fourier transform algorithm from MATLAB is used for computing. Because the Fourier transform generates both the positive and negative frequencies of matching magnitudes, the absolute value of the transform divided by its length is taken as a factor to scale the vector ranging from one to half the series length (MathWorks, n.d.). This is plotted relative to the frequency domain composed by scaling the vector ranging from zero to half the series length with the factor of the record frequency divided by this length (MathWorks, n.d.). Visually inspecting the figure allows to identify the frequency value of reoccurring signals in combination with the single sided amplitude value of this oscillation. Only peaks that stand out from the surrounding pattern are used. Taking the inverse of the frequency gives the period duration, while the single sided amplitude indicates how much the phenomenon deviates from the mean during the oscillating.

Autocorrelation allows to visualize the recognized periodic cycles because it is a time independent property retuning the dependence of the time series based on its own values (Pal & Prakash, 2017, p.37-38). An autocorrelation series is generated by shifting a duplicate of the time series parallel to itself for a specified lag and then computing the correlation coefficient amongst them (Pal & Prakash, 2017, p.38). Both a positive and negative time shift of up to half the series length is applied using lag intervals of the period between two possible data entries. To find an indication of the correlation strength of a period based on the previous one, the Fourier transform is again applied to the autocorrelation series. The peaks, of which now the frequency position is known, return the amplitude of the autocorrelation sequence for a shift of the lag of interest. This provides an indication of how similar succeeding cycles are.

Investigate spatial patterns amongst stations

To incorporate the spatial dimension of the data collection stations across the study area in understanding how the time series of a single metric type are dependent upon each other throughout space, attention is on spatial autocorrelation. A semivariogram allows to see if there is a relation amongst the readings from the different measuring points despite the space between them. Semivariance, defined as half the mean of the squared difference between the values recorded at both points (esri, n.d.-a) is a practical indicator. The figure of the relation of semivariance to the Euclidean distance between stations allows to visualize how quickly spatial dependence, deteriorates with increasing distance between pair points (Raposo, 2021). The semivariogram allows to interpret the distance range across which the phenomenon is spatially autocorrelated while uncovering potential error, through the nugget, and variance by the sill (Raposo, 2021). The range is the extent after which semivariance no longer appears to increase with distance while the sill is this stabilized semivariance level (esri, n.d.-b). The nugget refers to the vertical axis intercept indicting the error in the data, expecting a fit through the origin (esri, n.d.-b).

Correlation between system variables

In the context of the relational analysis of two metrics assessed per sensor station across time a direct correlation comparison is used. For the series considered in this strategy, it should hold that based on the temporal data collection resolution the record sets are not expected to noticeably be delayed with respect to each other. To compare two time series directly, for each time instant the respective values in the series compared can be plotted as a single pair point in a Cartesian plane. The Pearson correlation coefficient can consequently be used to assess similarity, complementing visual inspection. The Pearson correlation coefficient embodies the direction laden magnitude of the linear relation amongst the two system variables. It is defined as the covariance, measuring the combined variability between the variables in terms of the mean from the product of their difference with respect to the means from their individual series, divided by the product the sample standard deviation of each series (McClave & Sincich, 2018, p. 645). The comparison is performed for the longest range for which both series have records. The mean and standard deviation are computed across available instances per series to be most representative. Direct comparison is only done for instances where both series have an available entry.

Response of the system state to the input

In situations where a system state metric is expected to respond based on a temporal component to the system input, marked by precipitation, an event based analysis approach is used. This is justified by the numerous studies that extract events from time series for analysis (Ares et al., 2020; Black et al., 2021; Talei & Chua, 2012). Events of precipitation and its absence are delineated as described in section 4.1.1.

Firstly, attention is on how long it takes for precipitation to affect the water holding components of the system. Talei & Chua (2012) observe that literature tends to define lag time in terms of the time laps between the centroid of the rainfall event and either the centroid or the peak of the response. The latter option is used. The location of the centroid is identified by the point where preceding and succeeding rain quantity within the events bounds match. The identification of the corresponding peak in the response event of the metric analyzed is less evident following the numerous series to assess. A MATLAB script is therefore used with an implemented heuristic targeted at automatic identification of the response peaks.

Automatic lag time computation uses as input the precipitation events delineated alongside the series where these are derived from. The events centroids are subsequently computed. For each series, it is required to identify which events are included in the temporal range of the data. Locating all mathematical peaks then prompts the need to run through the applicable events to select the peak of the response event. This is possible by defining a tailored search range to select a peak. Two parameters introduced in section 4.1.1 are thereby used. First the minimum dry time parameter between events marks the minimal search range starting from the end of the precipitation series. This free of rain base search scope may be extended until actual precipitation falls. This is done by using the second minimum precipitation quantity cap defined. More precisely the end of the search range is located by systematically running through each instance subsequent to the end of the base search segment and verifying if the set criteria are met to conclude the range. The latter occurs if either the precipitation instance exceeds the smallest precipitation measuring unit of 0.2 mm or, alternatively, if the quantity is 0.2 mm then it is checked if up until now not more rainfall than the minimum precipitation quantity parameter has been included in the search range.

As the search range is defined per event, a peak needs to be selected from those present. This is done based on a ratio of peak magnitude and the distance it is from the centroid. Thereby favoring the close and high peaks in the search segment. The peak that has the maximum ratio is used to compute the lag time by taking the difference between the time of the peak and the instant of the centroid. To then judge if the calculated lag time is representative for the series, two further verification steps are applied. First, it is required to account for missing data in the search range. It was selected to not tolerate missing data entries in the basic search range but to allow five percent in the extended segment. Second, it is necessary to assess if the peak selected is clearly different from the rest of the local series. For this, it was chosen to compare the value of the peak with the mean of the records between the start of the event and centroid time. If the difference is less than twice the measurement error, then the peak is not considered significant. The measurement error is taken as the smallest unit of the sensing equipment.

To evaluate the performance of the MATLAB script that applies the presented criteria, its output is compared with manually delineated lag times. For each data type one time series is manually inspected and the peaks following from the used precipitation events recorded. The fit of the computed lag time to that observed is tested using a pairwise-t approach. This since both lists of records are expected to be correlated stemming from the same time series. The 95 percent confidence interval is used to test for significance. However, such a statistical test only compares those events for which both a peak was observed and one located by the script. As such lag times from peaks not located manually but by the script and the other way around are to be further discussed. If it is found that peaks are satisfactorily automatically located, its output is used after omitting five percent of the extremes to account for the possibility of some unrealistic lag times derived by the proposed method.

Secondly, to address the systems state response to precipitation absence an event based method is also implemented. During times marked as dry, a trend based regression analysis approach is used to study the rate of decline of a system state metric. Because following the method to identify dry events, presented in section 4.1.1, the start of an event is directly located after the end of a precipitation instance, it is to be accounted for how the precipitation may have had a response event. The start of the dry event over which a least squares linear regression can be computed is therefore adjusted using the third quartile of the computed lag times for the metric of interest. This requires reevaluating if the length of the dry event matches the minimum dry time also used here to ensure that the regression analysis can be applied to a period incorporating sufficient records. Finding the slope and associated coefficient of determination gives the basis to study the patterns of the changes in the metrics series in dry conditions.

3.1.1. Response of groundwater level to precipitation

Investigate patterns of a time series; Investigate spatial patterns amongst stations; Response of the system state to the input

This relation is targeted at identifying the responsiveness of groundwater level to precipitation while simultaneously considering how prolonged drought affects the groundwater table. Prior to determining the relation to precipitation through the event based lag time and trend analysis techniques proposed, the patterns in groundwater at each individual station are investigated using the time series data analysis strategy. This aims to reveal to what degree groundwater levels are precipitation dependent and prone to fluctuations. To complement understanding, the spatial interrelation amongst stations is also relevant to see if groundwater levels throughout the catchment depend on another.

3.1.2. Response of drain flow volume and surface water to precipitation

Investigate patterns of a time series; Response of the system state to the input

The predominant focus of this relation is to uncover the duration required for precipitation to be discharged through the surface water. To investigate runoff, the lag times for surface water level and drainage discharge response to precipitation are computed. How these components respond to rainfall absence is addressed in parallel, preceded by seeking to understand how these manageable factors of water level and drain volume are self-dependent. Indeed, drainage infrastructure is a means to locally control the retention and discharge of water supplied by precipitation while the channel network of the surface water allows to let water in or out directly, connecting to the outside of the catchment.

3.1.3. Relation of soil moisture content to groundwater and precipitation

Investigate patterns of a time series; Correlation between system variables; Response of the system state to the input

The contribution of rainfall on soil moisture cannot be studied in isolation from the effect of groundwater, following their combined effect on the soil layer. Hence after addressing the properties of the individual time series of soil moisture at multiple depths, focus is on the continuous gradual processes between the unsaturated soil and saturated ground layers above and below the groundwater table respectively. This relation can be investigated following the direct correlation approach described. Attention is on how the relation of groundwater to soil moisture depends on the depth within the soil where measurements are taken. The individual time series are then thirdly analyzed to see how inclined the soil moisture is to change at varying depths following precipitation absence or presence. For the latter a different procedure to the proposed lag time approach is used because manually studying the soil moisture content time series for multiple depths revealed the instantaneous response at the shallower layers with further, at increasing depths, response peaks becoming unnoticeable instead of shifted along the series.

The relation of the analysis of soil moisture to precipitation occurrence takes the form of an investigation to see if changes in soil moisture are attributable to the rainfall. Hence the difference between each successive soil moisture record is computed. It is then verified if this difference is smaller than zero and if there is precipitation. In cases where at least one of these conditions holds, the soil moisture difference instance is kept, otherwise it is replaced by zero. This is interpretable as considering all soil moisture changes during precipitation events while also including any increases that may not be linked to precipitation but have other causes. Further, this omits natural expected decreases during times of rain absence. Hence, the comparison is established between the precipitation quantity occurring in 15 minutes and the change in soil moisture that takes place in that time instance. The series response to dry periods can proceed as described only systematically using an input lag time of zero to determine over which period the trend is to be computed.

3.1.4. Relation of soil moisture content to vegetation vigor

Investigate patterns of a time series; Correlation between system variables

To investigate this relation, it is foremost necessary to characterize vegetation vigor, further discussed in section 4.1.2, to obtain a time series. The latter would have an entry possibility on a daily time scale. Therefore, the soil moisture series have been sampled up to a daily resolution by averaging over the entries for that duration period. Based on this lower temporal resolution the direct correlation approach is most suited to identify a relationship. This aims to extend the sole water quantity focus to look at the connection with land cover combined with any patterns in the latter.

3.2. Contextualizing agricultural drainage management

Drawing on the relational insights sought for with the method presented in section 3.1, the second central research question targets to contextualize the results in how the system functions. This, framed by the implications of drainage management to support land use in the catchment. According to Pal & Prakash (2017, p.6), time series data is useful to obtain insight into the underlying processes of the system to improve future practices. This is required because increasing concerns arise of how drainage interventions have reformed the hydrological characteristics of catchments (Blann et al., 2009).

Agricultural drainage decisions follow from the targets of the farmer and pressures from society. Hence ways to work with drainage can change with time. Jorjani (1990) proposes an overview of the influences drainage interventions have and how this can adapt through a feedback loop. Attention is thus not on evaluating the drainage system but on systematically discussing the adapted framework proposed in Figure 5 to identify what the observed relations can mean for the perception of local management. Attention is on how the performed analysis is embedded in the understanding of the studied drainage catchment that is managed accordingly. The main conclusions drawn for each of the five data supported system components are presented to two employees of Waterschap Noorderzijlvest, with backgrounds in integral water management and groundwater hydrology, for a discussion on their derivation and implications in context. Figure 5 is generated by adapting the framework published by Jorjani (1990) using supplementary insights from Oosterbaan (1994) to obtain a version that focuses on the hydrological segment of the physical drainage effects while acknowledging the social component in management.

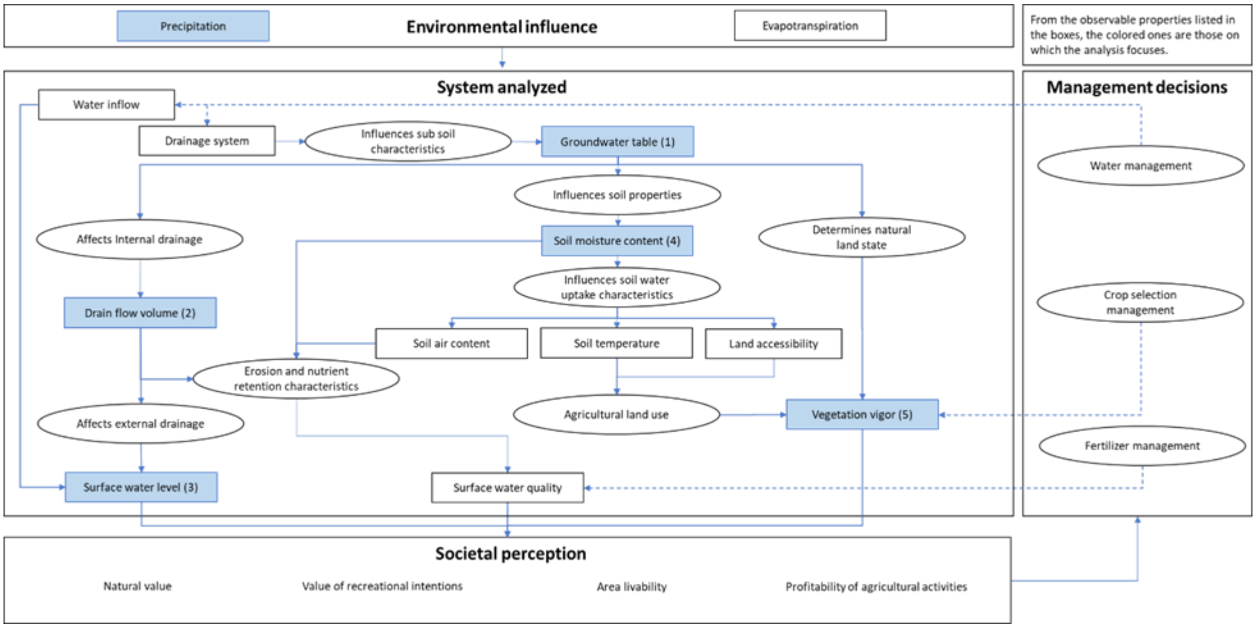

Figure 5: Framework of drainage influence on the studied catchment, adapted from Jorjani (1990) using Oosterbaan (1994)

The presented figure is not exhaustive and restricted in terms of what the analyzed relations and overall system data collection encompasses. It takes drainage schemes as to promote the use of agricultural land by supporting the opportunity of crops with higher value and succession at a reduced cost in land prone to waterlogging (Oosterbaan, 1994). Indeed, drainage leads to drier soil conditions by lowering the groundwater table, discharging the water from the system (Oosterbaan, 1994). This is intended to benefit soil aeration, structure and increased water storage capacity to reduce direct runoff from precipitation. Further, specifically this tries to favorize early crop production while enhancing land accessibility in combination with diversified crop opportunities (Oosterbaan, 1994). Nevertheless, it is required to be careful of how the disruption of the natural environment state engages damage to nature, facilitating drought and biological oxidation (Oosterbaan, 1994). Natural ecosystems are transformed through reduced surface water storage and enhanced discharges (Blann et al., 2009).

4. Processing data available for the analysis

To provide context for the generated results, the findings from the preliminary data are presented by first describing the strategy used to prepare the data to then report on the resulting data sets obtained.

4.1. Data preparation

The onsite collected data is provided as it is stored in the data base. Cleaning is required associated to subsequent manipulation to obtain inputs for the analysis. Further, the complementary remote sensing imagery needs to be processed to compute the vegetation index and generate a time series.

4.1.1 Onsite collected records

Executing presented strategies requires universal comparable files screened for faulty entries. To use precipitation records in a lag time analysis at stations where rainfall has not specifically been measured, an assessment of a series representativeness prepares for the further subdivision into events.

Reformatting retrieved data

The provided data files are expected to have entries for every date-time instance with 15-minute intervals. Nevertheless, several inconsistencies are present. To ensure a predictable universal format of the data files, reformatting is required. Using the start and end dates, all expected time instances have been generated and an identifier feature computed by sequentially concatenating the year up to the minutes into one number. This facilitates matching the available records that had a time instance corresponding to one of those expected with the reformatted data set. This ensures that there are no missing date-time entries while omitting doubtful records that have not been stored at the expected intervals. Absent data is marked as not-a-number, NaN. The reformatted files with their identifier to record combination are used in analysis, facilitating comparison amongst series of different time index positions.

System state data record validity

To identify when the unprocessed reformatted data has features that can be attributed to abnormal sensing conditions, either the patterns observed in the series examined can be used individually or in combination with comparable records collected at the same location. Because measurements of drainage volume alongside surface and groundwater levels are taken in isolation at the dedicated stations, the first option can only apply. Accordingly, soil moisture data can be screened using the dual approach.

For surface and groundwater level alongside drainage volume, the strategy used to locate outliers is based on the series rate of change. Attention is thereby on sudden jumps in the records rather than filtering based on a limit range of extremes. This strategy expects that to some degree records are dependent upon each other. Using the assumption that if a computed slope occurs frequently then it is characteristic for the time series, allows to identify a subset of date-time instances for visual inspection. Rates of change have thus been computed between each available entry. To facilitate further assessment, accounting for non-exact duplication of slope values, the frequency of occurrence is retrieved for predefined classes. The latter have been determined uniquely per series to accommodate for the number of available instances in determining the number of classes, with the basic initial rule of taking the square root of the count, used to select the class intervals following the available range of record values. Defining categories is done separately for positive and negative slopes to account for how a phenomenon may have the tendency to increase and decrease at different rates. A limit for extreme slopes is subsequently determined by applying the mentioned assumption in terms of selecting the last category that has an attributed frequency exceeding one. These positions of extreme slopes are marked in a plot of the data for visual feedback, allowing for a manual delineation of the range of untrustworthy data followed by replacement by not-a-number entries if appropriate. Because classes are not refined, it should be acknowledged that classification has influence on patterns it reveals. Hence, if a lot of outliers are perceived amongst the values extracted for visual inspection, the search range should be extended.

Soil moisture is recorded at multiple depths thereby yielding six time series at a single location that are expected to be related. Consequently, while applying the above presented slope based evaluation strategy a combined plot of all soil moisture data at the sensing location should be consulted as well. This gives background perspective for potential malfunctioning of sensing equipment for specific depths.

System input data record representativeness

The event based lag time assessment described in section 3.1 requires precipitation data to be compared to the records from all stations. Because at most stations there is no rainfall data, a single precipitation series that is representative of the study area allows for the most efficient analysis. Due to the central position the weather station, alongside its series record consistency, this data is most appropriate to serve as a reference point. Since the other four locations with rainfall data are providing good coverage of the study area, these are used to identify instances in the weather station data that are not representative.

Two rules have been applied to filter for non representative records between the range of the first and last common instance identifier of the five series available. Firstly, each record of the time series generated by the weather station was compared directly to each of the other series. If there was not one of those four record instances that matched the weather station in a range of 0.2 mm, it was selected as potentially non representative. The margin of 0.2 mm is tolerated since this is the smallest measurement unit for precipitation. Secondly, from those potential instances identified, a further selection was made based upon if the four series the weather station data is compared to overall show that it has rained or not. To acknowledge that not all series may have a record at the considered date-time instance the ratios of the number of dry and non dry records to the number of available records for the four series at each date-time instance is computed. If the dry based ratio exceeds the non dry it is taken that it was dry, while otherwise it is assumed that it rained. This is then compared to if the weather station showed that it rained or not. If the records do not match, they will not be kept in the representative series generated.

System input data event selection

Based on the representative precipitation time series from the weather station, events have been delineated. This is done by using a time increment to run through each instance of the series. The strategy incorporates a minimum precipitation quantity alongside dry time between events that are tailored to the local situation following the observed records. It is assumed that events occur randomly and thus reoccurrence is not self dependent.

The iterative computation is initiated by searching for the first precipitation instance. Having this selected, the consecutive hour in the time series is taken for assessment. If the accumulated rainfall quantity is smaller than or equivalent to the set limit, then the search for the next precipitation instance is renewed based on the current time step. On the other hand, if the rainfall in this succeeding hour exceeds the cap, the start instance of an event is found. Further incrementing the time step enables to locate the end of the now initiated event using the same procedure of considering the consecutive hour to the current time step. As the volume of precipitation over the subsequent hour to the current time step no longer exceeds the set limit, the event is closed. A new possible event initiating instance is then again located by continuing to skim through the time series from the end of the last hour used to evaluate that the preceding event ended. Missing data entries are treated as if no precipitation had fallen. However, events that incorporate such an empty instance have been removed in post processing of the obtained output.

Regarding the limit of the minimum precipitation quantity to be accepted over the combination of the evaluated instance and the subsequent one hour, an assessment of the number of identified events at limit values of increasing magnitude is performed. Considering the decrease in the number of located events based on increasing the cap allows to identify at what value an apparent stabilization in decrease rate is observed. As the decrease rate stabilizes, and increasing the cap leads to a similar reduction in events each time it is incremented, this suggests a suitable limit is found.

With the final minimum precipitation quantity cap implemented, the proposed procedure offers a preliminary way to accommodate for possible instances of no precipitation in an event. The one hour evaluation range, as a start to group precipitation instances, is expected to be inferior to the minimum dry time to be set. To justifiably find this minimum, the time between events is computed. Based on this, a logic matrix is generated to verify if this difference exceeds a set time, ranging from zero up to two days, using 15 minute intervals. Counting the frequency that each set separation is exceeded by that observed between successive events allows to determine the number of events that would be additionally grouped as the dry time is increased. To nuance the computation an hourly aggregation is used to determine how many events would additionally be merged if the minimum dry time limit is increased by one hour. At the point where the additional joining rate stabilizes the minimum dry time is selected. Correcting the event set found based upon the minimum dry time identified by joining those within the range yields the final set used in lag analysis.

Instead of using the times between precipitation events as dry times, a more representative approach is sought since the latter yields events disturbed by unselected precipitation and missing entries. Hence, an alternative approach is used that fundamentally functions the same as the precipitation event locating strategy but applies criteria tailored to selecting consecutive dry instances. The parameters of minimum dry time and precipitation cap found are reused in this analysis. Running though the time series, the first dry instance is selected. An evaluation is made of this instance and those in the subsequent half hour. If one of these is zero, this allows to initiate a dry event. This same evaluation is made for each consecutive instance, following the starting point, to decide if it is to be included in the dry event. This continues until the current and two subsequent instances are all non zero. Two conditional criteria are then applied to this possible dry event delineated. First it is evaluated if its length exceeds the minimum dry time. If this criterion is met, secondly, the sum of the values is found for each group of consecutive instances spanning over the minimum dry time in the potential dry event. The latter is evaluated on if it is inferior to the minimum precipitation cap. If both criteria are successfully passed, the dry event is stored while otherwise being discarded. The search for the next dry instance starts again to resume the iterative loop described. It should be noted that the dry events located in this way can not directly be used in further analysis. Indeed, before proceeding the typical lag time for the series evaluated should be taken into consideration.

4.1.2 Remote sensing records

A vegetation index as a model of biophysical characteristics of vegetation, based on radiometric remote sensing data (Jensen, 2007, p. 382), appears a justifiable and practical choice to characterize vegetation vigor. In terms of its dimensionless quantity, a vegetation index aims to maximize its sensitivity to a biophysical parameter it is linked to while simultaneously normalizing both internal and external effects related to the remote sensing approach and on ground phenomena respectively (Jensen, 2007, p. 382).

NDVI computation is based on the ground surface radiation reflectance from both the near infrared and red bands. The ratio is specifically related to the biophysical parameters of biomass and leaf area index, LAI, (Jensen, 2007, p. 383). The advantages of using NDVI include the possibility to analyze seasonal development in vegetation related to crop calendars while minimizing several multiplicative noise factors of concern such as illumination (Jensen, 2007, p. 386). Furthermore, although there is the possibility of NDVI being saturated at high biomass and LAI (Jensen, 2007, p. 386), NDVI may prove to be adequately responsive to the range in the Netherlands. The indicator is sensitive to the visibility of soil amongst the vegetation alongside additive effects related to non-reflective surfaces (Jensen, 2007, p. 386).

Before proceeding with generating a vegetation state time series, the data tiles available are processed to manageable file sizes. To identify suitable images in the period of interest, the quick view option provided by ESA in the access interface to their data base allows to make a judgement if the study area is not cloud covered. Suitable images have been downloaded. The provided files contain all image information for further manipulation in the SNAP desktop application. To make the images more manageable, all bands have been resampled to the lowest 10 m resolution characteristics of the bands of interest. Furthermore, computing a raster subset allows to select all 13 bands while restricting the extent to the study area, obtaining files of reasonable size. This product has been exported and saved as a GeoTIFF to later, if required, interpret the land cover based on a red green blue, RGB, composite.

The thematic land processing tool in SNAP is used for the computation of NDVI across the file. The NDVI is calculated by dividing the difference between near infrared and red band by its sum (Jensen, 2007, p. 385). The output image has been imported into MATLAB to, based on the image coordinates, extract the NDVI value at the locations where soil moisture data is collected. For improved acceptability of the NDVI value selected at a particular location in time, the 8 surrounding pixels are also chosen and an average taken. Associating this with the date of image capture yields the desired time series for each soil moisture station. Because entries are available at irregular days, the series have been reformatted as described in section 4.1.1 but with the expectation to have an entry for each day.

4.2. Data presentation

Following the data preparation processing presented, an overview is given of the inputs thereby available to initiate the targeted analysis.

4.2.1. Onsite collected data presentation

Overall, it appears that the sensing equipment has been operating as expected. However, for each data type, specific instances of likely equipment malfunction have been identified. Appendix 2 provides a full overview of the data used and potential reasons for the omission of sections. Attention has been focused on removing entries that are not supported by the data sequence itself.

Groundwater records

The collected groundwater level measurements are generally following steady patterns with only a few missing entries. Inconsistencies in the data that have been selected to be left out are all located in between instances of missing data, reinforcing the idea that these have been due to equipment malfunction. Three stations are further to be elaborated on due to their atypical time series. The data from the A723_865207 station features two distinct segments separated by a short period of missing records. Indeed, on the 16th of March 2020, prior to 12:00 the data fluctuates between 2.21 to 2.44 meters above NAP while after 16:15 a new period is initiated where the measurement range lies from 3.14 to 5.27 meters. Both segments appear readily plausible and consequently used in further computations where appropriate. Since both the level average and fluctuating range change, it appears unlikely that the change has to do directly with measurement equipment placement such as the height of the probe in the gauging tube. It would be interesting to have information about the local changes during the period.

Stations A723_865219 and A723_865220 both have a lower data collection limit with values of 3.51 and 6.2 meters above NAP respectively. When the water level goes below these, no records are available anymore. While the times of low groundwater levels have been left in the series since the records available above the presented limits are likely to be valid, interpretation should account for that there is a deficiency of data for the lowest range of groundwater tables due to the sensor positioning.

Surface water and drainage volume records

Surface water is recorded as expected. Some short equipment failures lead to few missing entries without hampering the potential of pattern recognition. A single invalid entry is removed in the A753_865222 station that features outside of the series minimum range while located in a period of data absence.

In terms of the drainage volume records, only the data from station A723_865215 supports the omission of an abnormal period. Nevertheless, while all other data has thus remained in the analysis, it is evident that recorded drain flow characteristics are frequently exceeding plausible maximum values. A generalized estimate of the drain flow capacity for the case of a gravity drained single walled pipe with the diameter of 5 cm is 300 to 800 liters in 15 minutes using information from Prinsco & University of Minnesota (2022). This is opposed to the maximum observed volumes ranging from 162440 liters in 15 minutes for station A723_865213 to 794140 liters at station A723_865211. It only appears that the base drainage flows are inside the estimated range. This leads to the unclear situation of observation reliability in the frame of the difficulty to make realistic estimates acknowledging how according to Prinsco & University of Minnesota (2022) pipe type and installation slope have a large effect on drainage volume.

Because the analysis to address the research questions makes use of all drainage data, except specified, it is important to understand what may be physically problematic with the records based on the used acquisition technique. Figure 6 gives an overview of the used set up. The drain water collected flows into the bucket where the water level is measured. Based on the buckets dimensions and specifications of the outlet this enables to compute outflow volume. An onsite visit revealed

Figure 6: States of the bucket used to measure drain flow. From left to right; as expected, outlet blocked, inundated

how the buckets were rather filthy. While cleaning them does result in the water level reaching a comparable state to the pre intervention condition, obstruction or dirt accumulation on the triangular shaped outlet is of concern. An alternative issue arises from the possibility of the equipment being flooded by the surface water body it discharges in.

Soil moisture content records

Few of these sensor locations are fully free of apparent problems. Often, several of the depths measured at a location feature inconsistencies. The latter can be reduced to three distinct, unacceptable, entry types aside from already missing records arising from integral sensor failure. Firstly, instantaneous drops to zero are indicative of individual sensor component fall out at a specific depth. In a couple of cases the drop is however not direct but gradual. The A723_865200 stations 40 cm depth alongside the 20 cm depth of the A723_865209 sensor features this characteristic. In such instances it would be expected that at least the top surface layer of soil, represented by the 10 cm depth, would fully dry out as well. Nevertheless, this does not occur. None of the other depths at the locations specified support the extreme decrease in soil moisture. Secondly, there are also reoccurring components of the time series that go suddenly to values around double those in the standard range. Specifically, the single depth abrupt increases are likely errors. It is observed that the A723_865200 station features a case where all depths unanimously increase to a higher level. The two series segments are separated by a period of missing data entries. Since the fluctuating range matches the interval of the rest of the series this could be indicative that there is a change to the sensor itself. The omission of this period is justifiable because of the incomparability of the last segment between 30 September 2021 and 12 April 2022. In all other cases, usually one depth is concerned with the exceptional two depths at once. Thirdly, a problem reoccurring only for the A723_865207 and 09 stations is that a single measurement from a 15 minute instance features a sudden drop to a lower value, sometimes even zero, compared to adjacent entries in the series. These have each been individually removed to conserve the patterns present in the record range.

Precipitation records

Comparing the precipitation time series available for the study area allows to enhance the representativeness of the weather station data. Subsequent gained understanding of the generated time series allowed to effectively decompose the data into events of the system input.

Representativeness of the records from the weather station is improved

The time range over which records are available from the five locations spans from the 15^{th} of March 2018 to the 12^{th} of April 2022. Some interruptions do occur in the data over this range. The precipitation time series have been compared both visually and numerically using a cumulative precipitation plot and correlation coefficient respectively, as shown in Appendix 3. In the first instance the centrally located weather station appears to poorly correlate with each of the surrounding stations. The cumulative plot generated by only using identifier instances where records are available from each series, reveals that the stations A723_865205 and 09 are the only ones that do not feature a sharp increase at a certain point in time. Those increases are not representative for the study areas rainfall but merely a local intensification of precipitation brought onto the collecting device. The proposed two phase method filtered out 124 records from the weather station series. From all edited records, only 52 exceed the magnitude of 1 mm with extremes attaining 38.6 mm of precipitation in 15 minutes when no other station collected any.

Precipitation is not self dependent

The characteristics of the generated representative series are revealed by applying the strategy to decompose a time series from Figure 4. As expected it does not incorporate a trend based on the regression analysis. Further, assessing periodicity with the Fourier transform plot generated does not yield any distinct peaks out of the noisy fluctuation range. As such, the fundamental assumption used in the methodology proposed to identified precipitation events is thus justified.

Events of precipitation occurrence characterize wet conditions

Testing the influence of the minimum precipitation cap parameter, introduced in section 4.1.1, allows to conclude that a limit of 1 mm is most sensible. Furthermore, the minimum dry time can similarly be set to 6 hours. Two figures are presented in Appendix 4 that support this decision. Using the presented parameter combination in the proposed method, yields 316 events from the representative precipitation series that can be used in lag time analysis if the time series to which these are applied has data records at that time. Throughout the time period of the representative precipitation series, each month has been allocated 16 to 37 events with no apparent pattern in the distribution.

The properties of the selected events are diverse. The precipitation total, duration and maximum instance are variable across events with coefficients of variation being 1.1, 0.93, and 1.1 respectively. This indicates that the standard deviation, taking the event set as a sample of the population, is almost equivalent to the mean. Because for each of these three characteristics of precipitation events, the mean exceeds the median that is in turn larger than the mode, it can be concluded that the events feature a positively skewed distribution. The events are thus best described by a median value of the characteristic assessed.

To understand if intensity as a metric combining the variables of volume and duration is appropriate to represent the properties of precipitation events, the correlation amongst these variables is computed. A Pearson coefficient of 0.727 is retuned, supporting the visually perceivable relation. Consequently the histogram in Figure 7 presents the distribution of intensity which allows to note that despite the variation in the plot the extremes are rarely reoccurring. To recognize how intensity varies throughout the year the scatter plot demonstrates that intensity tends to be highest and most variable during summer with a peak at July. Further while the minimum intensities found per month are stable, the maximums exceed the median strongly throughout the non winter months insinuating the reoccurrence of more extreme events.

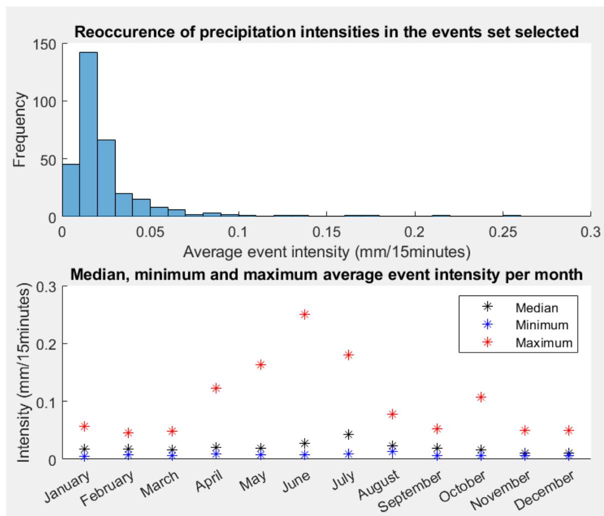

Figure 7: Presenting the frequency of event reoccurrence per intensity value followed by a decomposition of the median values on a monthly basis.

Events of precipitation absence characterize dry conditions

The proposed strategy to delineate times with little precipitation yields 229 periods. Located events range from just 7 hours to 23 days. Most events selected feature a duration smaller than 3 days with only 79 events exceeding this period. Before interpreting an analysis based on this event set it is foremost necessary to verify if there is a correlation between the duration and computed trend. An overview of the same properties of the dry periods as presented previously for the precipitation events but in terms of duration is featured in Appendix 5. Not all these events will be used in the related regression based analysis because their length needs to be further restricted following the found precipitation lag times.

4.2.2. Remote sensing data presentation

From the beginning of April 2018 to the end of March 2022 there are 102 cloudless images in the Copernicus open access data base from the European Space Agency (n.d.-a). In the four year period, each month has variably 4 to 10 files available with March and April excelling with 15 and 16 images respectively. Extracting the NDVI values, to characterize this system state variable of vegetation vigor, for each soil moisture station location allows to compose the series presented in Appendix 6 of which the properties are shown Figure 8. Stations A723_865200, 07 and 20 have lower NDVI values with there not being an apparent link to elevation while there seems a connection to soil type. The fields with those sensor stations are used for growing crops and thus plowed. All other stations are in grassland pastures apart from station A723_865204 that features in an area with deciduous trees. The standard deviation per location ranges around 0.15 with the exception for the two highest elevated stations that tend more to a value of 0.25. The latter two are located in the same parcel.

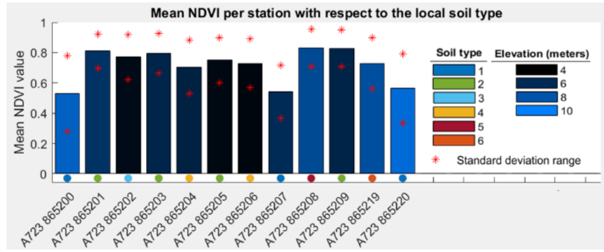

Figure 8: Overview of the mean NDVI, per soi moisture content data collection station, put in perspective by local soil type and elevation from NAP

5. Results

Applying the prepared data in the analysis allows to generate the results for the first component specific central research question that in turn founds the overall catchment perspective taken in the second.

5.1. Investigation of hydrological relations

Empirically analyzing the collected onsite water quantity time series alongside the processed remote sensing imagery for the locations of the sensing stations allows to interpret each relation of interest.

5.1.1. Response of groundwater level to precipitation

Describing the properties of the groundwater time series for each and amongst stations sets the context to discuss the subsequent influence of rainfall.

Groundwater time series characteristics

Groundwater records feature a positive trend

Initiating the individual time series decomposition by studying the linear trends, Figure 9 puts into perspective the observed tendencies from each series. While the coefficient of determination has been found, these statistics ranging from 0.08 to 0.44 and concentrated around 0.25 can not provide support for the regressions due to the seasonal fluctuations present. Only trends have been shown that are also visually apparent in the time series. Indeed, station A723_865207, due to its composite nature does not feature the gradual increases marked by all others. For the stations that have missing minimum records, the absent entries from A723_865220 do not hide the pattern while this is not so for station A723_865219. Elevation nor soil type influence trend magnitude while potentially being explained by dryer conditions marked by the precipitation time series for 2018 and 2019. Stations in proximity do not necessarily feature comparable values. The temporal extent of about 4 years limits interpretations to observations.

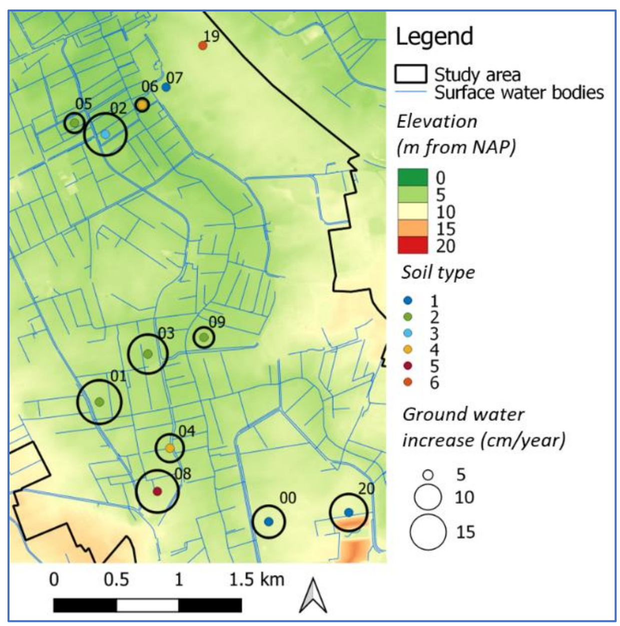

Figure 9: Trends in groundwater over the data collection period placed in perspective by ground elevation and soil type. Using layers from Actueel Hoogtebestand Nederland (2014–2019) and those provided by Waterschap Noorderzijlvest.

The amplitude of yearly groundwater level fluctuation changes with land elevation in the catchment

To proceed with the understanding of the seasonality and cyclic movements, eliminating the trend from the time series where it is apparently present, the Fourier transform based analysis consistently uncovers a yearly and a daily pattern. Appendix 7 presents an example of the plots used for determining this. The fluctuation frequency value returned is consistently indicative of these periods across all stations with the exception of A723_865207 for the daily component. As foreseen, the A723_865207 station also features a periodicity of two years due to the two distinct data segments. While the annual cyclicity would be expected, it is rather surprising to also locate the daily seasonality. Indeed, while the measurement frequency can adequately support such an oscillating pattern, the magnitude of the single sided amplitude is smaller than the minimum measuring unit for all stations expect A723_865200. This conclusion on the insignificance of the daily pattern is further highlighted by how the increase in correlation coefficient in the autocorrelation plot tends to be extremely small on the daily basis.

While the single sided amplitudes of the yearly cycles appear elevation related, this is not so for soil type. Consulting the station locations on the elevation map also in combination with Figure 10 allows to identify that those stations located at higher elevation are also further from the Grote Masloot. These two properties thus coincide with the higher differences in groundwater level in the yearly cycle. This may hint at the importance of the surface water body located at the lower elevated part of the catchment, with its potential to bring water into the system alongside discharging it, to stabilize the groundwater.

The autocorrelation analysis revealed how annual groundwater levels are related to the previous years, mostly yielding correlation coefficients exceeding 0.5. The low values for A723_865203 and 07 are explained by numerous missing entries and the dual level of the series respectively. A723_865202 has a rather atypical low groundwater level in the summer of 2018 which, shifted though the rest of the series, decrements the correlation. Station A723_865205 has a wider fluctuation range between the summer and winter time for 2018 and 2019 then in the rest of the series. Overall, the moderate correlation found, while supporting the cyclic pattern, demonstrates that there is an impact on groundwater from factors that do not follow similar patterns. The precipitation component will further be investigated accordingly.

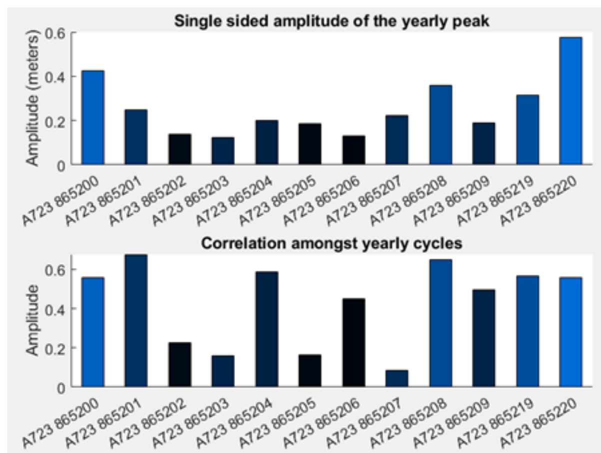

Figure 10 Amplitudes of the fluctuations attributable to yearly cycles, complemented by the correlation strength amongst them indicated by the amplitude of the autocorrelation series on those oscillating frequencies.

Relation amongst groundwater stations

Having presented how the observed groundwater measurements and patterns differs between the stations, the spatial dependence of the local measuring points is revealed by studying the semivariogram presented in Figure 11. A function is not fitted to the data because with the limited distance ranges in the study area the stabilization of semivariance is not observable. The scatter plot allows to perceive the pattern in spatial autocorrelation amongst the available sample points, indicating to what degree the time series become dissimilar as the distance between their collection location is increased.

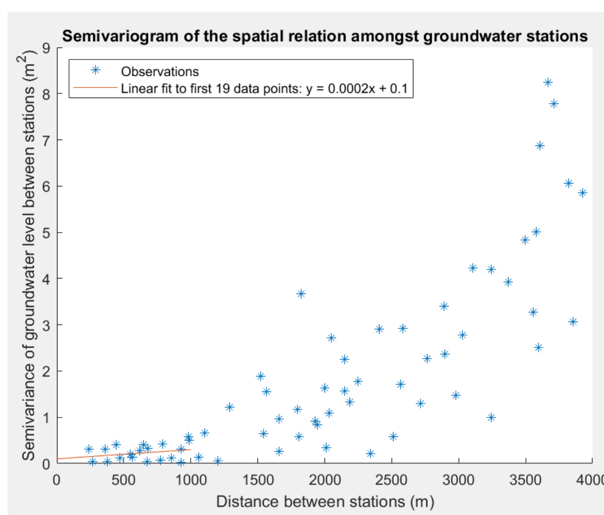

Figure 11: Spatial groundwater dependence amongst stations

Groundwater levels are spatially autocorrelated

Because the semivariance does not level out, no sill or range can be fully interpreted. For the latter however it can be stated that within the distance ranges found in the study area, the groundwater levels are spatially autocorrelated, with closer stations presenting time series that are more similar. As such the groundwater level at one point is dependent upon the tables figuring in the surrounding area allowing to interpolate a groundwater surface. Using the Spearman ranking coefficient, not expecting a linear relation, finds a correlation of 0.86. Thereby it can be concluded that the station spacing ranges presented are a good basis for any modeling of groundwater in between the measurement locations, can the appropriate interpolation parameters be retrieved.

Variability of groundwater table amongst stations is large

The nugget can be expected to have a semivariance value of about 0.1 m^2 based on the regression fit to the plot points that has a close to horizontal slope. As such there is still quite a large error relative to the magnitude of the groundwater level fluctuations. Therefore, the difference in groundwater level found between stations is not entirely explained by the distance amongst them based on the observed tendence of groundwater to spatially vary in the study area. Up to one kilometer, the semivariance oscillates around the same range. This indicates that up to this distance the data sets from the stations are similar to an equivalent degree. While there is no sill, to estimate the increase in variance of the data with distance amongst data collection points, the semivariance does rapidly inflate. This indicates that with increasing distance the similarity amongst the two stations compared differs at increasing rates. As such while the groundwater levels at the stations are correlated, the differences in their time series are not necessarily consistent with other station pairs located at comparable distances from each other. This potentially suggests the need to further investigate the directional component of the relation between two stations in terms of catchment characteristics.

Response of groundwater to precipitation

Automatic lag time computation is applicable

Manual delineation of lag time, to evaluate the performance of the implemented strategy to locate peaks in MATLAB, is executed using station A723_865200. The selection of peaks is rather straightforward with increasing groundwater level followed by stabilization or decreases, depending on the antecedent conditions, as a response to a precipitation event. However for a few cases where as the precipitation occurs there is groundwater decline, peak identification is not evident. In these situations it is not clear where the peak is because the decline coinciding with the occurrence of the precipitation event is followed by later reestablishment of the level that fits in the general pattern. After having selected the peaks, a new visual inspection was made of these cases to see how the automatic selection would perform. It was observed that the script tends to select the stabilizing instant as the level of the overall groundwater pattern is picked up again. Appendix 8 provides an example of the lag time derivation.

Statistically assessing the correspondence between the lag times recorded both manually and automatically yields a 95 percentage confidence interval ranging from -7.02 to 0.38 number of 15 minute instances. This includes zero and therefore supports the conclusion that the difference between the two series is not significant. Hence, the computed lag times suitably represent those observed. It can further be noted that because the low bound exceeds the high bound in magnitude, the manual lag time delineation has the tendency to yield lower results than the MATLAB script based on the order of computation. Addressing those lag time records for the events that do not have an entry in both series, peaks found automatically that were judged insignificant occur 10 times with there not being a pattern of including events with a particular lag time. One instance is excessively too large for the realistic data lag time set. This emphasizes the need to indeed omit 5% of the lag time extremes. Further, also only 10 peaks manually found are omitted by the automatic delineation with these predominantly featuring a tendency to omit short response times.

Lag time of groundwater level to precipitation occurrence is dependent on local conditions

Computed lag times are variable for each station and amongst them. Despite this, there is no correlation between lag time and precipitation intensity suggesting that the event type does not influence the time of groundwater response. The variation in lag time is thus to be attributed to the antecedent conditions of the system. With the median per station, which following Appendix 10 is a reasonable representation, allows to see in Figure 12 that soil types in which multiple stations figure also feature a similar lag time range.

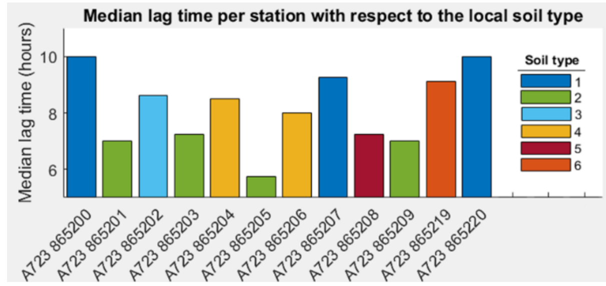

Figure 12: Median lag time as a response to a precipitation event for each of the groundwater stations put in perspective by the soil type.

Because groundwater fluctuates on a yearly basis while the precipitation series does not, it is possible that the lag time also features this periodicity if influenced by the level of the groundwater. Regrouping the lag times of events that had the centroid in the same month allows to deduce that the time of the year does not influence lag time. However, as suggested by Figure 13, there is a pattern showing that lag time per station is similar to the previous or successive month for winter but not during summer. This indicates how winter local conditions contribute to a more stable response to precipitation with less predictability in summer. Preluding to section 5.1.3 this can follow from the more saturated state of the soil in winter.

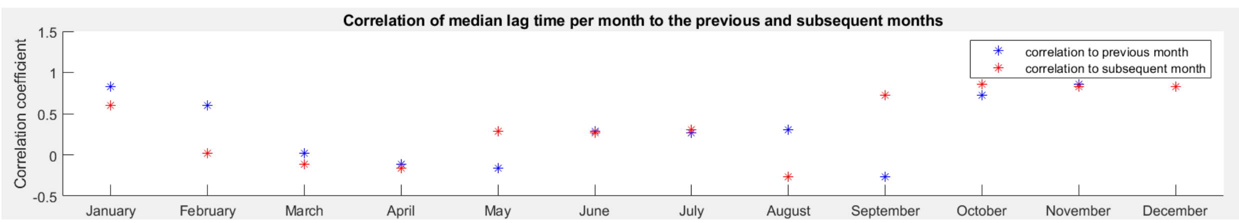

Figure 13: Correlation of median groundwater lag time per month across all stations to the previous and subsequent months.

Rate of change of groundwater during precipitation absence is linear but variable per event

For the response of the groundwater in dry conditions, the trends are overall well supported by high coefficients of determination. Appendix 9 offers a visualized example of the approach. Further, as presented in Appendix 10, the median characterizes the wide range of gradients computed. Groundwater change rates and the duration of event are not correlated. Figure 14 portrays the outcome per station. While the values of the stations A723_865207 and 19 are zero this outcome appears unrealistic but explainable following the limitations of these series discussed in section 4.2.1.

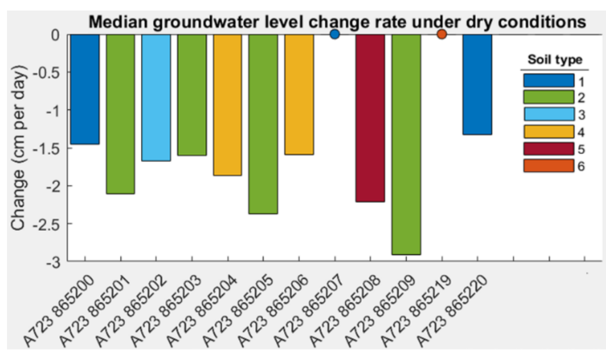

Figure 14: Median rate of change of groundwater level per station under conditions of precipitation absence.

5.1.2. Response of drain flow volume and surface water level to precipitation

Following from the discussed groundwater storage, the components that discharges water from the local system are further addressed. While the drainage infrastructure collects excess soil moisture from the land to discharge it into the surface water bodies, the latter do maintain the water in the catchment while facilitating its movement downstream. It is to be kept in mind how the surface water level can be supplemented by letting water into the catchment at the upstream end of the Grote Masloot. First the individual time series properties are again discussed prior to addressing the response to precipitation.

Surface water time series characteristics

All but one surface water time series do not feature a directional trend

In decomposing the surface water time series for each station, none but one location showed to more constantly fluctuate around the series mean when detrended, based on the linear regression computed for that series, than prior to removing the trend. As such only station A723_865218 can be designated as featuring a mean annual increase of 1.85 cm over the data collection period with all other stations already centered around a neutral level. Visually inspecting the record series indeed confirms that the base level from which peaks occur in the water level record series of A723_865218 is increasing. This is additionally seconded by the 0.42 coefficient of determination that adequately supports the regression fit, considering how numerous water level increases are apparent from the base line range. Indeed, with surface water being regulated in the area it can be expected that any deviations occur from this base line. The A723_865218 location is the second measuring point in the Grote Masloot taken from upstream. The weir at which it is located is itself just an overpass weir and so is not likely that the increase is intentional through direct regulatory procedures at the location.

Surface water level only changes minimally based on a yearly cycle

The Fourier based transform analysis reveals that each measuring location features a yearly cyclicity in water levels. The single sided amplitude of this fluctuation about the mean ranges from 1 to 4 cm leading to the conclusion of this being negligible based on that the smallest measuring unit is 1 cm. Computing the autocorrelation series for the surface water levels for each station further reveals that as expected the similarity between the successive years is not existent, yielding correlation coefficients from 0.08 to 0.2. Therefore, the time series is dominated by the event based deviations from the water level that local water management seeks to conserve.

Drain flow time series characteristics

Drain flow volumes do not feature a directional trend

With the drain flow volumes departing from the base line of no drainage, no trend is recognized. It is observed though that especially in the more recent years of 2021 and first few months of 2022 the base discharge values are more elevated than previously. This is especially the case for the A723_865210 location. However, this property is likely attributable to the meteorological conditions reported by the precipitation series. Indeed, the discussed period does have a tendency to portray more rainfall than previous years. It is further worth noting that the A723_865210 location is the most upstream drainage sensor in the catchment and is not located directly along the Grote Masloot.

Each successive cycle of an oscillating pattern present in the drain flow time series is only weakly similar

In terms of the Fourier transform analysis, this depicts that the previously mentioned A723_865210 station is the only one featuring a cyclic pattern of 470 days. Although this is rather distant from the more readily expected year period, visual inspection of the autocorrelation series does tend to support an annual pattern that is disturbed principally by the already discussed abnormal peaks in the original series. The autocorrelation value of 0.19 based on this lag shift does show that, despite the yearly cycle present, each year is not really similar to the previous one.

It is further uncovered that a daily seasonality is present for each station with the exception of A723_865212 which is rather surprising since it is only located a few meters away from A723_865213 that is on the opposite side of the road. Visual inspection of the autocorrelation series supplemented by two moving averages taken over half and a quarter of this seasonality period does support the periodic fluctuation around the yearly cycle path. Nevertheless the extracted single sided amplitudes of this seasonal movement returns correlation coefficients of zero to one decimal place, demonstrating that over the data collection period each day is not similar to the previous one.

Response of surface water level to precipitation

Automatic lag time computation is applicable

Response events can usually be clearly delineated based on a combination of the precipitation and surface water plots. Manually locating peaks for the validation of the approach to recognize peaks using the implemented heuristic revealed that it often occurs that there is no real change in surface water and hence no peak could be designated. Comparing the lag times based on the manually located peaks with those identified automatically for the A723_865216 station through a paired t test shows that there is not a significant difference between the lag times. The confidence interval of -8.66 to 2.51 in terms of number of 15 minute instances indeed includes zero, using the 95% confidence level. The skewed confidence interval does reveal that the automatically generated results do tend to overestimate the lag time slightly. Inspecting the combination in the Cartesian plane shows that indeed a minimal number of points deviate significantly from a line with slope 1 through the origin. To further discuss those instances not located both automatically and manually, 17 events are concerned of which only three lag times do not fit in the found range. Response events that the automatic peak delineation fails to pick up are counted at 16 events from which most are with very small lag times.

Lag time of surface water level to precipitation is generally consistent across the catchment

The station where there is a trend and that has the minimum amplitude fluctuation also has the minimum lag time. This median lag time of 5 hours and 30 minutes is rather different from the other stations that range from 6 hours and 30 minutes to 7 hours. There is thus no difference in the lag time to precipitation based on the position in the catchment. The computed lag time is further not correlated to rainfall intensity, insinuating that it is dependent upon the conditions of the local system. Considering the median lag time per month, there is no visually recognizable monthly dependence pattern in the correlation coefficient of the lag time of each station with the values from the preceding or succeeding month.

Rate of change of surface water during precipitation absence is very variable per event

For the response of surface water to dry conditions, it is found that the spread of recorded trends from the surface water time series during the times labeled as dry, spans a wide range while being poorly characterizable by the median value as portrayed in Appendix 11. Nevertheless, while this median value is supported by good coefficients of determinations this cannot be stated about the more plausible trends that lie around zero that occur with highest frequency. Overall, it appears that surface water is variably affected by dry periods suggesting the potential differences in management decisions taken.

Response of drainage volume to precipitation

Automatic lag time computation is applicable

Response events to precipitation tend to be clearly visible in the time series. However, on occasions it is difficult to identify which maximum to select because peaks follow up without there being new precipitation. In those cases the manual peak delineation resorts from a value judgment on closeness and magnitude using insights from the properties of the precipitation event. The automatic computation of lag time does not deviate from the manual selection based on a paired t test using the 95% confidence level. It is however revealed by the confidence interval found, ranging from -9.75 to 0.99 number of 15 minute instances, that the automatically generated lag times are more overestimating the suspected value than with surface and groundwater. This is not surprising based on the rapid and numerous changes of drainage volume that the series encompasses. A further 20 response events not manually delineated are picked up by the script. The lag time values for those are within the usual range based on the rest of the matching lag times. Additionally, the script does fail to return values for 39 events of which the lag time characteristics do not appear to tend to a particular value. Hence, overall the results from the script should provide a representative output of lag times based on the input precipitation events.

Lag time of drain flow to precipitation occurrence exceeds that for surface water

The analysis has resulted in that the drain volume response times exceed the surface water lag times for stations A723_865214, 11 and 15 that are placed at drains discharging directly in the Grote Masloot downstream of the weirs where surface water level is recorded at stations A723_865218, 16 and 17 in the order of the most upstream to downstream sensor. Hence it takes longer for the rainwater discharging from the fields to peak than the actual surface water that is in the subsequent stage of the discharge sequence. With the differences between the medians being 3.5, 1.75 and 2.5 hours respectively, this shows that there is no relation with the order in which stations are located along the Grote Masloot. Further, Figure 15 depicts that there is no lag time relation to local soil type while only stations A723_865211 and 12 have lower response times than the others. These two stations are in proximity and feature amongst the stations that are in fields with highest elevation alongside station A723_865210. The difference is however that the mentioned two stations are furthest away from the Grote Masloot. Finally based on the limited number of events useable to compute lag time on, the latter does not appear to differ systematically from the median on a monthly basis with no further pattern in the correlation of the lag times from one month with respect to the previous and succeeding months across the station set.

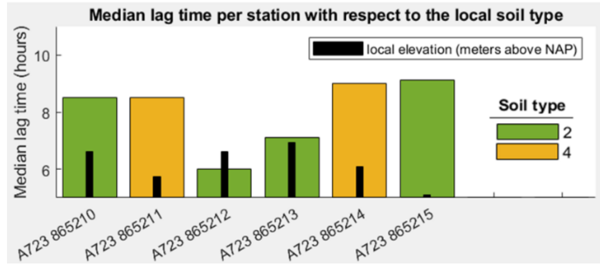

Figure 15: Median response delay for each drain flow station to precipitation put in perspective of soil type and elevation.

Drain flow volume during precipitation absence is fluctuating

Little is found in terms of the trend of drain volume during dry condition. The gradients returned have a tendency to be close to zero. Nevertheless, the regression fits are frequently not well supported by the coefficients of determination, as presented in Appendix 12. This prompts the idea that drain flow is variable during the dry events, as was already insinuated by the presence of the daily periodicity.

5.1.3. Relation of soil moisture content to groundwater and precipitation

To study the soil layers connection to both input factors of groundwater and rainfall, the soil moisture records are deconstructed to subsequently address each of these relational components respectively.

Soil moisture content time series characteristics

Soil moisture content does not feature a directional trend

No general trends are observed that directionally alter the yearly average. The regression analysis does return indicative slopes supported by coefficients of determination, however for each of these a visual inspection of the plot further complemented with the data on the other soil depths at the studied location lead to not support the linear pattern.

The amplitude of the yearly soil moisture content fluctuation decreases with depth

The subsequent series decomposition has been limited to the depths of 10, 30 and 50 cm. Figure 16 presents an overview of the yearly cyclicity for each depth. The daily peaks that do reoccur for a few stations in the plot of the Fourier transform are not supported by visually interpreting the autocorrelation series. The latter do strongly support the yearly fluctuating pattern for the depths of 10 cm and 30 cm but are clearly less pronounced for the 50 cm depth. For stations A723_865201, 5 and 9 of the 50 cm depth series the Fourier analysis also no longer picks up the yearly cycle. The absence of the daily periodicity is surprising in the frame of its presence with the drain flow records. This can however be explained by how those are only validated based on the tendencies from the series themselves and not corrected to eliminate theoretically unrealistic entries. As expected, for each year decline in soil moisture is initiated late spring with recharge steadily occurring from around the end of autumn The exact time is year related and linked to a similar cyclicity as observed with groundwater for the 10 and 30 cm depths at least.

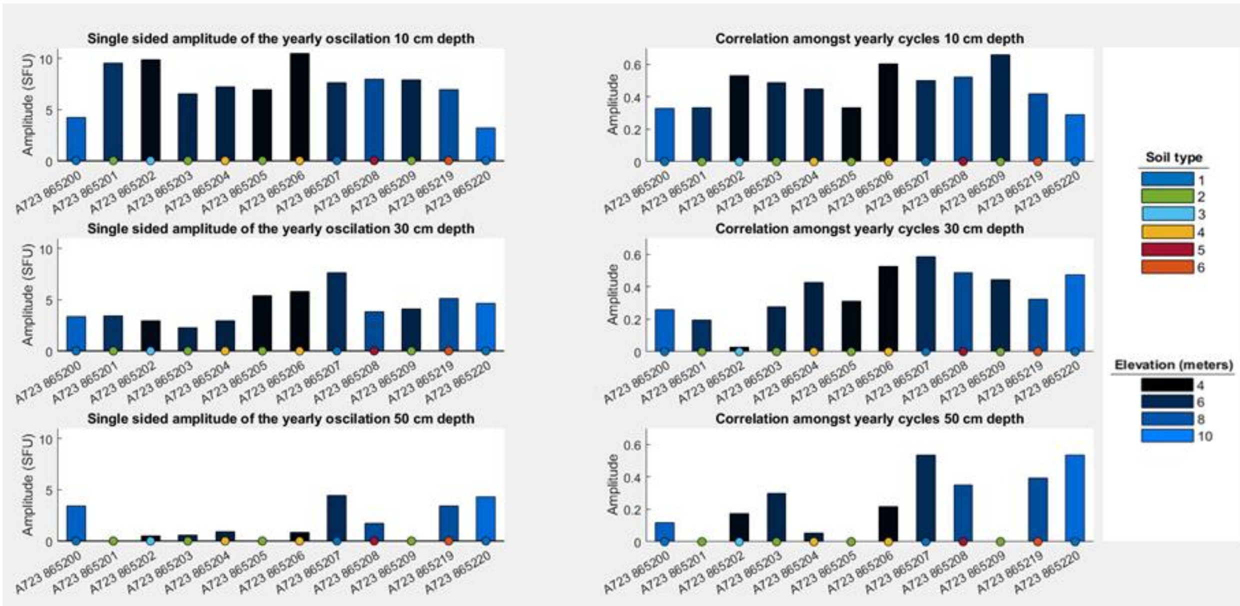

Figure 16: Presenting the yearly single sided amplitude fluctuation range for soil moisture content in the scaled frequency unit, SFU, alongside the correlation amongst these yearly cycles for each stations using the depths of 10, 30 and 50 cm.

Figure 16 shows that the top soil layer features the largest amplitude annual fluctuations which decreases for deeper soil layers. This decrease in oscillation influence is most apparent for the stations is the less elevated parts of the catchment. Those locations start with the highest oscillations but only have a reduced amplitude at 50 cm depth. This while for the stations in the more elevated parts of the catchment, that have initially relative to the other stations rather small amplitudes, the oscillating range changes less as the depth is increased. There is however no visible link to soil type. Further the similarity of succeeding years tends to decrease with depth, but to different extents for each station. It should be noted how this analysis is impacted by missing data entries which can span prolonged periods.

Correlation of soil moisture to groundwater

Soil moisture content correlates with groundwater based on the coinciding yearly cyclic movement

Directly correlating the time instances available for both the groundwater and soil moisture time series reveals that the data sets follow similar patterns. Weak correlations have all been identified to originate from unexpected, atypical, fragments in the soil moisture data. An overview of the Pearson correlation values on a per depth basis is provided in Appendix 13. There is no apparent connection to location, local elevation or soil type. A summary of the mean correlation coefficients across all stations is provided in Figure 17 to indicate the magnitude of the correlation coefficients along the tendency that this decreases with depth. The less oscillating time series from the depths of 50 and 60 cm are attributed lower values. However, this does not imply a weaker connection. The more stable properties of the deeper layers do insinuate that it is maintained towards a more saturated state by an underlying influence. This seems particularly applicable for the locations with lower land elevation following the cyclic movement amplitude decrease with increasing soil moisture sensing depth below the surface for those stations.

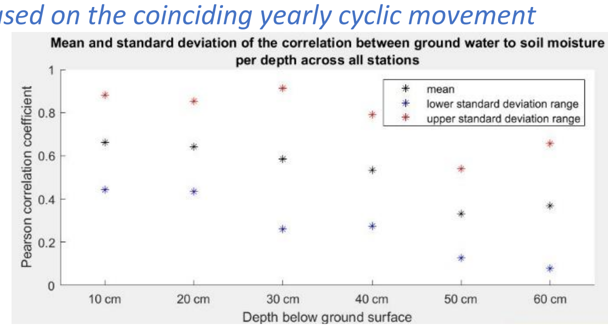

Figure 17: Mean correlation coefficient per soil moisture content sensing depth taken across all stations.

Response of soil moisture content to precipitation

Only the shallow soil layers respond strongly to rainfall

Applying the alternative to the lag time analysis to study the relation between soil moisture content and precipitation is justified by the obtained output as presented in Figure 18.

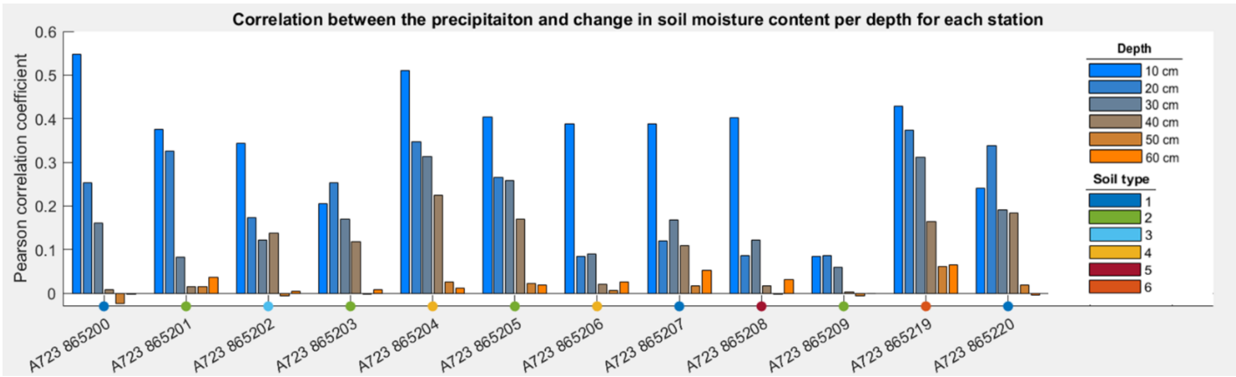

Figure 18: Correlation of the change in soil moisture content as positive during precipitation absence and any change during precipitation occurrence on a per station basis for each depth.

A direct response effect to precipitation, based on the data collection frequency, is observed for the upper soil layers. Overall, the shallower soil layers respond strongly to the occurrence of a precipitation event with influence decreasing with depth. This supports the expectation of the shallower layers responding instantly, based on the 15 minute data collection temporal scale, to the infiltration of precipitation water. Because rainfall volumes are in the majority of events analyzed not very large, based upon the analysis performed in section 4.2.1, it is likely that the precipitation quantity is just sufficient to fill up the pore space in the top soil layers with then only a slow and gradual potential exchange with the deeper layers if the shallower ones tend to saturate. This often will not occur, leading to stored water merely evaporating again. Nevertheless, it can not be ruled out that a possible deterioration in correlation is due to a lag time shift. However as was previously mentioned applying the lag time script poses problems and visual identification of most peaks is more difficult as depth increases, nuancing the validity of this observation.

Only the shallow soil layers respond strongly to dry periods

Figure 19 demonstrates how the shallowest soil layers are clearly induced a negative trend by the absence of precipitation while the deeper soil layers do not respond. Appendix 14 shows that the medians used are representative of the range of change rates found. For the shallow depths, where the 10 cm was explicitly tested the coefficients of determination strongly supports the found trends. This is less so for the deeper depths for which analysis focused on the 50 cm depth exemplar case. It is not really apparent if soil type affects the median rate of change since values are rather different amongst stations.

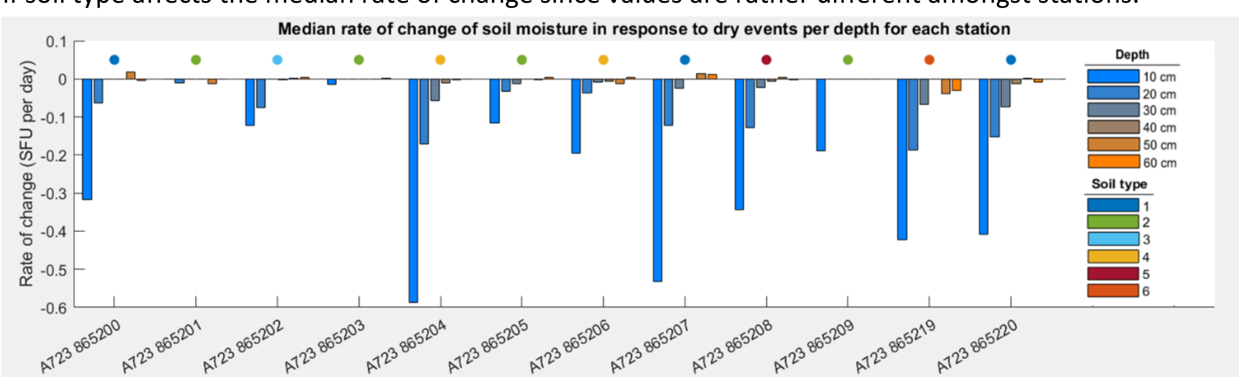

Figure 19: Median rate of change of soi moisture in response to dry conditions put in perspective by local soil type.

5.1.4. Relation of soil moisture content to vegetation vigor

Studying the NDVI time series supports the subsequent correlation with soil moisture content evaluation

NDVI time series characteristics

NDVI does not feature a directional trend and periodicity is not returned for agricultural grassland

There is no directional trend in any of the generated series of NDVI value at the locations of the soil moisture content monitoring stations. In terms of periodicity, in these series with coarser temporal resolution, this is featured by stations A723_865200, 04 and 20. The Fourier transform unanimously returns a period of 362 days referring to a yearly cycle. Further, A723_865207 features a cyclicity of 181 days according to a pattern of half year periods. Each of these oscillations is visually perceivable in the time series. An autocorrelation time series gives a distorted view due to the numerous data gaps following the low temporal resolution. It is interesting that their NDVI fluctuation range is very similar with values of 0.18, 0.17,0.13, and 0.11 in the order of the stations for which periodicity is mentioned. Hence the action of clearing and plowing an area induces the same NDVI fluctuation range as trees losing their leaves.

Correlation of NDVI to soil moisture

For grassland parcels NDVI is not correlated to soil moisture content

Because soil moisture does feature cyclicity for each location at the shallower depths, this is already not promising to find a correlation between NDVI and soil moisture content for most stations except those mentioned. Figure 20 provides an overview of the computed correlation coefficients when investigating the relation between vegetation vigor, characterized by NDVI, and soil moisture. Station A723_865204 is the only one that features the expected pattern with decreasing magnitudes of the negative correlation coefficients found with increasing depth below the ground surface. Indeed, vegetation vigor is highest during the summer period that coincides with the lowest soil water content. This relation, that is not direct, is a result of the confounding variable of the time of year and the attributable characteristics for each series during that time. Decreasing magnitude with depth appears logical in the frame of how it was previously observed that deeper soil layers feature a more constant moisture content all year round for this station in Figure 16 of section 5.1.3. This follows on to the steady correlation per depth for station A723_865207 that was shown to less feature decrease in soil moisture oscillating magnitude with depth.

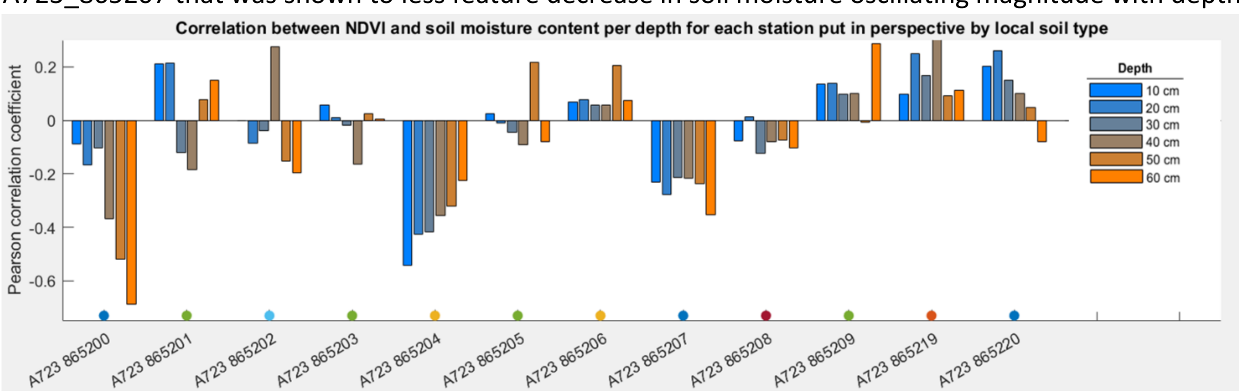

Figure 20: Correlation of NDVI to soil moisture content at each sensing depth with respect to the local soil type.

Soil moisture content and NDVI time series for non grassland parcels are out of phase

With correspondence being absent for most stations or not necessarily meaningful as with station A723_865200 that has increasing negative correlations with depth only because both series compared are more temporally aligned than with the shallower depths. The latter observation induces the idea that there may be a temporal delay between changing soil moisture content and NDVI values. Hence it was investigated if shifting the soil moisture content time series along that of the NDVI improves correlation. For each of the stations where cyclicity is present, this does yield a steady pattern of correlation coefficient value change. Appendix 15 gives the results obtained for these four stations. Shifting any series that does not have cyclicality does not systematically improve the correlation and are not further discussed.

Because both series compared feature the same yearly oscillating periodicity, momentarily neglecting that half the value has been observed for the A723_865207 location in the NDVI series, allows to compare how much the series are out of phase. Firstly A723_865204 is perfectly out of phase with respect to the soil moisture content for the depths of 10 to 30 cm. Then with increasing depth the correlation decrements with the loss of seasonality in the deeper soil layers observed for this location. While the latter problem is also featured by the A723_865200 station, an improved pattern of correlation change with lag is still apparent. Indeed, with increasing depth the two series are more perfectly out of phase by the half year period. However, for the shallower depths, it first requires about 50 days before they are completely so. Similarly, stations A723_865207 and 20 require approximately 100 days for all depths. This explains the poor correlation coefficients in Figure 20 while the oscillating patterns correspond. It is thereby noted that this pattern does not fully coincide for the A723_865207 location while the correlation between soil moisture and NDVI is still strongest after the lag applied. This can follow from the few points in the half a year NDVI drop during summer, insinuating further that this drop in the growth season is of brief duration.

Deciduous tree land cover optimally fits the soil moisture yearly cyclic movement

While grassland greenness is not particularly related to the time of year or soil moisture content, it can be observed from the perfect out of phase situation in the natural conditions at station A723_865204 that the crop cultivation at the other three stations may be responsible for this partial out of phase condition. While this presents the anthropogenic influence on land use, it can be concluded that soil moisture is at its lowest as vegetation is in growth stage, gaining vigor with increasing NDVI. This instead of the natural situation for A723_865204 where soil moisture is minimum when NDVI is at its maximum. Despite that only one station is in natural vegetation cover, the stableness and predictable nature of it are striking.

5.2. Contextualization of agricultural drainage management

Artificial agricultural drainage facilitates the discharge of water when the natural conditions do not fit the desired moisture conditions of a parcels land use (Oosterbaan, 1994). In the study area both subsurface and surface gravity based drainage is found. While the former internal system lowers the groundwater table in the fields the latter external component seeks to discharge the water to the lower point in the catchment (Oosterbaan, 1994). Using Figure 5 of section 3.2, observations on the local drainage system are presented. This discussion is restricted on what the analysis of section 5.1 revealed about the system state and thereby would need to be extended to encompass the water quality, agricultural practices and societal component. The five system variables, numbered according to Figure 5, are separately addressed.

Groundwater level differences amongst stations are not explained by the distance between them alone

Following Figure 5, the drainage system intends to maintain groundwater tables [box 1] at a lower level than the natural condition. Draining the land and discharging the water from the catchment does in principle raise concern about groundwater recharge (Jorjani, 1990). However, this likely does not apply following the stable nature of groundwater fluctuations observed. Ideally drainage is implemented so that the groundwater table remains as high as possible without inducing waterlogging problems from saturated soil layers. Agricultural groundwater level management could well influence the surroundings based on the distance related dependency amongst groundwater stations revealed. Hence the natural land can be expected to have a table to some degree relatable to the anthropogenic controlled surroundings. However, the variability observed also hints at the possibility for groundwater level differences not being fully accounted for by distance. This thereby does insinuate that drainage can have local effects. After discussing this with the two employees from Waterschap Noorderzijlvest, it is confirmed that they expect internal drainage systems to have localized effects, but when combined with the external system the effects should be more widely influential. They suspect that differences in groundwater tables observed are likely related to influences of local upward groundwater seepage patterns.

Drain flow volume appears unaffected by yearly groundwater fluctuations

The effect of the groundwater levels on the internal drainage system are characterized by the drain flow volumes [box 2] in Figure 5. Because groundwater tables have distinct yearly periodicity while drain flow has not, it appears that winter water tables are not rising sufficiently to trigger extra drain flow. This prompts enhanced attention to the benefits gained from drainage if the drain flow itself would not be enhanced by the high winter groundwater tables. However this is likely not the case because of the unreliability of the drain flow records. Focusing on how close the groundwater comes to the land surfaces in Appendix 16, it is observed that for the stations with lower land elevation the groundwater table does rise in winter to levels where the soil moisture content is measured and consequently expected to affect drain flows. Indeed, accordingly, the drain flow sensors are all placed in those lower elevated areas. The discussion on this revealed how it is expected that drain flow discharges are more rainfall related than groundwater while there is a clear tendency to support the usefulness of drainage for land workability.

Surface water level peaks are not enhanced by drain flow peaks due to their longer response delay

With the drain flow volumes contributing to the surface water level [box 3] of the Grote Masloot, the data allows to conclude that the internal drainage does not contribute to the peak discharges in the external system because surface water tends to peak before the drain flow. Such a condition is desirable and explained by how Oosterbaan (1994) states that the increased pore space following from the drainage intervention offers more room in the soil to accommodate for water from rainfall. Thereby, reducing the potentially negative consequences an intense rainfall event could have on surface runoff from fields. The surface water body of the Grote Masloot is well controlled with the water level annually oscillating in a restricted range. Resorting to the insights gained during the discussion, Waterschap Noorderzijlvest seeks to have enhanced water tables in summer while limiting them in winter through water inflow and weir management respectively. This, as perceivable, rules out natural expected seasonal variations. Further, it is expected that the regulation of surface water results in groundwater level not decreasing below its currently observed minimums. Indeed as a drainage system outlet, the Grote Masloot has the potential to set the standard for the limit at which further water drainage is hampered, with the reverse of replenishment not holding. The societal perception on this level, determining management decisions, do dictate the tendency of water to be drained from the land.

Soil moisture content in low elevated grassland becomes more stable with increasing depth

According to Figure 5, the drainage system lowers groundwater tables, influencing the soil moisture content [box 4]. The latter is the principal component the implementation of drainage seeks to improve for agricultural purposes. Soil moisture becomes increasingly stable deeper in the ground and is well correlated with groundwater. This stable nature is most prominent at stations in the lower elevated parts along the Grote Masloot for which the groundwater table is also closest to the land surface. Although the private drainage infrastructure network is not consulted to place this in perspective, those are also the locations with the highest potential of waterlogging and thus probably have internal drainage to stabilize the fluctuations of soil moisture content at the deeper soil layers monitored that were not identifiably affected by periods of dry conditions. Thereby this tends to support that the soil moisture is strongly upheld by the groundwater table that is close to these depths with excess soil moisture being effectively discharged by the drains. This complements the observation noted during the discussion that drainage seeks to maintain soil moisture at a desired state by reducing groundwater replenishment.

Vegetation vigor characterized by NDVI is unaffected by the cyclicity of soil moisture content for grassland

With the drainage systems influencing soil properties through its moisture content, as presented in Figure 5, the vegetation is impacted directly on internally drained parcels to improve yields through promoting vegetation vigor [box 5]. It was observed how NDVI values are not apparently influenced by soil moisture content on grassland parcels all year round. This can be an indication of well sustaining the groundwater level, that was shown to correlate with soil moisture content, for grass growth. However, it could also be that a higher groundwater table would not so much harm the production. McFarlane et al. (1994) observes how grassland that is waterlogged can retain a higher soil moisture content across spring. Nevertheless, the additional growth this yields in late spring does come at the expense of vigor at the end of winter and early spring. Further drainage does tend to promote the establishment of deeper reaching roots of crops in general (University of Minnesota, 2018), while land accessibility is a practical aspect of concern. Indeed, the discussion confirmed the importance of the practicality aspect with landholders seeking to maximize the production of the grassland. As such Oosterbaan (1994) suggests to search for the water table that has optimal crop yield without lowering the groundwater level unnecessarily, because this will not present increased yields, considering societal perception in the management decisions for the system.

6. Discussion

The analysis strategies and data used have been described to place the found outcomes in perspective for transparency on the restricted applicability of findings. However, several specific limitations could have been better planed for while alternatives of how the research can be extended have become apparent.

The processing strategies influence the observations made on the relational insights sought.

In the first part of the analysis targeted at empirically studying the relations between the collected time series, the data validation would have benefited from a theoretical basis. Especially for drain flow data that has an unrealistic nature, an improved literature search and identification of the onsite internal drainage system properties are necessary. Further to ensure the methods used in the analysis executed in MATLAB perform as expected, the two verification strategies of manual quantitative replication and visual feedback allowed to judge performance on a case specific basis. However these types of approaches do lack in integral reliability while ensuring that overall performance is in lines with expectations.

While verification and validation has been restricted to a case specific approach, the analysis itself principally has attention for general features that characterize the time series. This diverts awareness away from event specific interpretation. The latter is more resource intensive but could complement the analysis with interpretations of more atypical cases. Especially, the response event delineation that is an important part of the analysis is of concern despite its target to seek robustness. Even with the tuning of the selection choices made to try ensuring supported methodological decision, differences in input events and the following peak selection choices will induce variation in outcomes. It would be valuable to further look into the effect of the latter in the light of uncertainty. Accordingly the manual delineation used for verification purposes is also still value judgement prone, using a similar mentality as when composing the MATLAB script written for automatic identification. An integral dissociation between both would be desirable, with efforts seeking to improve the replicability of manual identification to be supplemented by extending the validation to more series.

The interpretation is only as insightful as the contextualized relational insights found

The second research component seeking to interpret the established qualifications of the relations amongst the time series is restricted in how context is brought in from a non diversified angle. Therefore, although a discussion with two employees from Waterschap Noorderzijlvest is complementarily used, it is expected that a reflection on the outcome by people of different backgrounds will broaden the scope.

A redirected research perspective would benefit integral system understanding

The analysis subject chosen focuses on the empirical analysis of the time series. However, interpretation is deficient in incorporating an overview of the full drainage system. Additionally an elaboration of what soil type properties imply for the water quantity relations adjoint to comparing soil moisture content amongst fields that are internally drained and those that are not should promote understanding of soil moisture replenishment. Further, despite constant surface water level, the onsite visit showed that the water at the weirs was well flowing even after prolonged antecedent dry conditions. This directs attention on what the balance is between the artificial inflow and the flow drained from the catchment.

7. Conclusion

The onsite data collection scheme offers extensive potential for the exploration of local properties, extending to the more integral catchment perspective. The executed analysis to obtain insight in the hydrological relations in the frame of discussing the drainage management is supported by using of the available records but does need to be improved by supplementary system awareness while acknowledging the influence of the analysis strategies selected on the revealed patterns. Further the used remote sensing data offers complementary information but is limiting in terms of temporal resolution.

Amongst the most insightful findings from empirically analyzing the hydrological relations is that soil moisture rapidly responds to meteorological conditions. Shallow soil layers up to 40 and 20 centimeters in depth respond most to precipitation occurrence and absence respectively, with the effect most attenuated for the deeper layers on the grassland. Nevertheless groundwater, due to the widespread contribution to its level, does responds perceivably. The delay of the response of drain flow peaks found is plausible featuring in between those of surface and groundwater recharge despite the unreliability of drainage records. Groundwater lag times are variable amongst the locations while most median surface water response times are similar per station. This also holds for drainage volume that for all, but one case, does not feature yearly cyclicity. Groundwater tables do have yearly periodicity with similar successive cycles. While this also holds for soil moisture where the amplitude fluctuation decreases with depth, surface water level is kept in a constant range with deviations being principally event determined.

Using the relational insights to discuss support of the drainage system for land use, acknowledging the management and environmental influences, allows to positively observe how drainage outflow does not strain the surface water system by simultaneously having peak discharges. While drain flow records do not feature corresponding cyclicity with groundwater tables, the superficiality of the latter does support the usefulness of drainage to counter waterlogging. Adjoining that the current variations in soil moisture do not influence grassland vigor, to that the time of lowest soil moisture content in fields used for crops coincides with vegetation vigor increases, prompts interest for an evaluation of the desired balance.

8. Recommendations

The applied analysis strategies are entirely data driven and a more profound evaluation of the relations found with respect to literature, should improve support for more generalizing conclusions across the catchment. However, the study of the system state response metrics to the environmental input of precipitation has been more insightful than the investigation on fluxes amongst system state components that proved to require complementary information. So, some practicalities are observed for the broader sustainable agricultural water management project context where the sensor network originated from.

Following the unrealistic entries in the drain flow time series it would be valuable to improve monitoring in terms of the data reliability for the prevailing stations. Further subsequent attention to enhance the combined monitoring of drainage and groundwater level, seconded by soil moisture content, in the same parcels is expected to provide a better indication of the value drainage has locally. Additionally, the balance between the water let into the catchment and the water that naturally or artificially drains would be interesting to investigate in the frame of how the Grote Masloot rapidly increases in water holding capacity as moving downstream. Especially focusing on how much water is contributed by which section may allow to locate areas of concern. Moreover, accounting for the role of groundwater extraction for irrigation, can be useful in this two way connection between ground and surface water.

For a more environmental perspective, from the current aim of supporting agricultural practices, it can be interesting to reinforce monitoring of nonagricultural parcels. Being aware of how groundwater and soil moisture content respond to meteorological conditions could allow to put in perspective the water quantity demand of agricultural activities from the land to benefit open minded management decisions.

References

Actueel Hoogtebestand Nederland. (2014–2019). *AHN3* [Dataset]. PDOK. https://www.pdok.nl/downloads/-/article/actueel-hoogtebestand-nederland-ahn3-

Ares, M. G., Varni, M., & Chagas, C. (2020). Runoff response of a small agricultural basin in the argentine Pampas considering connectivity aspects. *Hydrological Processes*, *34*(14), 3102–3119. https://doi.org/10.1002/hyp.13782

Bing. (2021). *Bing Aerial* [Dataset]. Bing. https://ecn.t3.tiles.virtualearth.net/tiles/a{q}.jpeg?g=1

Black, A., Peskett, L., MacDonald, A., Young, A., Spray, C., Ball, T., Thomas, H., & Werritty, A. (2021). Natural flood management, lag time and catchment scale: Results from an empirical nested catchment study. *Journal of Flood Risk Management*, *14*(3). https://doi.org/10.1111/jfr3.12717

Blann, K. L., Anderson, J. L., Sands, G. R., & Vondracek, B. (2009). Effects of Agricultural Drainage on Aquatic Ecosystems: A Review. *Critical Reviews in Environmental Science and Technology*, *39*(11), 909–1001. https://doi.org/10.1080/10643380801977966

Boermarke Zeijen. (2021, August 23). *Over ons*. Retrieved April 30, 2022, from https://boermarkezeijen.nl/over/

Copernicus. (n.d.). *Discover our satelites*. Copernicus Infrastructure Overview. Retrieved April 30, 2022, from https://www.copernicus.eu/en/about-copernicus/infrastructure/discover-our-satellites

Eamus, D., Zolfaghar, S., Villalobos-Vega, R., Cleverly, J., & Huete, A. (2015). Groundwater-dependent ecosystems: recent insights from satellite and field-based studies. *Hydrology and Earth System Sciences*, *19*(10), 4229–4256. https://doi.org/10.5194/hess-19-4229-2015

European Space Agency. (n.d.-a). *Copernicus Open Access Hub*. Copernicus Scihub. Retrieved April 30, 2022, from https://scihub.copernicus.eu/dhus/#/home

European Space Agency. (n.d.-b). *Data Products*. Sentinel Online. Retrieved April 30, 2022, from https://sentinel.esa.int/web/sentinel/missions/sentinel-2/data-products

European Space Agency. (n.d.-c). *MultiSpectral Instrument (MSI)*. Sentinel Online. Retrieved April 30, 2022, from https://sentinel.esa.int/web/sentinel/missions/sentinel-2/instrument-payload

European Space Agency. (n.d.-d). *Sentinel-2*. Sentinel Online. Retrieved April 30, 2022, from https://sentinel.esa.int/web/sentinel/missions/sentinel-2

esri. (n.d.-a). *Modeling a semivariogram—ArcGIS Pro | Documentation*. Arc GIS Pro Help. Retrieved May 25, 2022, from https://pro.arcgis.com/en/pro-app/latest/help/analysis/geostatistical-analyst/modeling-a-semivariogram.htm

esri. (n.d.-b). *Understanding a semivariogram: The range, sill, and nugget—ArcGIS Pro | Documentation*. Arc GIS Pro Help. Retrieved May 25, 2022, from https://pro.arcgis.com/en/pro-app/latest/help/analysis/geostatistical-analyst/understanding-a-semivariogram-the-range-sill-and-nugget.htm

Glansbeek, T. (2021, July 7). *Project Duurzaam Agrarisch Waterbeheer*. Boermarke Zeijen. Retrieved February 4, 2022, from https://boermarkezeijen.nl/project-duurzaam-agrarisch-waterbeheer/

Jensen, J. R. (2007). *Remote Sensing of the Environment* (2nd ed.). Pearson Prentice Hall.

Jorjani, H. (1990). *Analysis of subsurface drainage for land use planning*. Wageningen Agricultural University. https://www.wur.nl/en/Publication-details.htm?publicationId=publication-way-3133343837

Matalas, N. C. (1963). *Autocorrelation of Rainfall and Streamflow Minimums* (No. 434-B). United States Department of the Interior. https://pubs.usgs.gov/pp/0434b/report.pdf

MathWorks. (n.d.). *Fourier Transforms - MATLAB & Simulink*. Help Center. Retrieved May 25, 2022, from https://www.mathworks.com/help/matlab/math/fourier-transforms.html

McClave, J., & Sincich, T. (2018). *Statistics* (13th ed.). Pearson Education.

McFarlane, D. J., Cransberg, L., Glencross, A., & Glencross, R. (1994, January). *Managing waterlogging and inundation in pastures*. Department of Agriculture Western Australia. https://www.researchgate.net/publication/329138808_Managing_waterlogging_and_inundation_in_pastures

Oosterbaan, R. J. (1994). Agricultural Drainage Criteria. In *Drainage Principles and Applications* (second revised edition, pp. 635–656). International Institute for Land Reclamation and Improvement. https://edepot.wur.nl/183099

Pal, A., & Prakash, P. K. S. (2017). *Practical Time Series Analysis* (1st ed.) [E-book]. Packt Publishing.

Prinsco & University of Minnesota. (2022). *Drainage Calculator by Pipe Size*. Prinsco Water Water Management Solutions. Retrieved May 26, 2022, from https://www.prinsco.com/resources/drainage-calculator-by-pipe-size/

Raposo, P. (2021, September 28). *Spatial Patterns and Interpolation* [Slides]. University of Twente HTHT Geographic Information Systems (2021–1A). https://canvas.utwente.nl/courses/9059/files/2583273?module_item_id=268613

Rozemeijer, J., Verweij, S., Hunink, J., Visser, M., van Heeringen, K., van Rotterdam, D., & Ros, G. (2020, December). *Opzet eerste fase real time informatiesysteem voor DAW pilot Boermarke Zeijen* (No. 11202761–000-BGS-0002). Deltares, NMI

Talei, A., & Chua, L. H. (2012). Influence of lag time on event-based rainfall–runoff modeling using the data driven approach. *Journal of Hydrology*, *438–439*, 223–233. https://doi.org/10.1016/j.jhydrol.2012.03.027

University of Minnesota. (2018). *How agricultural drainage works*. University of Minnesota Extention. Retrieved June 5, 2022, from https://extension.umn.edu/agricultural-drainage/how-agricultural-drainage-works#frequently-asked-questions-1362415

van Rotterdam, D., & van Doorn, M. (2021, February). *Nutriëntenbenutting verbeteren en emissies beperken, Bodem- en bedrijfsonderzoek Boermarke Zeijen* (1746.N.19, pp 45). Nutriënten Management Instituut BV.

Vinkenvleugel, S. (2019, November 26). Boeren en waterschap meten in Zeijen waterpeil en kwaliteit met sensoren. *RTV Drenthe*. https://www.rtvdrenthe.nl/nieuws/154649/Boeren-en-waterschap-meten-in-Zeijen-waterpeil-en-kwaliteit-met-sensoren

Waterschap Noorderzijlvest. (2021, August). *Jaarplan 2022 inclusief meerjarige doorkijk 2022–2025*. https://www.noorderzijlvest.nl/_flysystem/media/jaarplan-2022.pdf

Appendix 1 Available onsite data

Onsite collected records are derived from one of the sensor station types presented in Figure 21. Rainfall is collected and the additional quantity transmitted to the database. The Soil moisture content equipment is a rod with multiple sensors for each depth. Water level is recorded on the upstream side of a weir. The drain volume is a derived quantity based on the water level in the bucket. Finally, groundwater is measured based on a pressure transmitter in the shown gauge tube. For each of the sensing locations, an overview of the data and its characteristic is provided in Table 2.

Figure 21 Examples of the four data collection station types. Left to right; precipitation and soil moisture content (groundwater gauging tube not visible); surface water level; drainage volume; groundwater level (soil moisture content probe not visible).

Table 2: Overview of the data collected per sensing station in the study area based on the information provided by Waterschap Noorderzijlvest

Identifier	x coordinate *	y coordinate *	Sensor type	Data collected (1)	Unit	Data from	Data collected (2)	Unit	Data from	Data collected (3)	Unit	Data from
A723 865201BV_P	232109	564950	Soil moisture and ground water	soil moisture content	SFU (a)	15 March	ground water level	m (b)	15 March			
A723 865200 BV_P	233465	563990	Soil moisture and ground water	soil moisture content	SFU (a)	15 March	ground water level	m (b)	15 March			
A723 865202 BV_P	232157	567097	Soil moisture and ground water	soil moisture content	SFU (a)	15 March	ground water level	m (b)	15 March			
A723 865203 BV_P	232497	565335	Soil moisture and ground water	soil moisture content	SFU (a)	15 March	ground water level	m (b)	15 March			
A723 865204 BV_P	232673	564580	Soil moisture and ground water	soil moisture content	SFU (a)	11 May	ground water level	m (b)	11 May			
A723 865205 BV_P	231909	567188	Soil moisture and ground water	soil moisture content	SFU (a)	15 March	ground water level	m (b)	15 March	precipitation	mm	15 March
A723 865206 BV_P	232451	567334	Soil moisture and ground water	soil moisture content	SFU (a)	5 June	ground water level	m (b)	5 June			
A723 865207 BV_P	232643	567476	Soil moisture and ground water	soil moisture content	SFU (a)	5 June	ground water level	m (b)	5 June			
A723 865208 BV_P	232573	564233	Soil moisture and ground water	soil moisture content	SFU (a)	4 May	ground water level	m (b)	4 May			
A723 865209 BV_P	232946	565468	Soil moisture and ground water	soil moisture content	SFU (a)	6 March	ground water level	m (b)	6 March	precipitation	mm	6 March
A753 865219 BV_P	232937	567810	Soil moisture and ground water	soil moisture content	SFU (a)	15 March	ground water level	m (b)	15 March	precipitation	mm	15 March
A753 865220 BV_P	234106	564064	Soil moisture and ground water	soil moisture content	SFU (a)	6 March	ground water level	m (b)	6 March	precipitation	mm	6 March
A723 865216 WP	232915	564984	Surface water level	surface water level	m (b)	4 July						
A723 865217 WP	233197	566348	Surface water level	surface water level	m (b)	5 July						
A723 865218 WP	233039	564253	Surface water level	surface water level	m (b)	9 July						
A753 865221 WQ_P	233156	563357	Surface water level and water quality	surface water level	m (b)	20 June						
A753 865222 WQ_P	232123	567935	Surface water level and water quality	surface water level	m (b)	20 June						
A753 865223 WS	232887	566059	Weather station	precipitation	mm	8 February						
A723 865210 DF	232863	566063	Drain flow	drained volume	l	5 June						
A723 865211 DF	233279	563816	Drain flow	drained volume	l	4 July						
A723 865212 DF	232898	565013	Drain flow	drained volume	l	28 May						
A723 865213 DF	232056	564772	Drain flow	drained volume	l	28 May						
A723 865214 DF	232124	564789	Drain flow	drained volume	l	9 July						
A723 865215 DF	233039	564259	Drain flow	drained volume	l	6 July						
RA440 51817	233197	566368	Soil moisture and ground water	Data incompatibility								

(a) scaled frequency unit for each of the six records taken at 10 cm intervals in the range of 10-60 cm below the ground surface
(b) to NAP **

* Amersfoort RD New coordinate reference system
** Amsterdam ordnance datum

Appendix 2 Not used system state data

Below an overview is provided of the omitted onsite collected system state data from the analysis.

			Segment not used		**(ymdhm = year, month, day, hour, minutes)**
	Station		**Start (ymdhm)**	**End (ymdhm)**	**Reason for omission**
Surface water level					
	A723_865216		N/A		
	A723_865217		N/A		
	A723_865218		N/A		
	A753_865221		N/A		
	A753_865222		202002031045	202002031045	Removed the minimum record of time series that is located in isolation in between a series of absent entries
Drainage volume					
	A723_865210		N/A		
	A723_865211		N/A		
	A723_865212		N/A		
	A723_865213		N/A		
	A723_865214		N/A		
	A723_865215		202102071000	202102080800	Increase to an extreme high value that is followed by absent entries. The extreme value is resumed again to gradually decrease back to the normal level.
Ground water level					
	A723_865200		N/A		
	A723_865201		201910111900	201910140945	Period scattered with missing entries, the available records in the range drop and suddenly jump up again in an unpredictable manner
	A723_865202		202003161045	202003161615	A sudden snip out of the time series that features a ground water level with about 1.5 m difference that is bound on either side by 4 missing entries
	A723_865203		N/A		
	A723_865204		N/A		
	A723_865205		202202041500	202202041500	Single instance extremely out of line that has one missing entry on either side
	A723_865206		N/A		
	A723_865207		202003161200	202003161615	Sparse record series in between the two major components of this time series (that differ), surrounded by missing entries on either side
	A723_865208		N/A		
	A723_865209		N/A		
	A723_865219		201803150000	201803230915	The initial part of the series is too low compared to the rest. After a single missing entry the series continues at a higher level from which it consequently logically progresses
	A723_865220		N/A		
Soil Moisture		**Depth**			
	A723_865200	10cm	202109300730	202204120045	A data gap occurs that is then followed by a record sequence that is scattered by missing entries that continues at a higher level overall.
		20cm	202106091830	202106151600	Instantaneous drop to zero
			202109300730	202204120045	A data gap occurs that is then followed by a record sequence that is scattered by missing entries that continues at a higher level overall.
		30cm	202109300730	202204120045	Features a sharp increase to then drop to 0. The series resumes at a higher level than before with a record sequence that is scattered by missing entries
		40cm	201911081500	202001171330	Non instantaneous drop to zero
			202012050300	202104211145	Instantaneous drop to zero
			202109300730	202204120045	Features a sharp increase to then drop to 0. The series resumes at a higher level than before with a record sequence that is scattered by missing entries
		50cm	202010152300	202106151600	Instantaneous drop to zero. The series resumes at a higher level than before, but then instantaneously drops back to the usual range.
			202109300730	202204120045	Features a sharp increase to then drop to 0. The series resumes at a higher level than before with a record sequence that is scattered by missing entries
		60cm	202109300730	202204120045	Features a sharp increase to then drop to 0. The series resumes at a higher level than before with a record sequence that is scattered by missing entries
	A723_865201	10cm	N/A		
		20cm	N/A		
		30cm	N/A		
		40cm	N/A		
		50cm	N/A		
		60cm	202006031645	202204120045	Sudden extreme increase not featured by any of the other depths. At this higher level the values do not stabilize around a central range. Decrease to the normal level is gradual.
	A723_865202	10cm	202104030300	202104211300	Although gradual, the series increases to about double the maximum value of the rest of the series. The drop to the normal level is instantaneous.
		20cm	N/A		
		30cm	201909242000	202001171315	Instantaneous increases to about double the maximum value of the rest of the series where it stabilizes. The drop to the normal level is instantaneous.
			202009101645	202104211245	Instantaneous increases to about double the maximum value of the rest of the series where it stabilizes. An instantaneous decrease is followed by a more gradual decrease that is marked by a short frequency fluctuation.
		40cm	N/A		
		50cm	N/A		
		60cm	N/A		
	A723_865203	10cm	N/A		
		20cm	N/A		
		30cm	N/A		
		40cm	N/A		
		50cm	N/A		
		60cm	N/A		
	A723_865204	10cm	N/A		
		20cm	N/A		
		30cm	201906260900	201907151445	Instantaneous drop to zero
		40cm	N/A		
		50cm	202101200330	202104211215	Instantaneous increases to about double the maximum value of the rest of the series where it stabilizes. A data gap is followed by the series resuming on the normal level again
		60cm	N/A		

			Segment not used		
Soil Moisture	**Station**	**Depth**	**Start (ymdhm)**	**End (ymdhm)**	**Reason for omission**
	A723_865205	10cm	N/A		
		20cm	N/A		
		30cm	N/A		
		40cm	N/A		
		50cm	N/A		
		60cm	N/A		
	A723_865206	10cm	N/A		
		20cm	N/A		
		30cm	N/A		
		40cm	N/A		
		50cm	N/A		
		60cm	N/A		
	A723_865207	10cm	201809171630	201908190800	Instantaneous 15 minute lasting extreme drops, of which some directly to zero (removed 356 instances)
			202011051345	202108051915	Instantaneous 15 minute lasting extreme drops, of which some directly to zero (removed 202 instances)
			202110080845	202204120045	Instantaneous 15 minute lasting extreme drops, of which some directly to zero (removed 116 instances)
		20cm	201809171630	201908190800	Instantaneous 15 minute lasting extreme drops, of which some directly to zero (removed 254 instances)
			202011051345	202108051915	Instantaneous 15 minute lasting extreme drops, of which some directly to zero (removed 137 instances)
			202110080845	202204120045	Instantaneous 15 minute lasting extreme drops, of which some directly to zero (removed 79 instances)
		30cm	201809171630	201908190800	Instantaneous 15 minute lasting extreme drops, of which some directly to zero (removed 295 instances)
			202011051345	202108051915	Instantaneous 15 minute lasting extreme drops, of which some directly to zero (removed 178 instances)
			202110080845	202204120045	Instantaneous 15 minute lasting extreme drops, of which some directly to zero (removed 111 instances)
		40cm	201809171630	201908190800	Instantaneous 15 minute lasting extreme drops, of which some directly to zero (removed 443 instances)
			202011051345	202108051915	Instantaneous 15 minute lasting extreme drops, of which some directly to zero (removed 188 instances)
			202110080845	202204120045	Instantaneous 15 minute lasting extreme drops, of which some directly to zero (removed 120 instances)
		50cm	201809171630	201908190800	Instantaneous 15 minute lasting extreme drops, of which some directly to zero (removed 302 instances)
			202011051345	202108051915	Instantaneous 15 minute lasting extreme drops, of which some directly to zero (removed 202 instances)
			202110080845	202204120045	Instantaneous 15 minute lasting extreme drops, of which some directly to zero (removed 94 instances)
		60cm	201809171630	201908190800	Instantaneous 15 minute lasting extreme drops, of which some directly to zero (removed 382 instances)
			202011051345	202108051915	Instantaneous 15 minute lasting extreme drops, of which some directly to zero (removed 231 instances)
			202110080845	202204120045	Instantaneous 15 minute lasting extreme drops, of which some directly to zero (removed 138 instances)
	A723_865208	10cm	N/A		
		20cm	N/A		
		30cm	N/A		
		40cm	N/A		
		50cm	N/A		
		60cm	N/A		
	A723_865209	10cm	202008302315	202009091215	Instantaneous extreme fluctuations (removed 916 instances)
			202009111315	202010071315	Instantaneous extreme fluctuations (removed 19 instances)
			202102271815	202104211230	Instantaneous extreme fluctuations (removed 4 instances)
		20cm	201804082300	201808120245	Instantaneous extreme fluctuations (removed 12016 instances)
			202008310000	202104211200	Instantaneous extreme fluctuations(removed 22417 instances)
		30cm	202010090945	202010091745	Instantaneous extreme fluctuations (removed 4 instances)
		40cm	201809200315	201905071245	Instantaneous extreme fluctuations (removed 2022 instances)
			202008302315	202009091215	Instantaneous extreme fluctuations (removed 916 instances)
			202010251515	202010270945	Instantaneous extreme fluctuations (removed 171 instances)
		50cm	202008301330	202009091200	Instantaneous extreme fluctuations (removed 913 instances)
			202011091100	202104211200	Instantaneous extreme fluctuations (removed 15653 instances)
			202106151300	202110271330	Instantaneous extreme fluctuations (removed 12867 instances)
		60cm	201807192215	201905071245	Instantaneous extreme fluctuations(removed 27995 instances)
			202008301330	202009091215	Instantaneous extreme fluctuations(removed 914 instances)
			202009220645	202010270945	Instantaneous extreme fluctuations(removed 3373 instances)
			202103171000	202104211200	Instantaneous extreme fluctuations(removed 3368 instances)
			202107091145	202110271345	Instantaneous extreme fluctuations (removed 10568 instances)
	A753_865219	10cm	202204020315	202204120045	Instantaneous increases to about double the maximum value of the rest of the series where it stabilizes, while maintaining a high level of fluctuation.
		20cm	201906220545	201907151445	Instantaneous drop to zero
			202201170330	202204120045	Instantaneous drop to zero
		30cm	N/A		
		40cm	201906261145	201907151445	Instantaneous drop to zero
			202109292200	202204120045	Instantaneous drop to zero
		50cm	N/A		
		60cm	201904180445	201907151445	Gradual increase to a higher level, non extreme level, than the rest of the series while depths do not change. A gradual decrease brings the series back to a normal level again. However the subsequent series continues to jump up and down between the higher and normal level again in the time of just 15 minutes. Stabilization occurs on the higher level again followed by a instantaneous drop to the normal level.
	A753_865220	10cm	N/A		
		20cm	N/A		
		30cm	201905140315	201905161630	Instantaneous drop to nearly zero, then completely to zero
			202008182300	202009091230	Instantaneous increases to about double the maximum value of the rest of the series where it stabilizes. A data gap is followed by the series resuming on the normal level again
		40cm	201905161600	201907151330	Instantaneous drop to zero
		50cm	N/A		
		60cm	201905161545	201907151330	Instantaneous drop to zero

Appendix 3 Representativeness of the data from the weather station

Because the series collected by the weather station is not representative for the study area based on a comparison with the other precipitation data sets available, untypical records have been removed. As a result, the dashed line of Figure 22 shows a more balanced fit of the representative series while further supported by the significantly improved correlation coefficients to the other non altered series. The cumulative line of station A723_865220 is not fully captured in the plot because it attains a final value of 13365.8 mm.

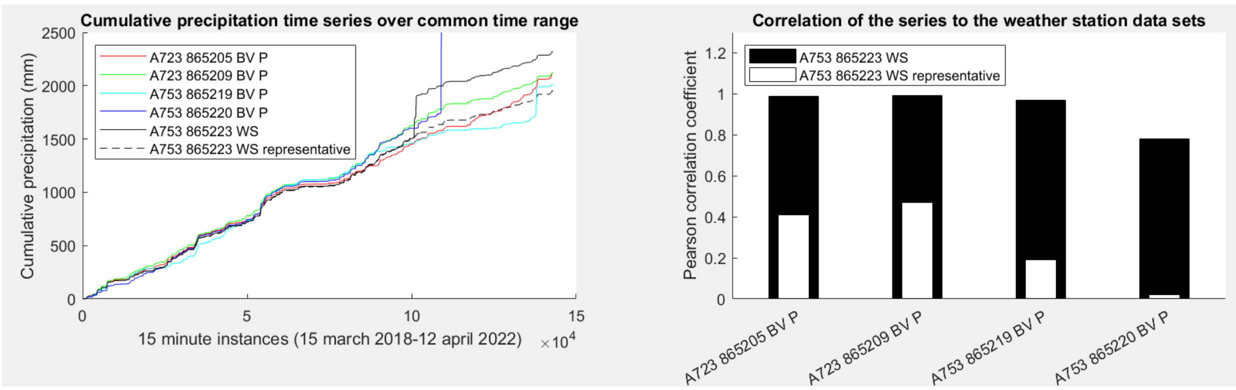

Figure 22: Comparing the cumulative precipitation accumulation across the five data sets and the edited representative series (left). Portraying the correlation coefficients between each time series to both the direct and edited records from the weather station (right).

Appendix 4 Parameters for identified precipitation events

To support the decision of the parameters of the minimum rainfall quantity for an event and the set dry time limit to separate these, Figure 23 is presented. It is judged that after the selected limit there is a stabilization in the rate of the effect these two parameters have on the number of events as further increased.

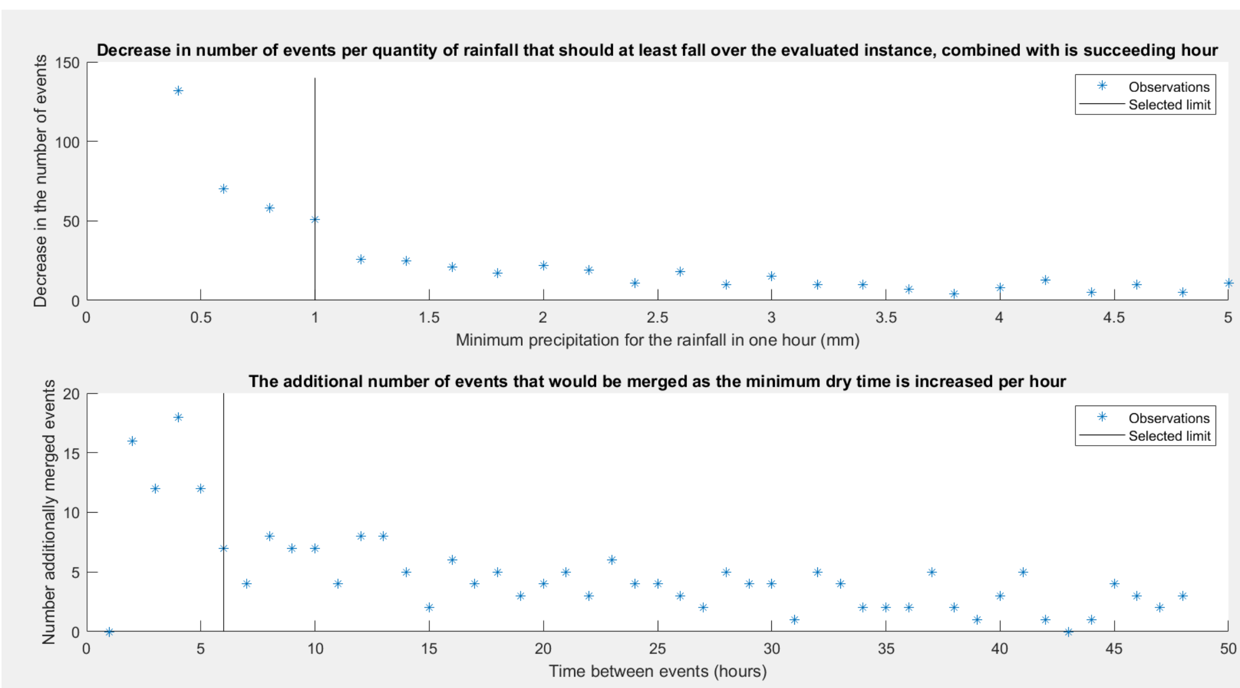

Figure 23: Selecting a limit for the minimum precipitation quantity to initiate an event followed by determining the minimum dry time between events.

Appendix 5 Unprocessed dry period characteristics

Figure 24 gives an indication of the characteristics of the dry events selected. It should be noted that the histogram of dry time duration frequency is not necessarily reflecting all dry periods in the data set. Indeed the event selection procedure will exclude dry segments if first selected as a single entity but disturbed by as shorter than 45 minutes event that exceeds the minimum precipitation cap. This is further exemplified in Appendix 9. On a per monthly basis, the minimum dry time is rather consistent per month with the maximum values increasing particularly over the spring periods with the medians following a similar pattern.

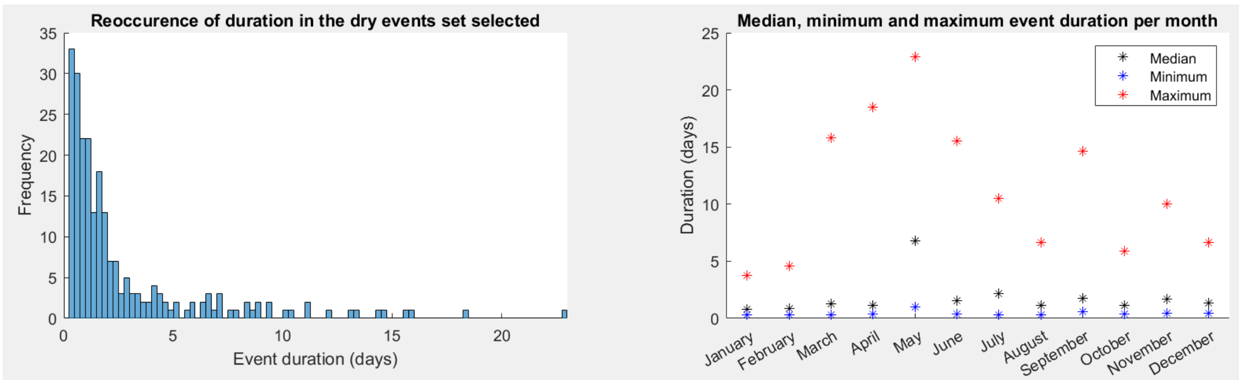

Figure 24: Presenting the frequency of dry event reoccurrence per duration value followed by a decomposition of the median values on a monthly basis.

Appendix 6 Generated NDVI series

To give an overview of the data not provided by Waterschap Noorderzijlvest that is also used in the analysis, Figure series 25 is proposed to offer the possibility to individually look at a specific time series.

Figure series 25: Overview of the generated NDVI series based on the processed remote sensing data from (European Space Agency, n.d.-a)

Appendix 7 Time series characteristics

The data from groundwater monitoring station A723_865200 is used as an example to demonstrate how the seasonally and cyclic movements have been retrieved from time series. Figure 26 presents the data used to obtain the Fourier transform plot, shown at multiple zoom levels in Figure 27, used in identifying periodicity and the amplitude of such an oscillation. Further computing the autocorrelation series, shown in Figure 28, reveals that both a yearly and daily pattern is visible. Fitting moving averages to the autocorrelation series has proven useful in cases where the oscillating patterns are not as smooth as with this groundwater exemplar. Figure 29 finally shows the reapplication of the Fourier transform to the autocorrelation series to retrieve the magnitude of how subsequent cycles are related.

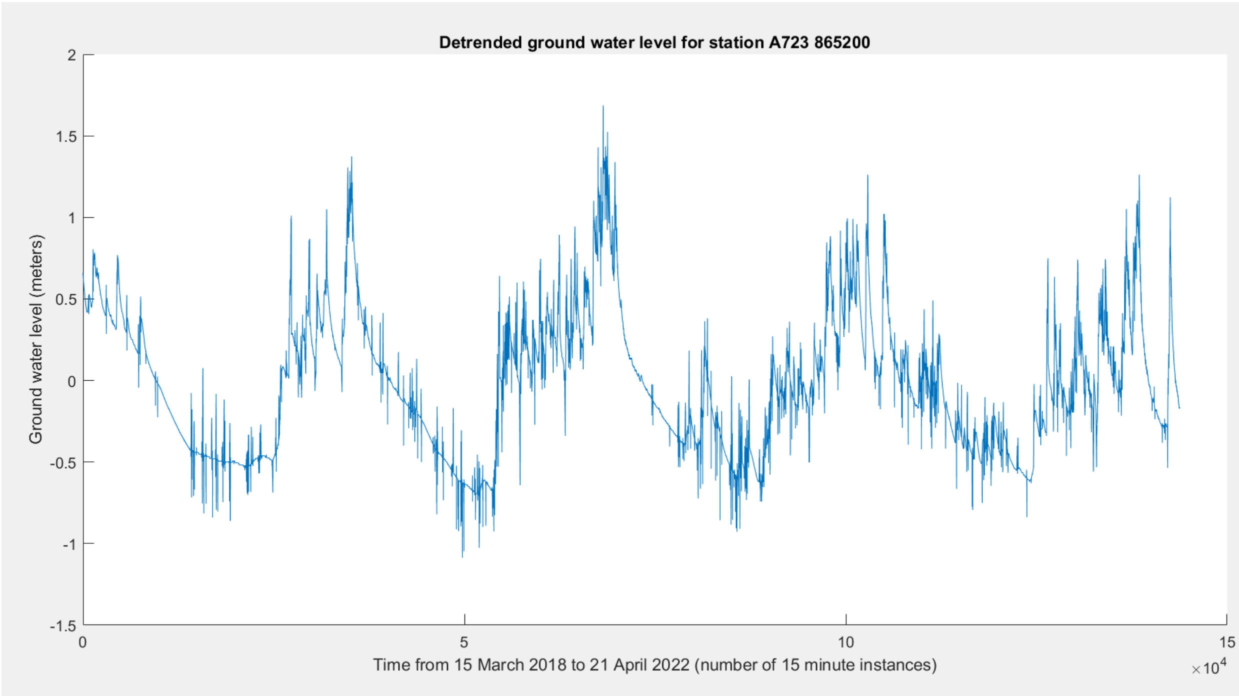

Figure 26: Detrended groundwater time series collected at A723_865200

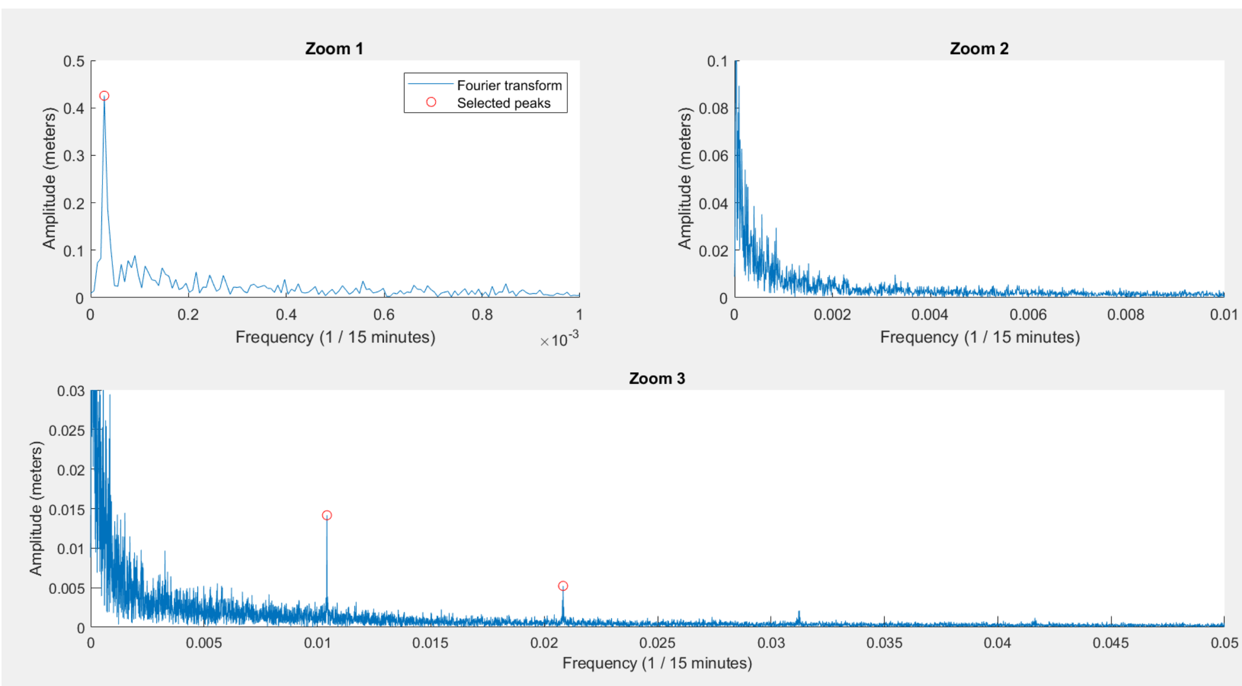

Figure 27: Plot based on the Fourier transform of the time series for the A723_865200 station shown at three different zoom levels to perceive the local peaks at the frequencies of a reoccurring period.

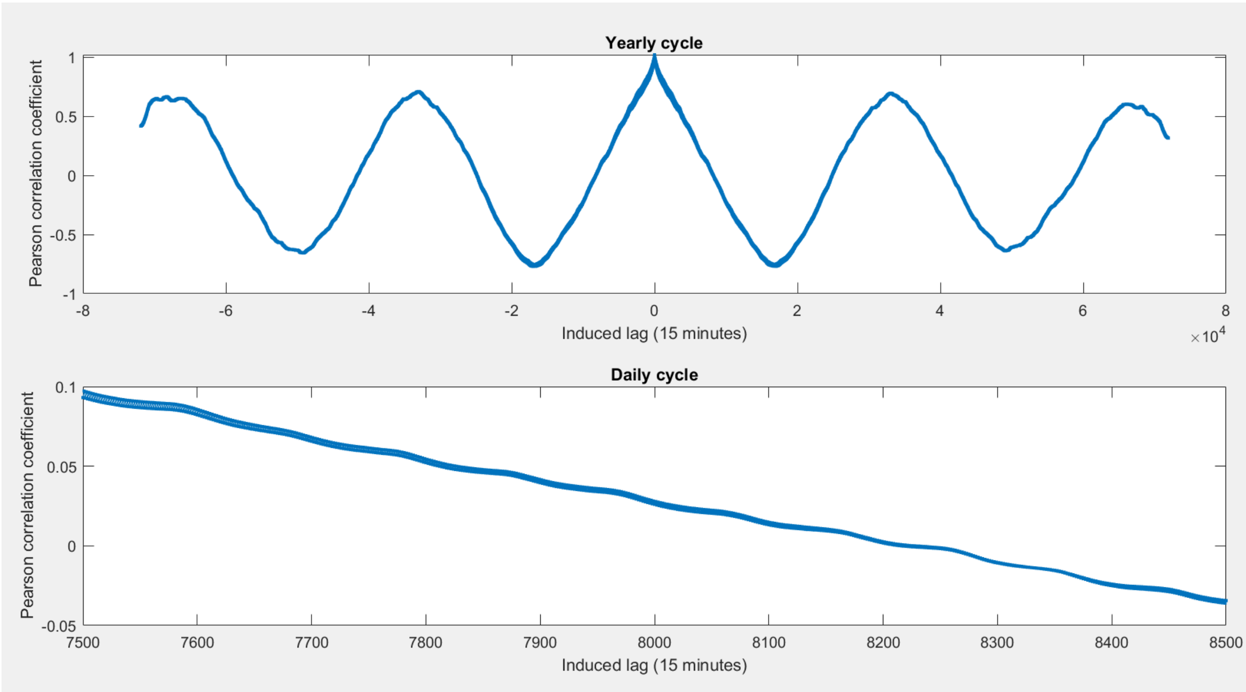

Figure 28: Autocorrelation sequence showing the daily and yearly cycle based on the zoom level for station A723_865200.

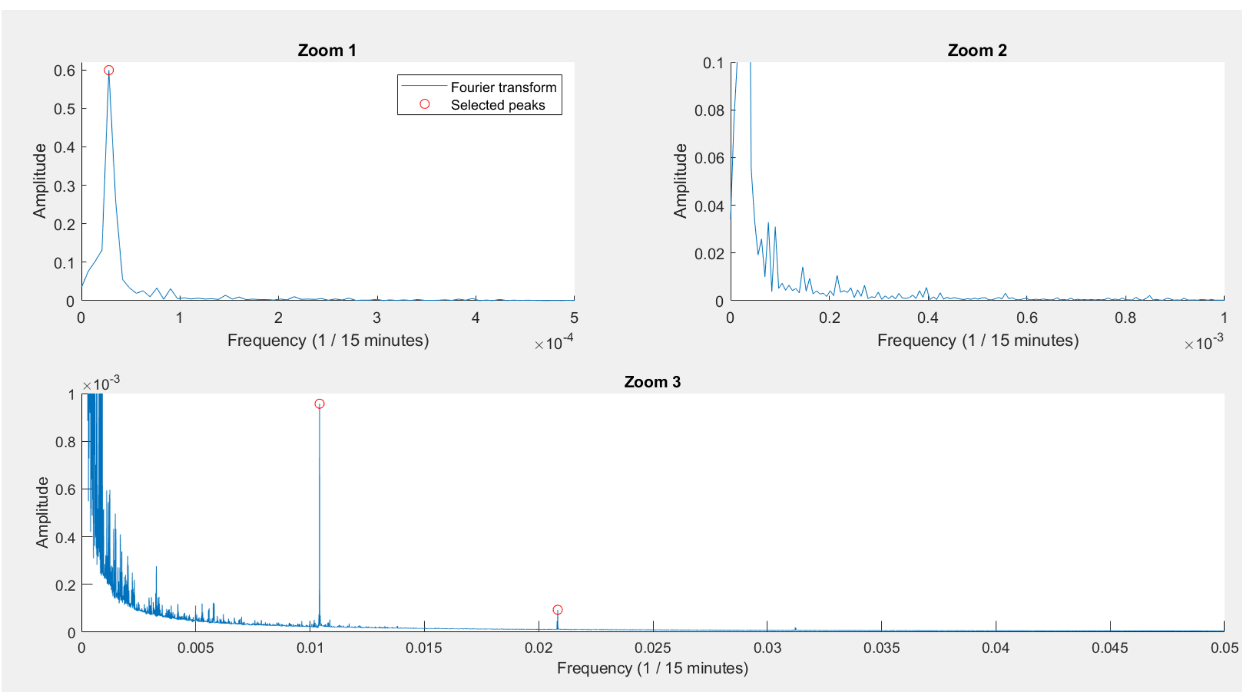

Figure 29: Plot based on the Fourier transform of the autocorrelated series for the A723_865200 station shown at three different zoom levels to retrieve the correlation amplitudes at the frequencies of a reoccurring period.

Appendix 8 Lag time to a precipitation event

Based on groundwater monitoring station A723_865200 Figure 30 serves as an example to demonstrate the automatic delineation of peaks based on the located precipitation events. It is firstly apparent how only precipitation instances attributable to a significant event are used. Overall peaks are correctly selected with the first event shown not featuring a clear response and so the peak is omitted in the lag time calculation as desired. Further for the last event portrayed, the data gaps in the series lead to no peak being selected.

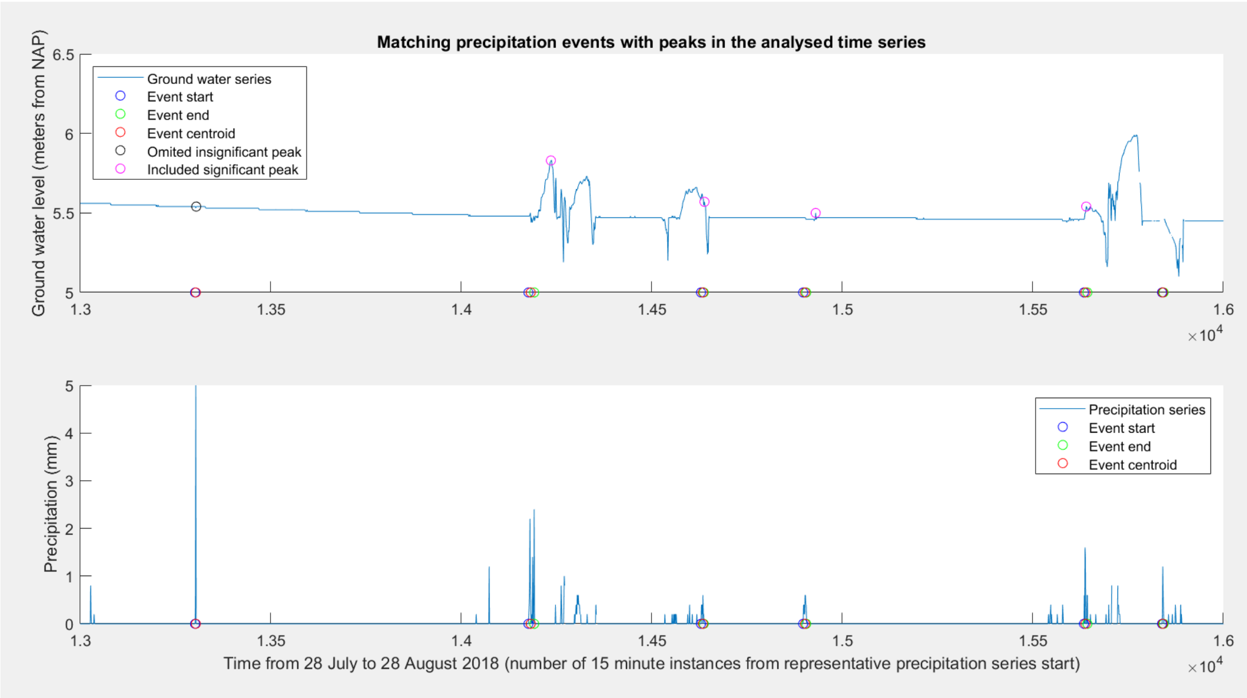

Figure 30: Locating peaks as a response to precipitation events. Example based on the A723_865200 groundwater monitoring station.

Appendix 9 Trend in a period of precipitation absence

Presenting an example, using groundwater monitoring station A723_865200 in Figure 31, for the linear regression analysis applied on segments of rainfall absence allows to justifiably see the potential of this technique. In this case the gradual declines are effectively captured by the trend lines with event starts being shifted according to the lag time that the series has to respond to rainfall. With the series not always featuring a clear directional trend, the coefficient of determination should provide a good indication of if the data closely follows any linear regression fitted.

It can be observed that the long dry conditions period on the most left side of the plot is not selected while this could have yielded additional valuable information. The omission can however be explained in terms of the method applied, parallelly revealing the limitations of the latter. The dry events delineation strategy proceeds with accumulating a potential event until three successive data entries are not dry. Hence short precipitation occurrences can feature in the range. Applying the verification step, to see if during the time range of the minimum dry time the precipitation volume does not exceed the minimum precipitation required to initiate a precipitation event, it is possible to reject a dry event if such short, but intense, rainfall has taken place. This, without the possibility to reuse the dry components on either side of this moment of rainfall. The situation portrayed is rather abnormal, and it is thus expected that such omissions of dry periods do not frequently reoccur.

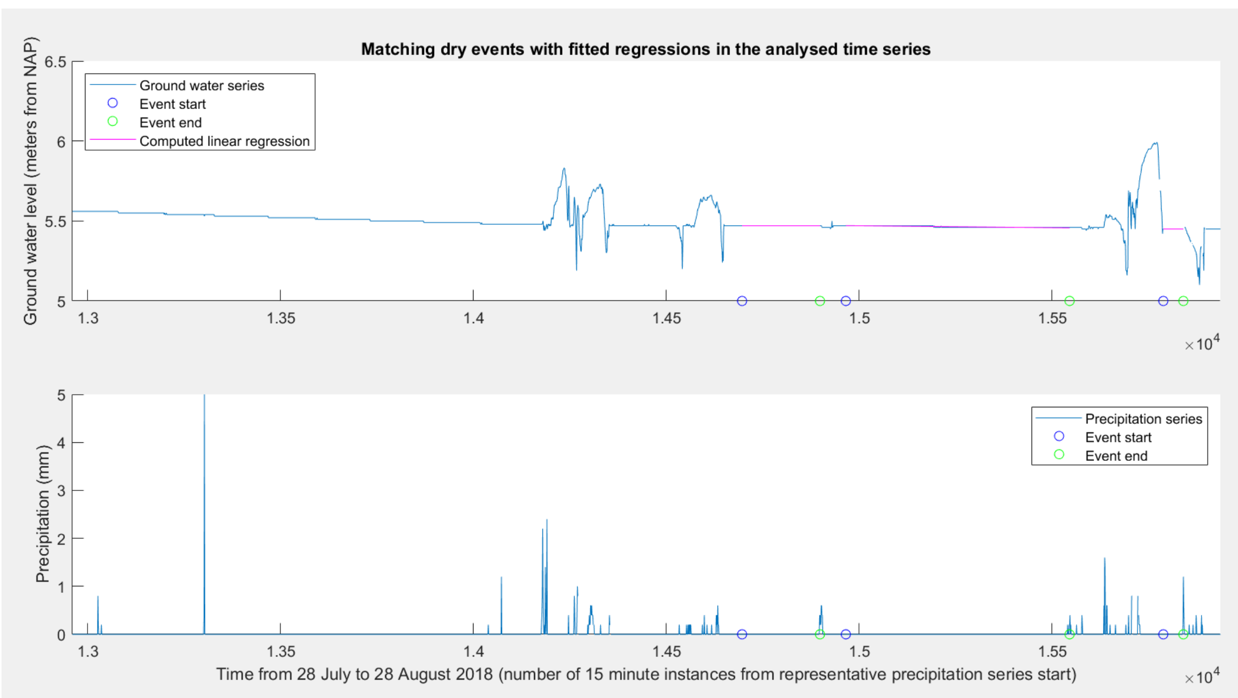

Figure 31: Locating trends as a response to dry conditions. Example based on the A723_865200 groundwater monitoring station.

Appendix 10 Groundwater response to precipitation

To support the described conclusions, Figure 32 and Figure series 33 provide an overview of the computed lag times to rainfall events and the trend, with associated properties, during dry conditions respectively. The found lag time ranges are well focused around the median found. In turn the regression trends computed are often more variable and supported to different degrees by the coefficient of determination.

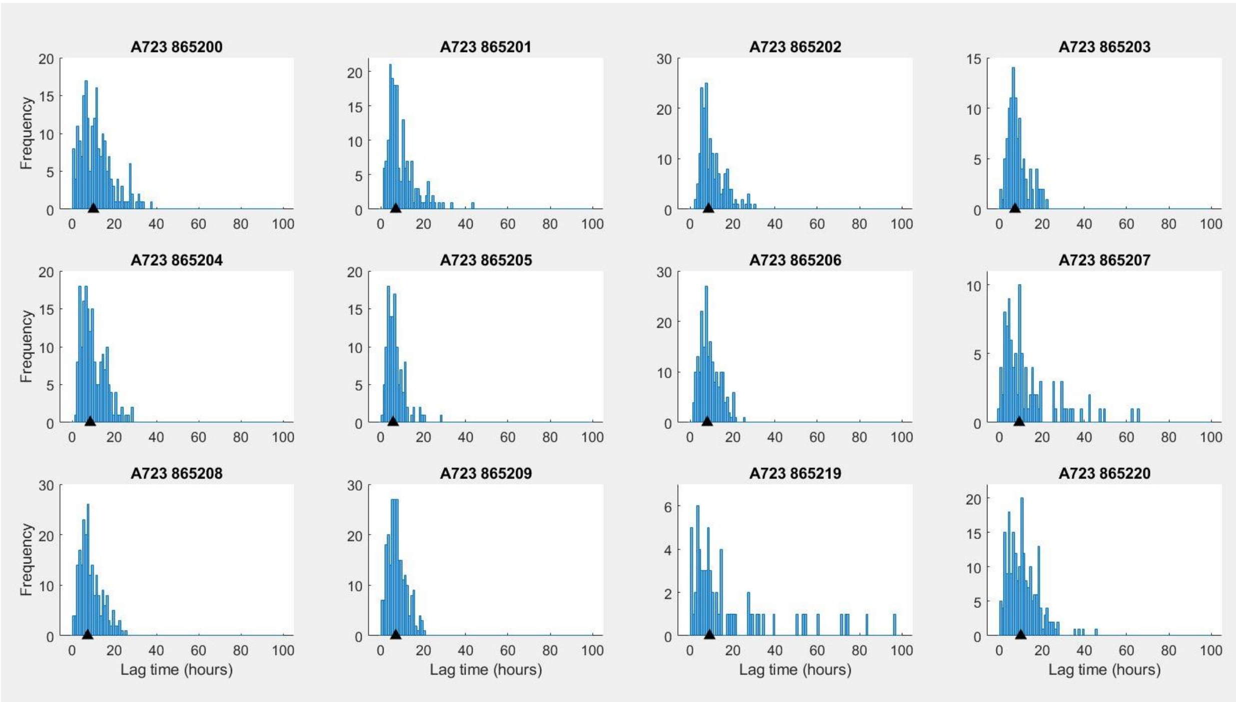

Figure 32: Histograms of the lag time computed for groundwater for each station supplemented by the median value indicated by the black triangle.

Figure series 33: Histograms of observed trend values put in perspective by the associated range of coefficients of determination for each groundwater monitoring station.

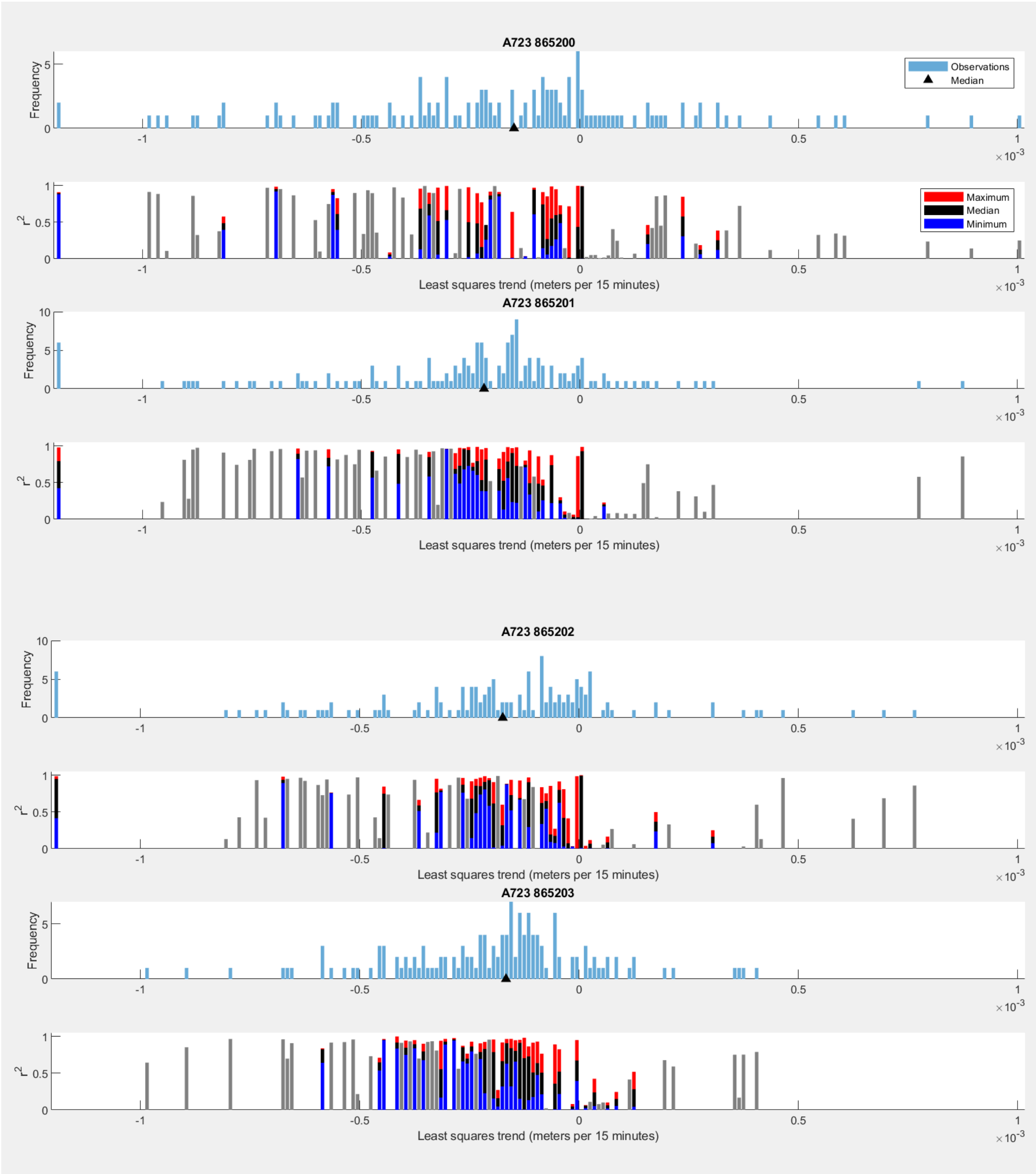

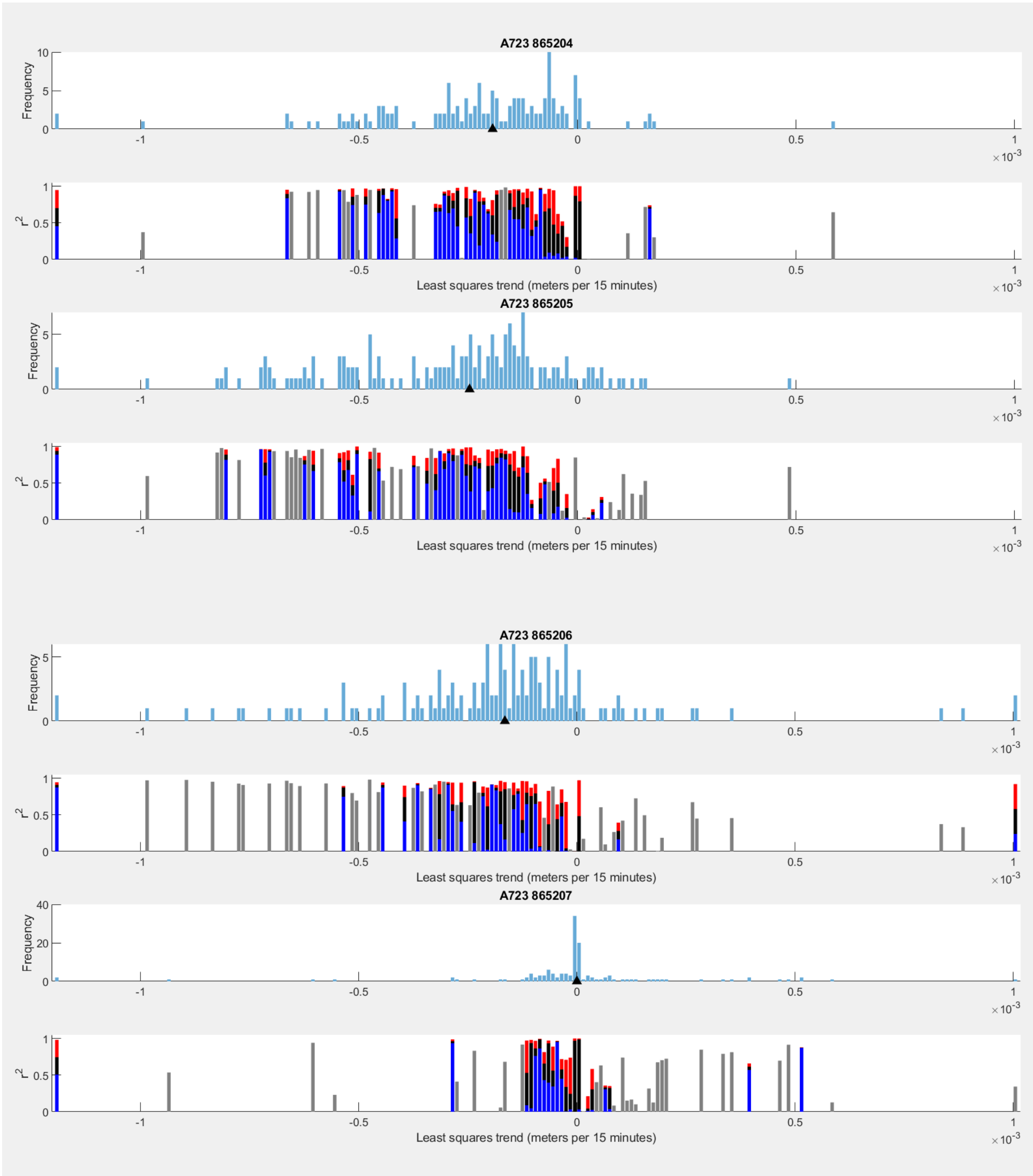
A723 865204
Frequency
r2
Least squares trend (meters per 15 minutes)
A723 865205
Frequency
r2
Least squares trend (meters per 15 minutes)
A723 865206
Frequency
r2
Least squares trend (meters per 15 minutes)
A723 865207
Frequency
r2
Least squares trend (meters per 15 minutes)
× 10-3

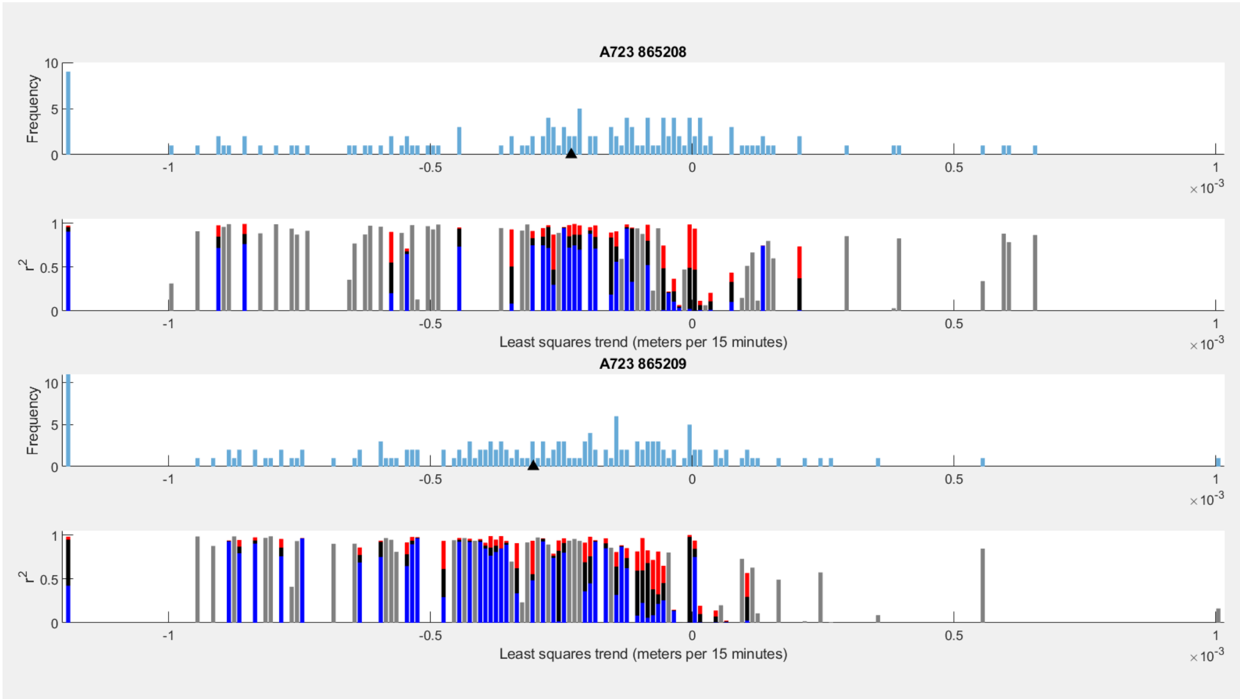
A723 865208
Frequency
r²
Least squares trend (meters per 15 minutes)
×10⁻³
A723 865209
Frequency
r²
Least squares trend (meters per 15 minutes)
×10⁻³

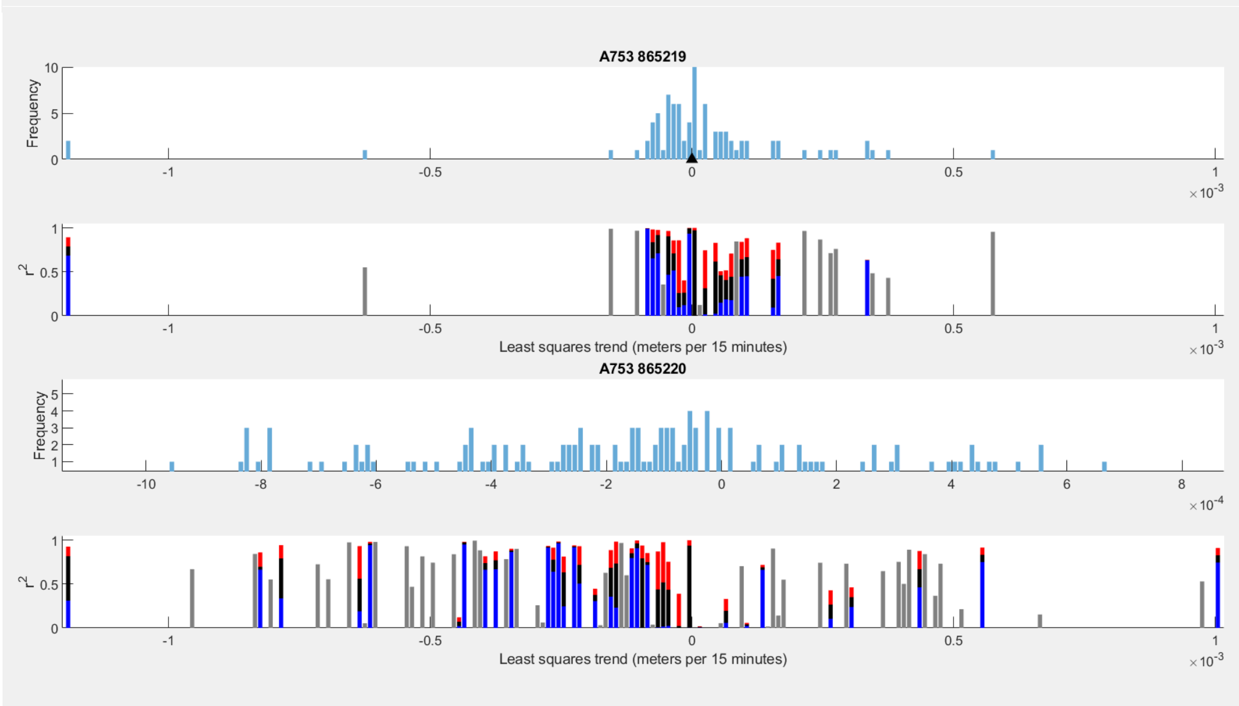
A753 865219
Frequency
r²
Least squares trend (meters per 15 minutes)
×10⁻³
A753 865220
Frequency
×10⁻⁴
r²
Least squares trend (meters per 15 minutes)
×10⁻³

Appendix 11 Surface water response to precipitation

Figure 34 and Figure series 35 provide an indication of the variability in the retrieved lag times and trends, with associated characteristics, found.

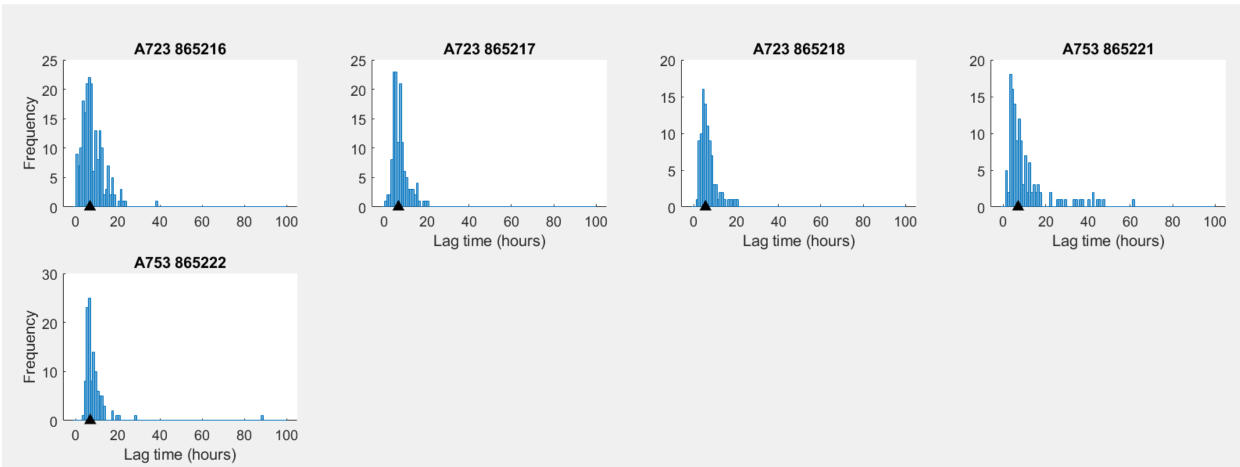

Figure 34: Histograms of the lag time computed for surface water for each station supplemented by the median value indicated by the black triangle.

Figure series 35: Histograms of observed trend values put in perspective by the associated range of coefficients of determination for each surface water monitoring station.

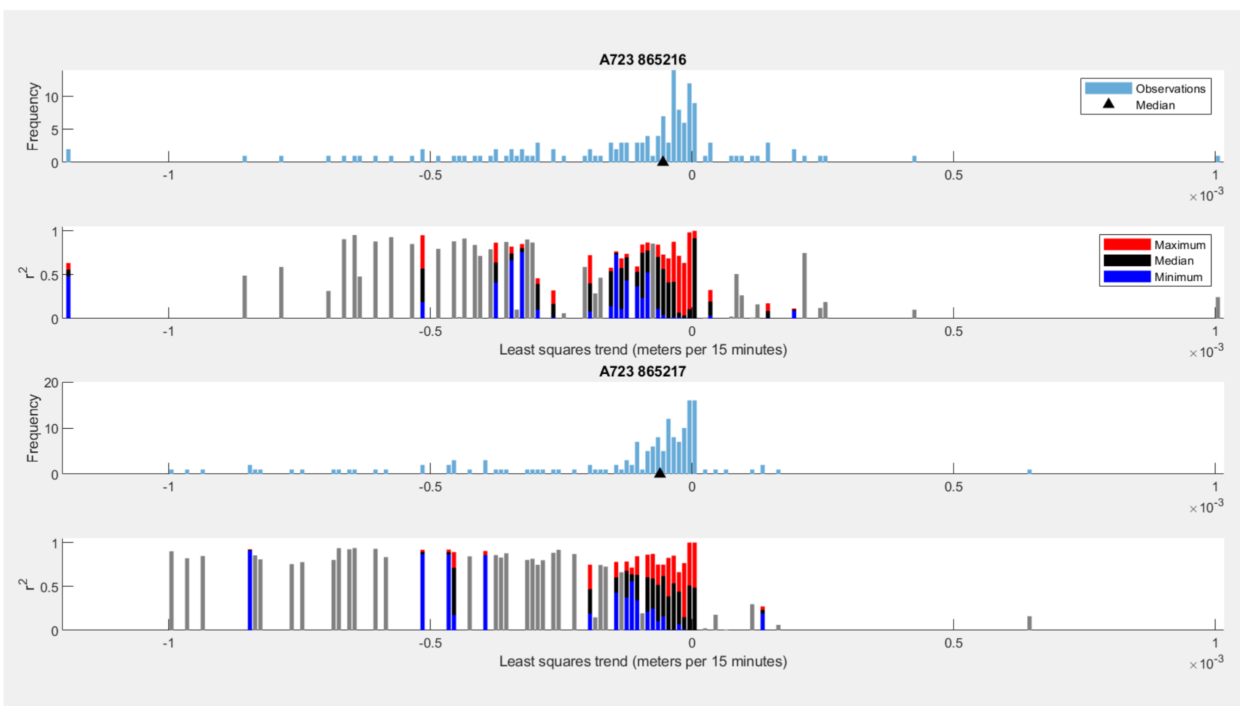

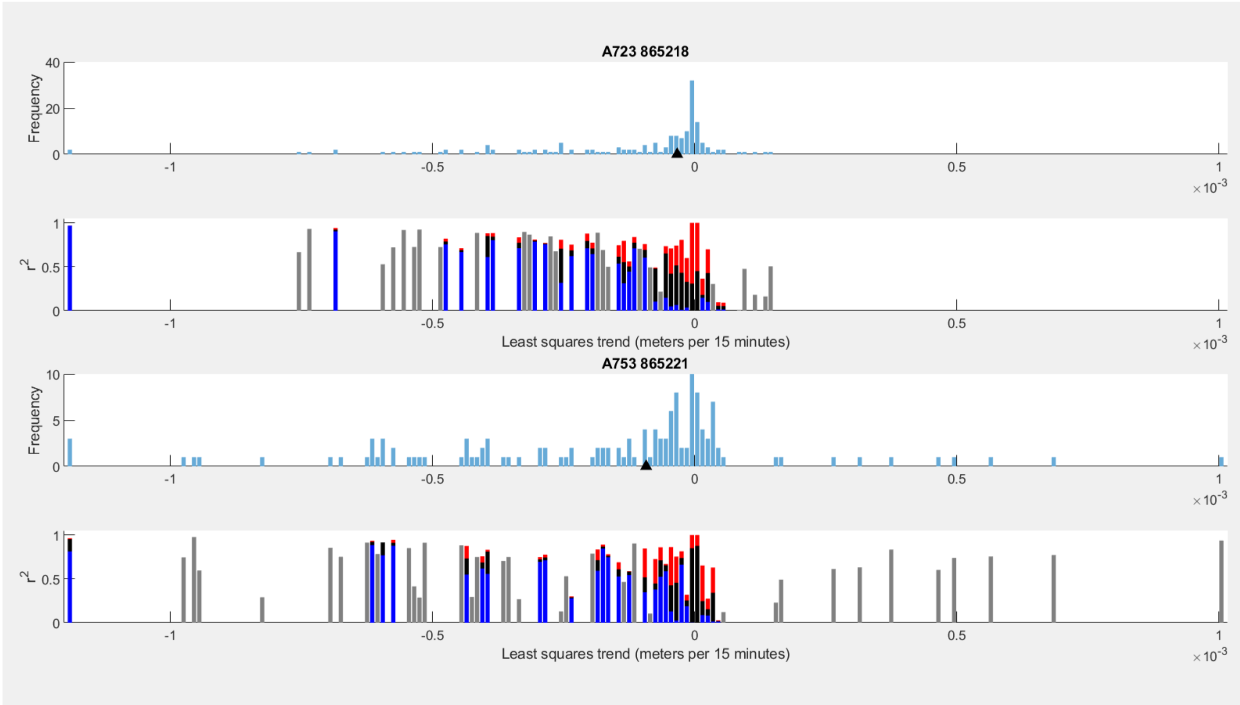
A723 865218
Frequency
r2
Least squares trend (meters per 15 minutes)
A753 865221
Frequency
r2
Least squares trend (meters per 15 minutes)

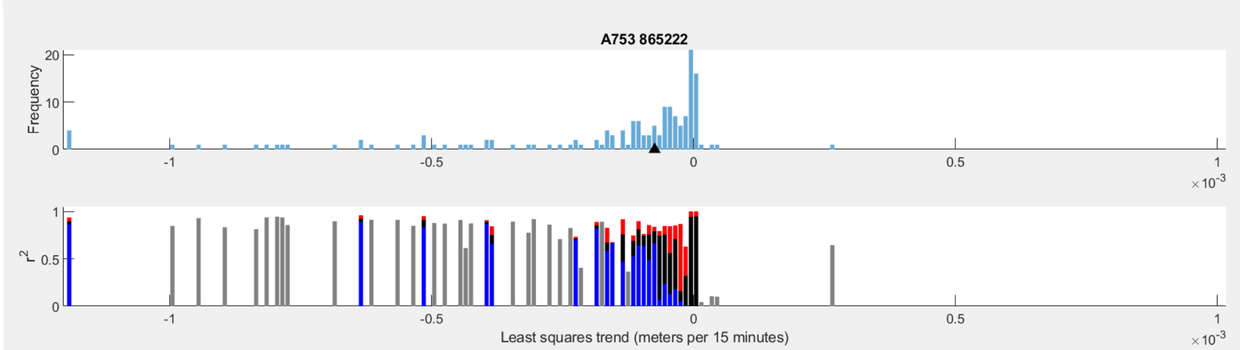
A753 865222
Frequency
r2
Least squares trend (meters per 15 minutes)

Appendix 12 Drainage volume response to precipitation

Figure 36 and Figure series 37 provide an indication of the variability in the retrieved lag times and trends, with associated characteristics, found.

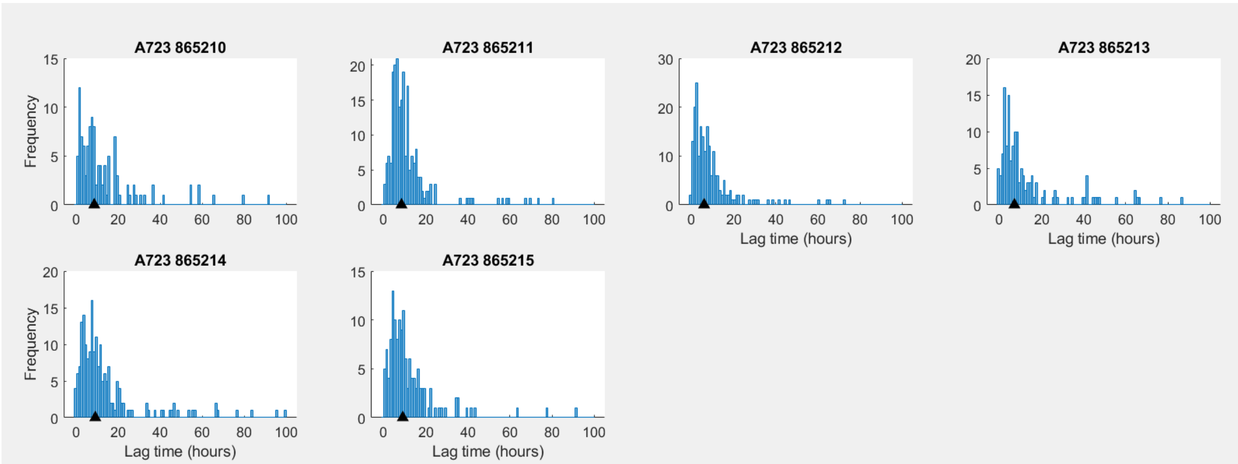

Figure 36: Histograms of the lag time computed for drainage outflow for each station supplemented by the median value indicated by the black triangle.

Figure series 37: Histograms of observed trend values put in perspective by the associated range of coefficients of determination for each drain flow monitoring station.

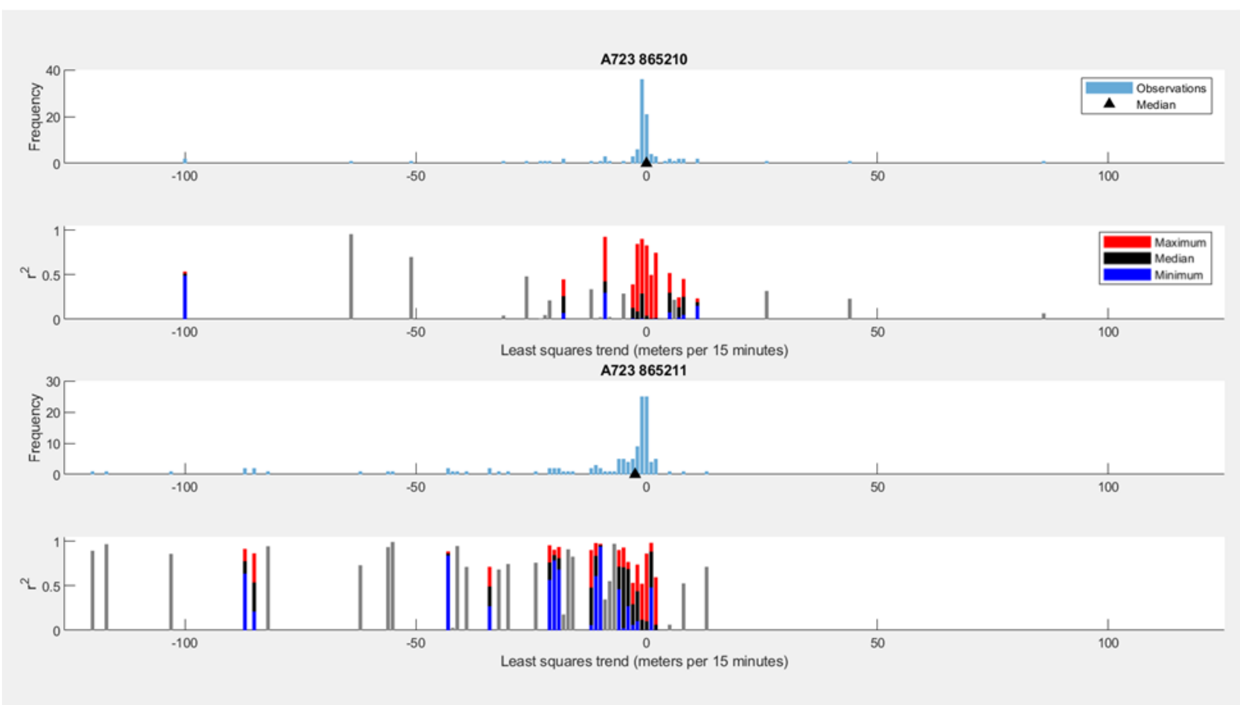

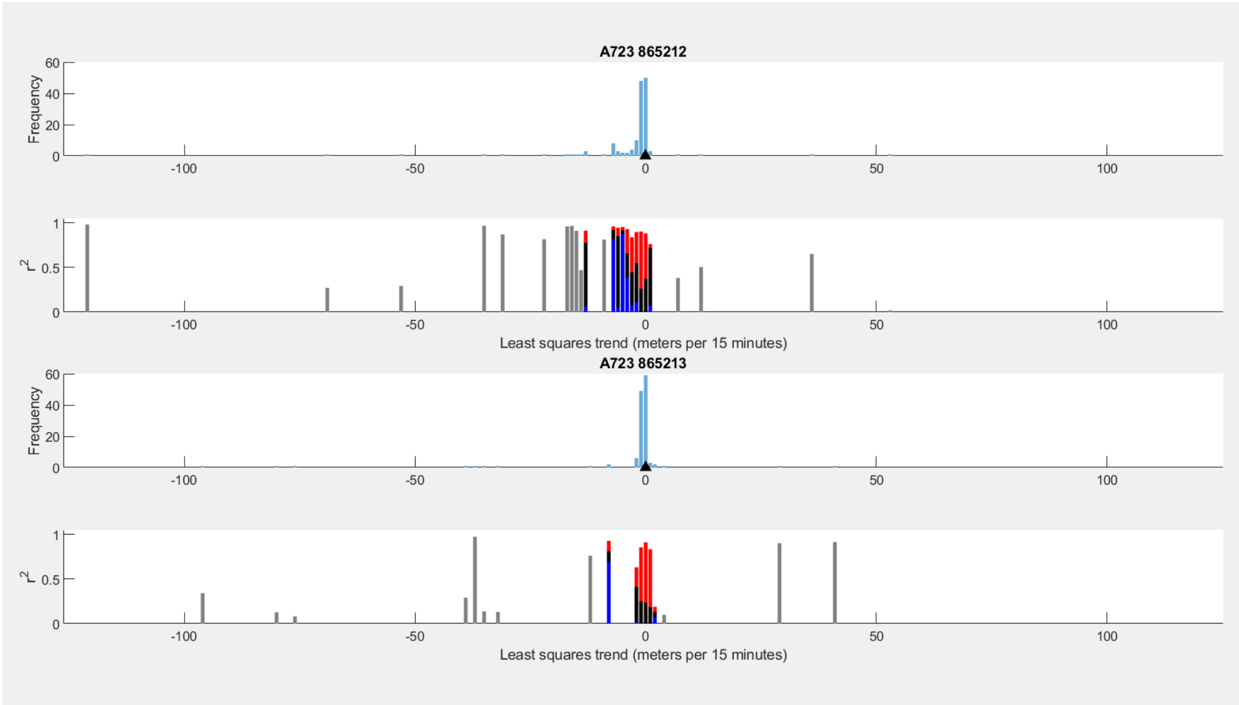
A723 865212
Frequency
r2
Least squares trend (meters per 15 minutes)
A723 865213
Frequency
r2
Least squares trend (meters per 15 minutes)

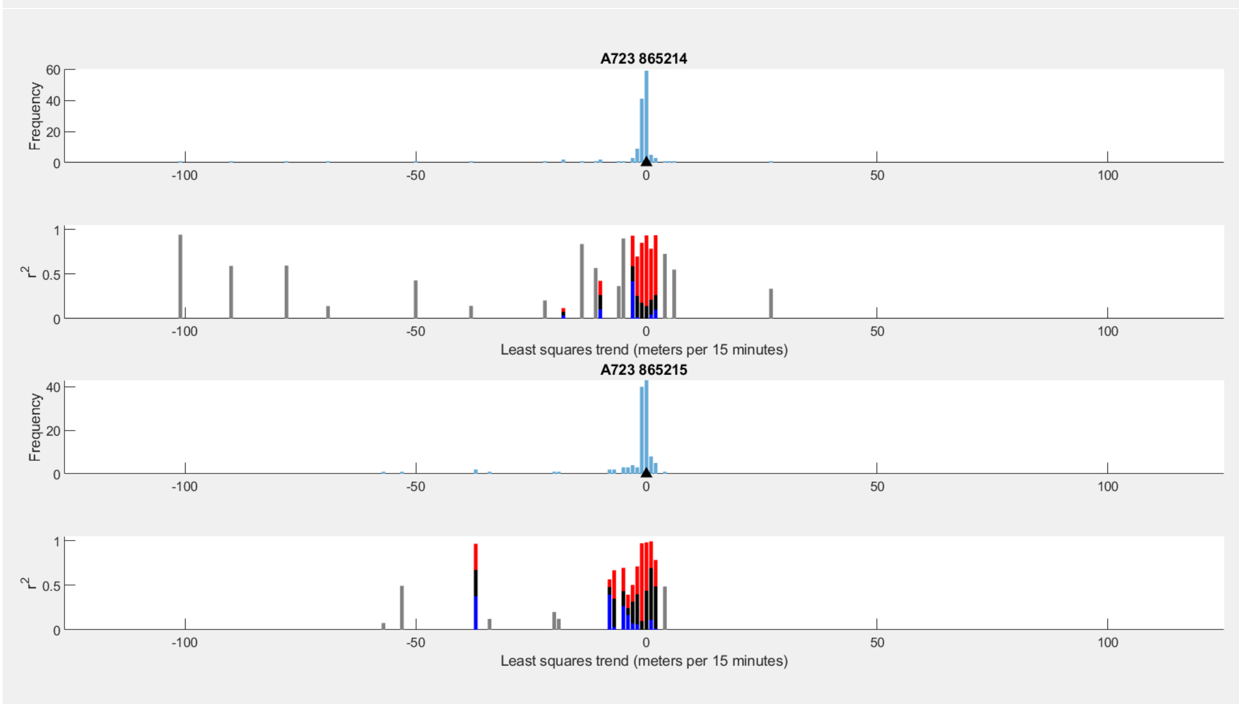
A723 865214
Frequency
r2
Least squares trend (meters per 15 minutes)
A723 865215
Frequency
r2
Least squares trend (meters per 15 minutes)

Appendix 13 Correlation of groundwater to soil moisture

For reference, Figure 38 gives an overview of the computed correlation coefficients when investigating the relation between groundwater level and soil moisture. Despite there being a correlation there is no apparent pattern in terms of at which depth the soil moisture content is retrieved.

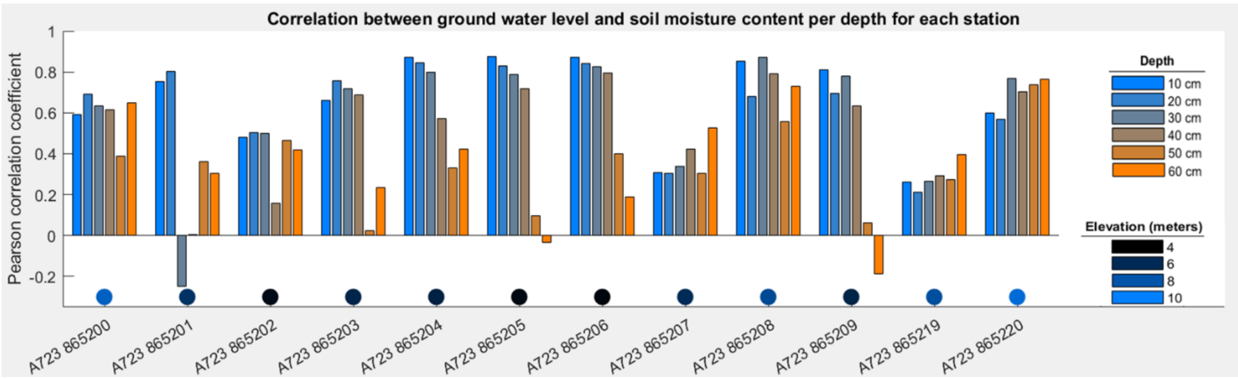

Figure 38: Found correlation coefficients comparing groundwater level and soil moisture content

Appendix 14 Influence of precipitation absence on soil moisture

To give an indication of the response of soil moisture to dry conditions, the found trend values are provided for the depths of 10 cm and 50 cm because these represent either spectrum end of the medians observed. The two exemplar cases are presented sequentially in Figure series 39 and Figure series 40.

Soil moisture content at 10 cm depth

Figure series 39: Histogram of observed trend values put in perspective by the associated range of coefficients of determination for each soil moisture content monitoring station for the 10 cm depth.

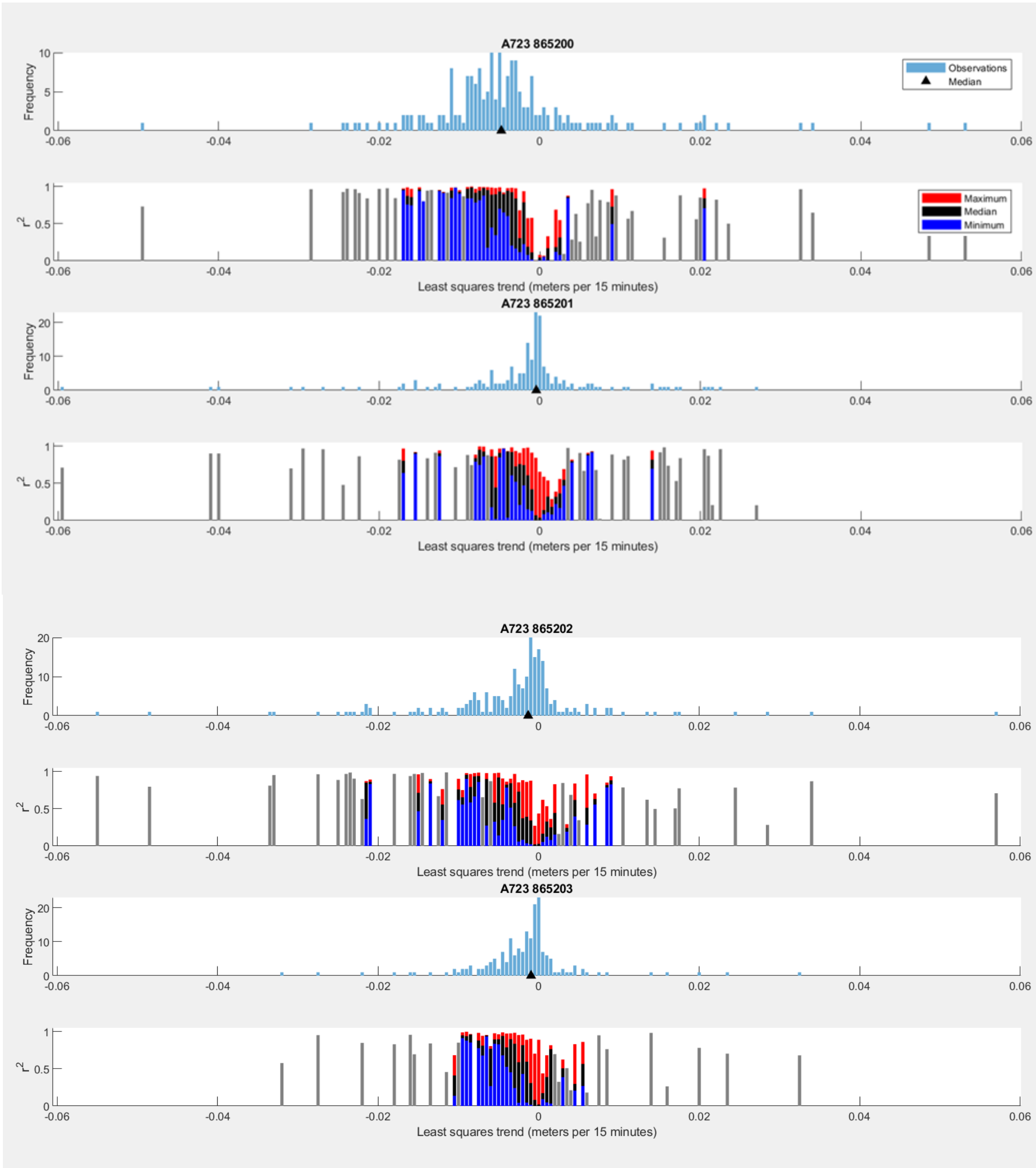

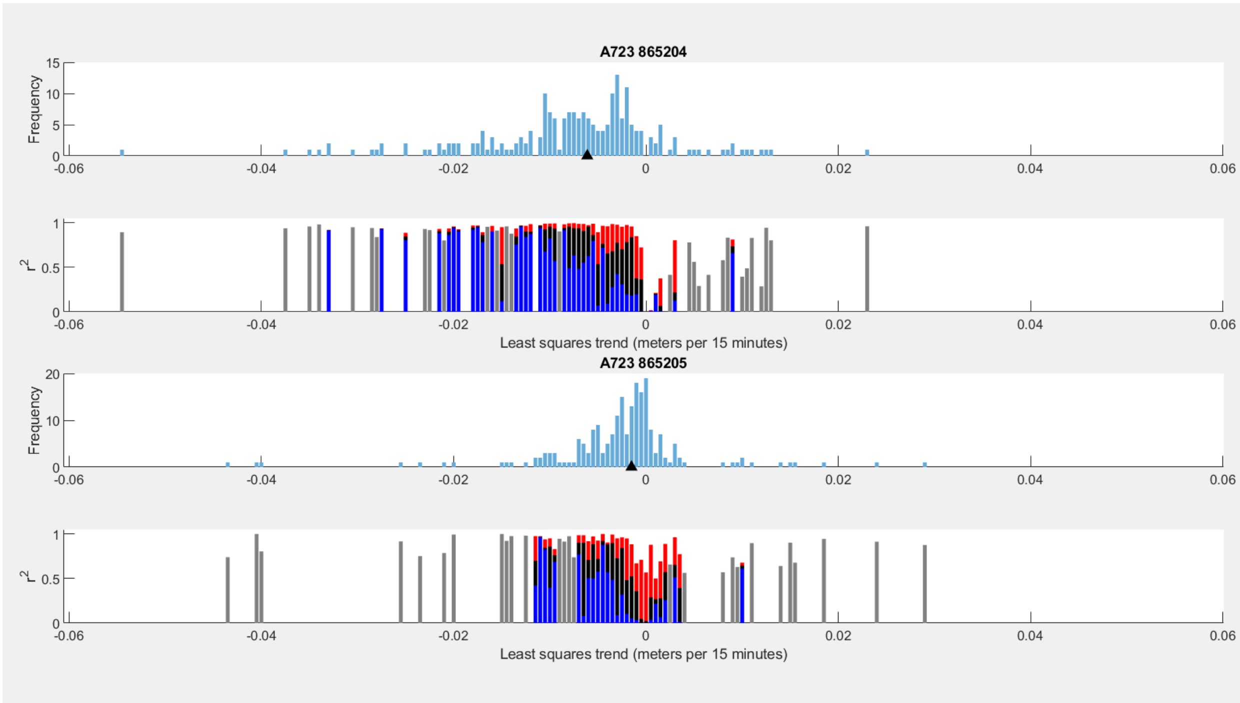
A723 865204
Frequency
r^2
Least squares trend (meters per 15 minutes)
A723 865205
Frequency
r^2
Least squares trend (meters per 15 minutes)

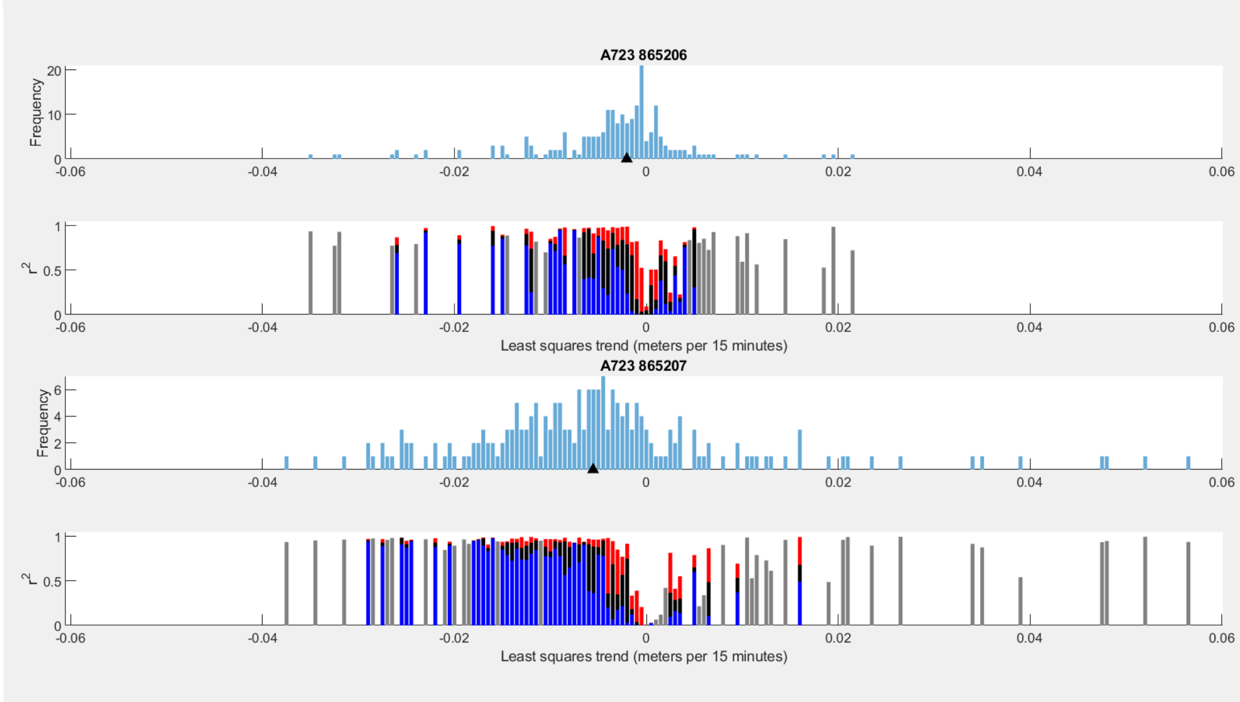
A723 865206
Frequency
r^2
Least squares trend (meters per 15 minutes)
A723 865207
Frequency
r^2
Least squares trend (meters per 15 minutes)

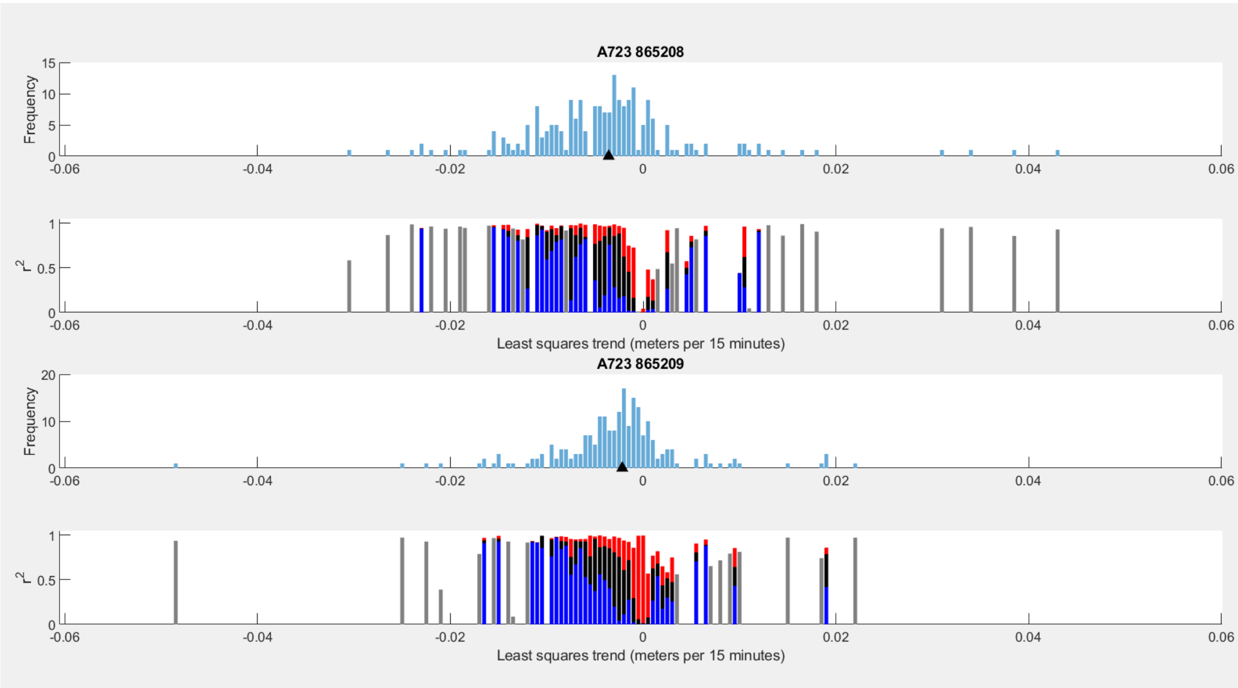
A723 865208
Frequency
r2
Least squares trend (meters per 15 minutes)
A723 865209
Frequency
r2
Least squares trend (meters per 15 minutes)

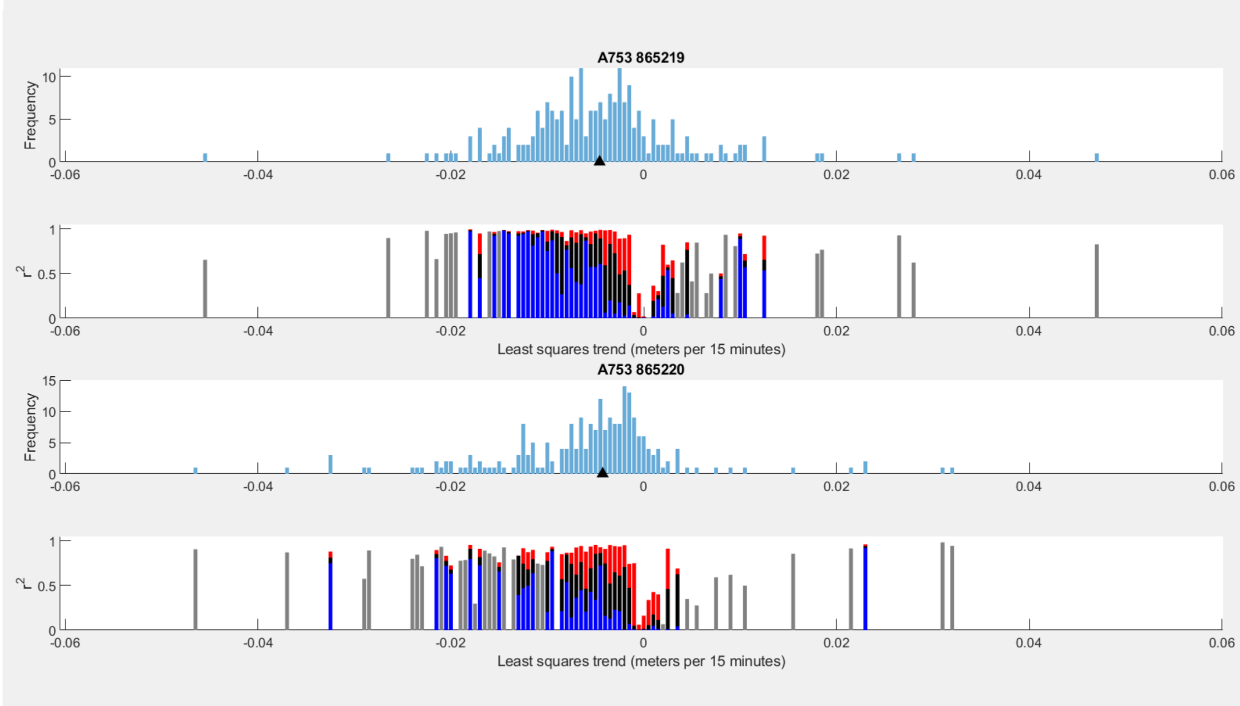
A753 865219
Frequency
r2
Least squares trend (meters per 15 minutes)
A753 865220
Frequency
r2
Least squares trend (meters per 15 minutes)

Soil moisture content at 50 cm depth

Figure series 40: Histogram of observed trend values put in perspective by the associated range of coefficients of determination for each soil moisture content monitoring station for the 50 cm depth.

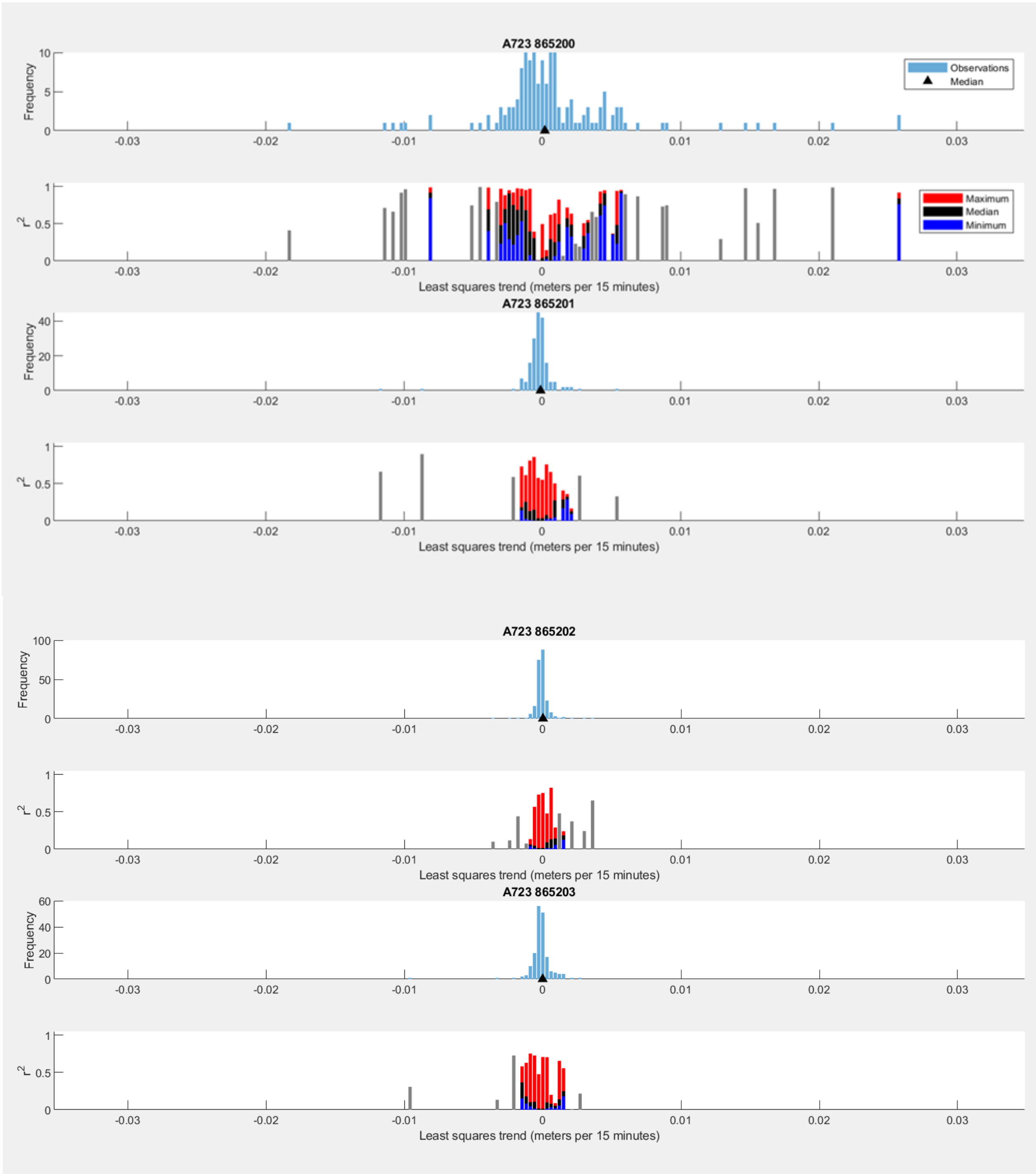

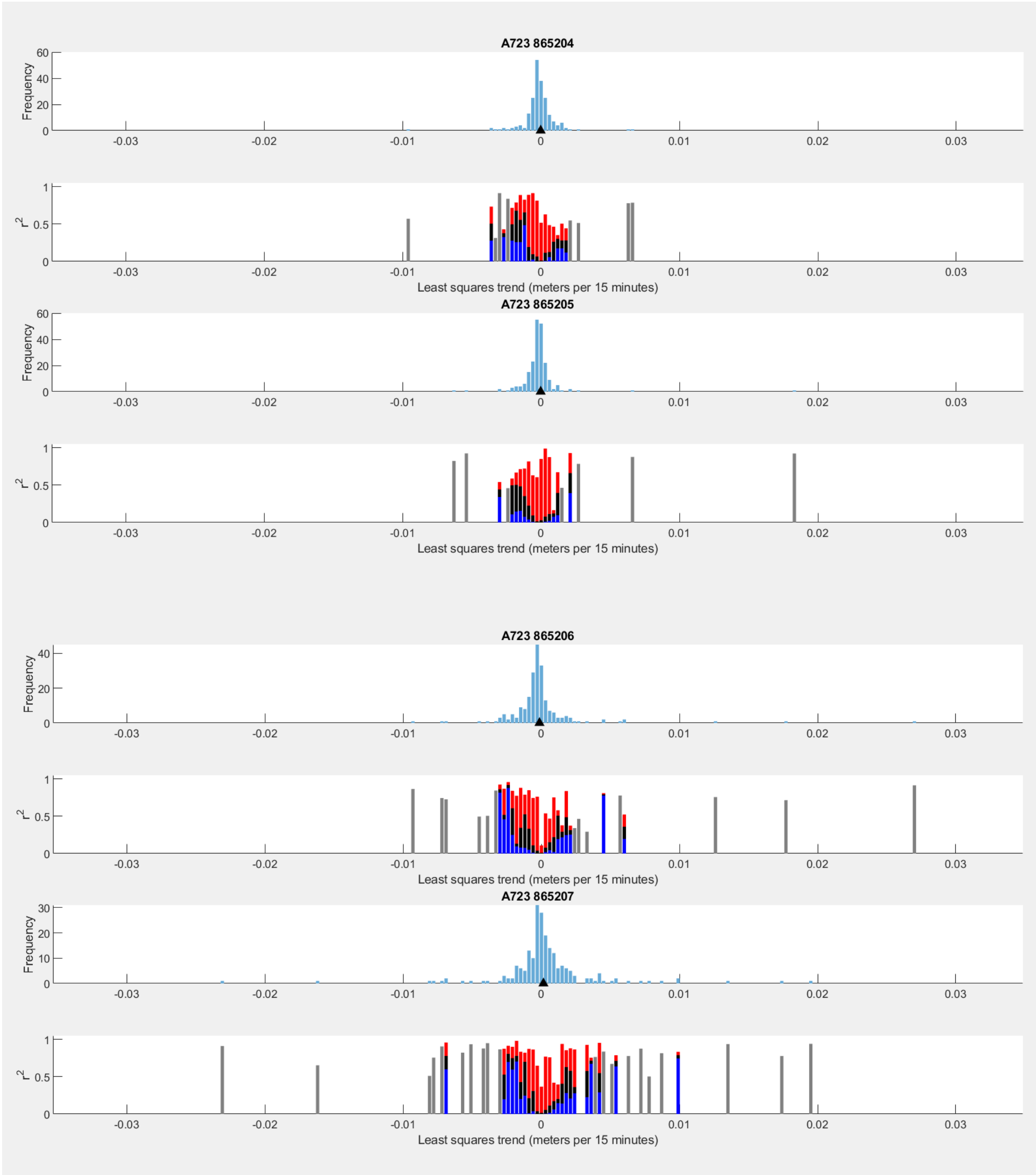
A723 865204
Frequency
r2
Least squares trend (meters per 15 minutes)
A723 865205
Frequency
r2
Least squares trend (meters per 15 minutes)
A723 865206
Frequency
r2
Least squares trend (meters per 15 minutes)
A723 865207
Frequency
r2
Least squares trend (meters per 15 minutes)

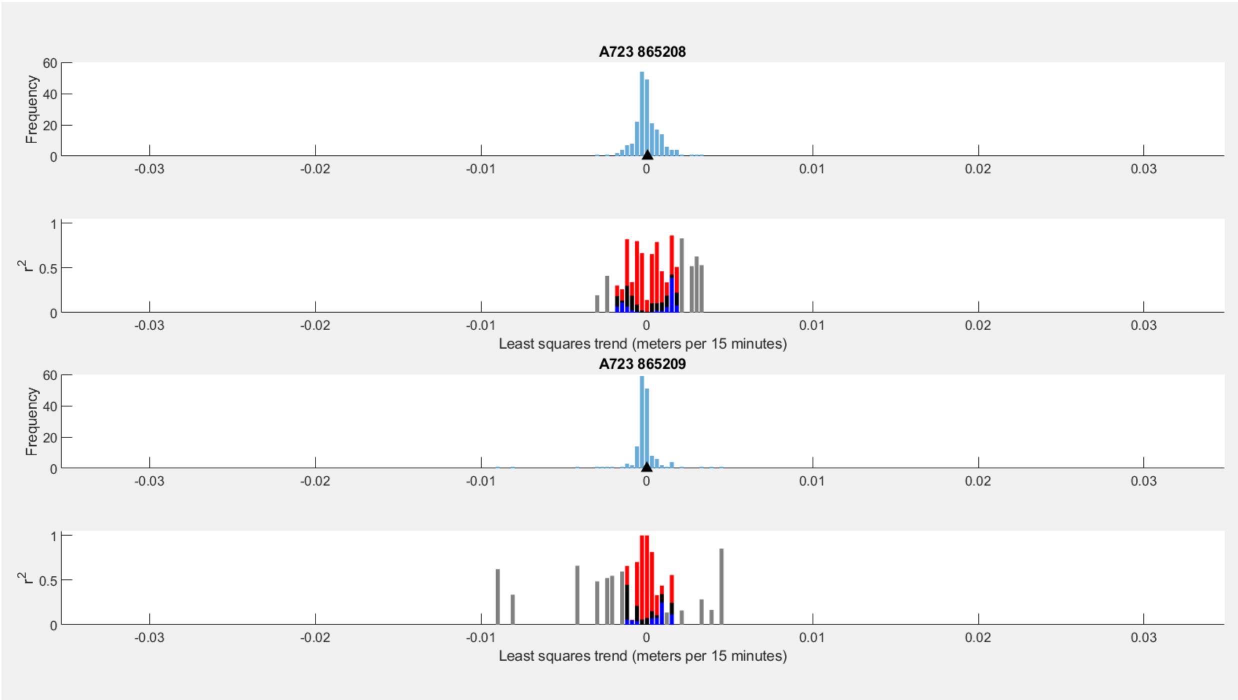
A723 865208
Frequency
r2
Least squares trend (meters per 15 minutes)
A723 865209
Frequency
r2
Least squares trend (meters per 15 minutes)
-0.03
-0.02
-0.01
0
0.01
0.02
0.03

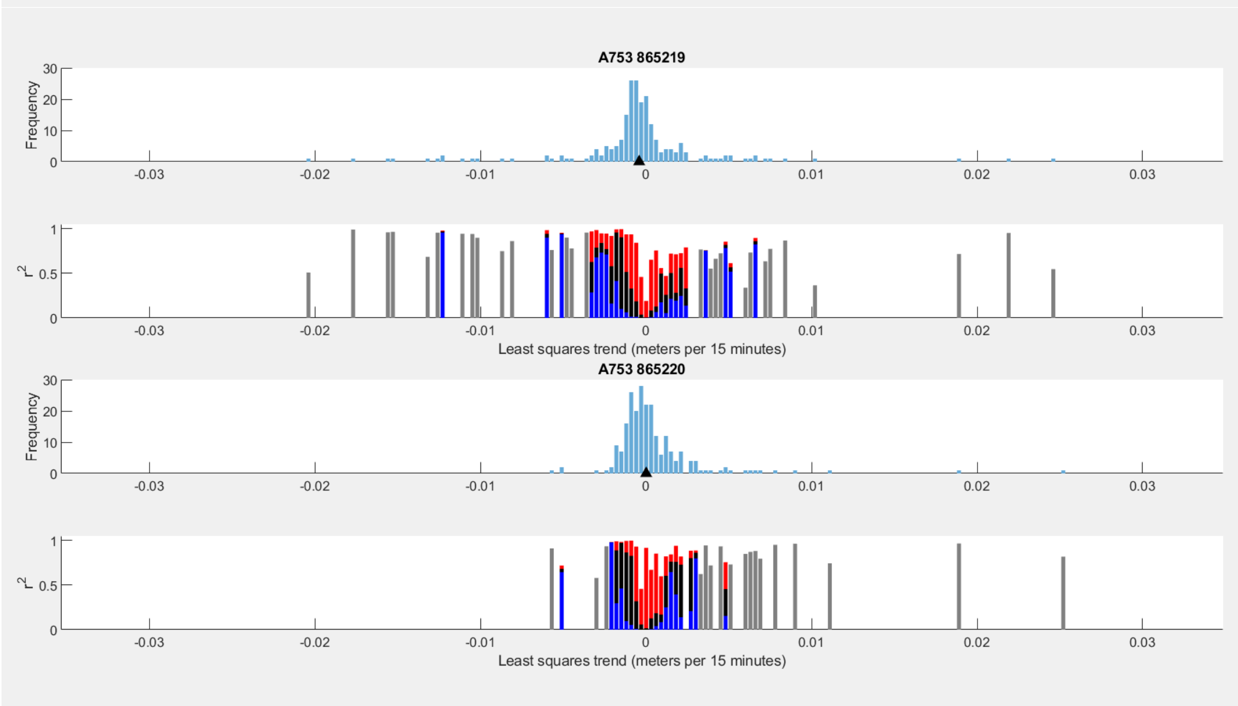
A753 865219
Frequency
r2
Least squares trend (meters per 15 minutes)
A753 865220
Frequency
r2
Least squares trend (meters per 15 minutes)
-0.03
-0.02
-0.01
0
0.01
0.02
0.03

Appendix 15 Correlation of NDVI to soil moisture

Shifting the soil moisture time series of each depth along the NDVI data set with both positive and negative lag for the four station locations where NDVI features periodicity, allows to present Figure 41. This shows the differences per depth in the correlation outputs as well as the degree in which the two series compared by a correlation coefficient are out of phase while further displaying the maximum coefficients observed when correcting for this time shift component

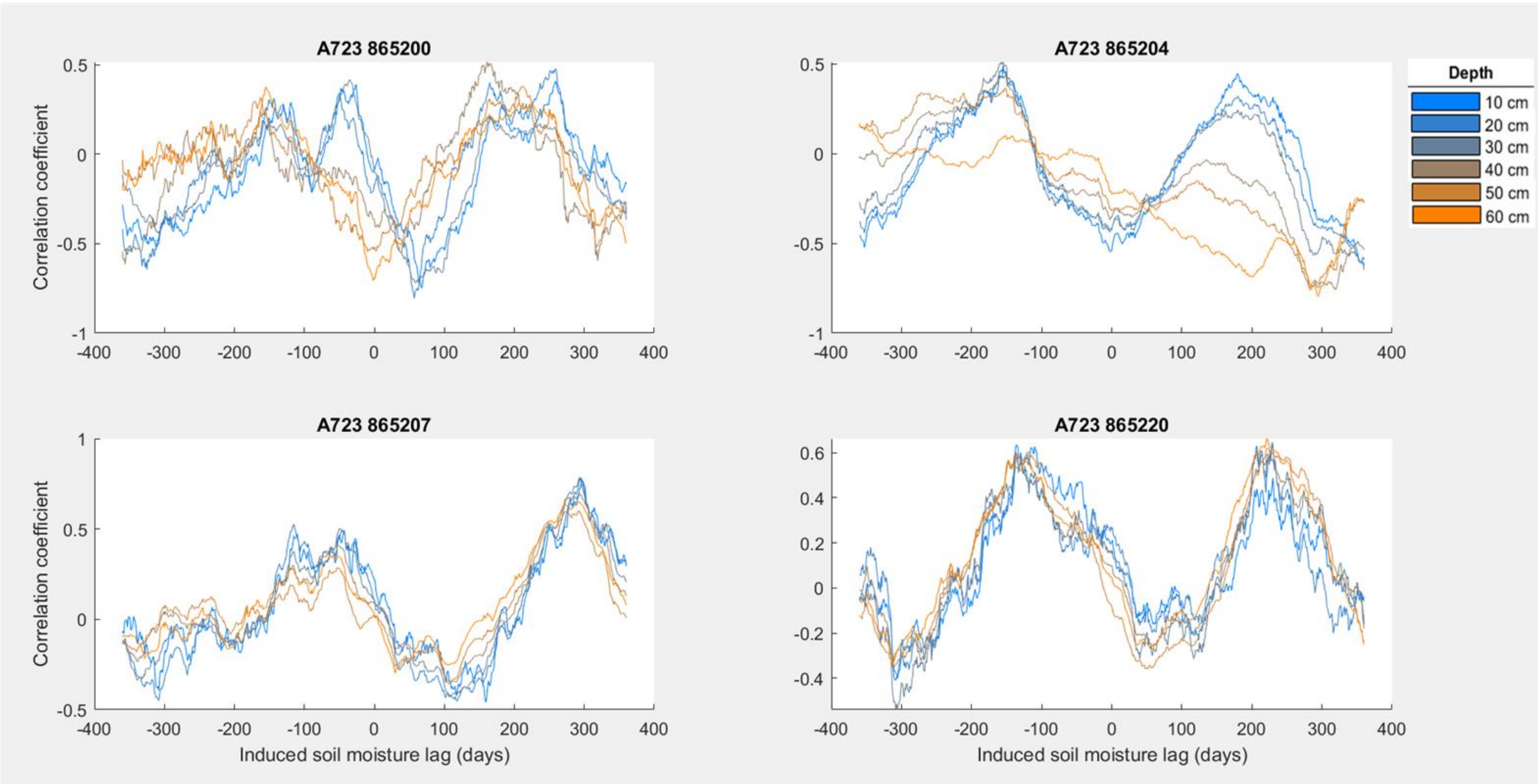

Figure 41: Correlation between NDVI and soil moisture, based on a series of induced soil moisture lag shifts with respect to the common recording time of both series compared, for each of the stations featuring periodicity in the derived NDVI time series for the locations where soil moisture is measured.

Appendix 16 Soil moisture saturation frequency

To obtain an overview of how often the groundwater level rises, during its annual cycle, to fully saturate the soil around the moisture sensor for each of the depths ranging from 10 to 60 cm below the ground surface, Figure 42 is proposed. The latter is derived using the conversion of groundwater level measured from NAP to the table with reference to the local ground surface. The data recorded every 15 minutes is aggregated per day by taking the average. For each of the complete years of 2019, 2020 and 2021, the number of days for which the groundwater level exceeded each of the depths below the ground surface, used in measuring soil moisture content, is found. However, because of missing data entries, it does occur that for some days no value is available. In most cases based on the restricted temporal extent of such missing entries, accompanied by the stable nature of the adjoining records, a linear interpolation seems suited for an indication. This intervention is used to complete the time series for station A723 865201 in 2021, A723 865204 in 2019 and all three years for station A723 865205. Further, in 2021, stations A723 865220 also requires interpolation. However, based on the missing entries for station A723 865203 in 2019 and 2021 alongside the series of A723 865202 from 2021, such interpretation is not realistic. Hence, as for the time series of A723 865207 of which the limitations have been discussed, these are not used.

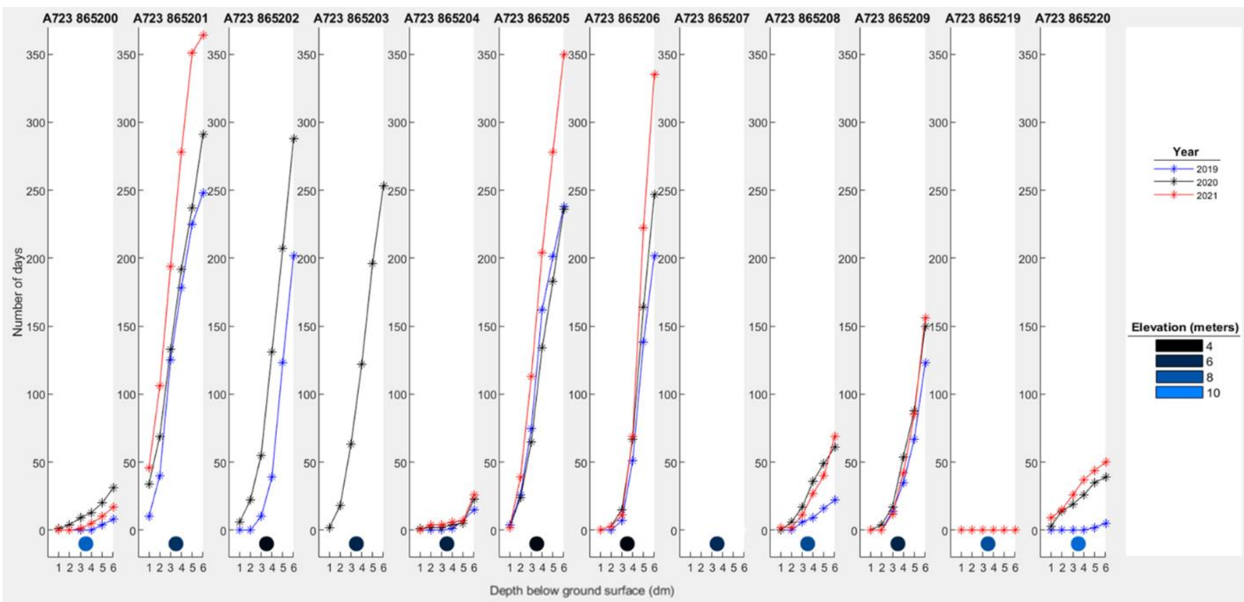

Figure 42: Number of days that the groundwater level saturates each of the six depths at which soil moisture is recorded for each station for the completely observed years of 2019, 2020 and 2021.